



# Nuclear Reaction Mechanisms in Heavy Ion Collisions

Nasirov A.K.<sup>1</sup>

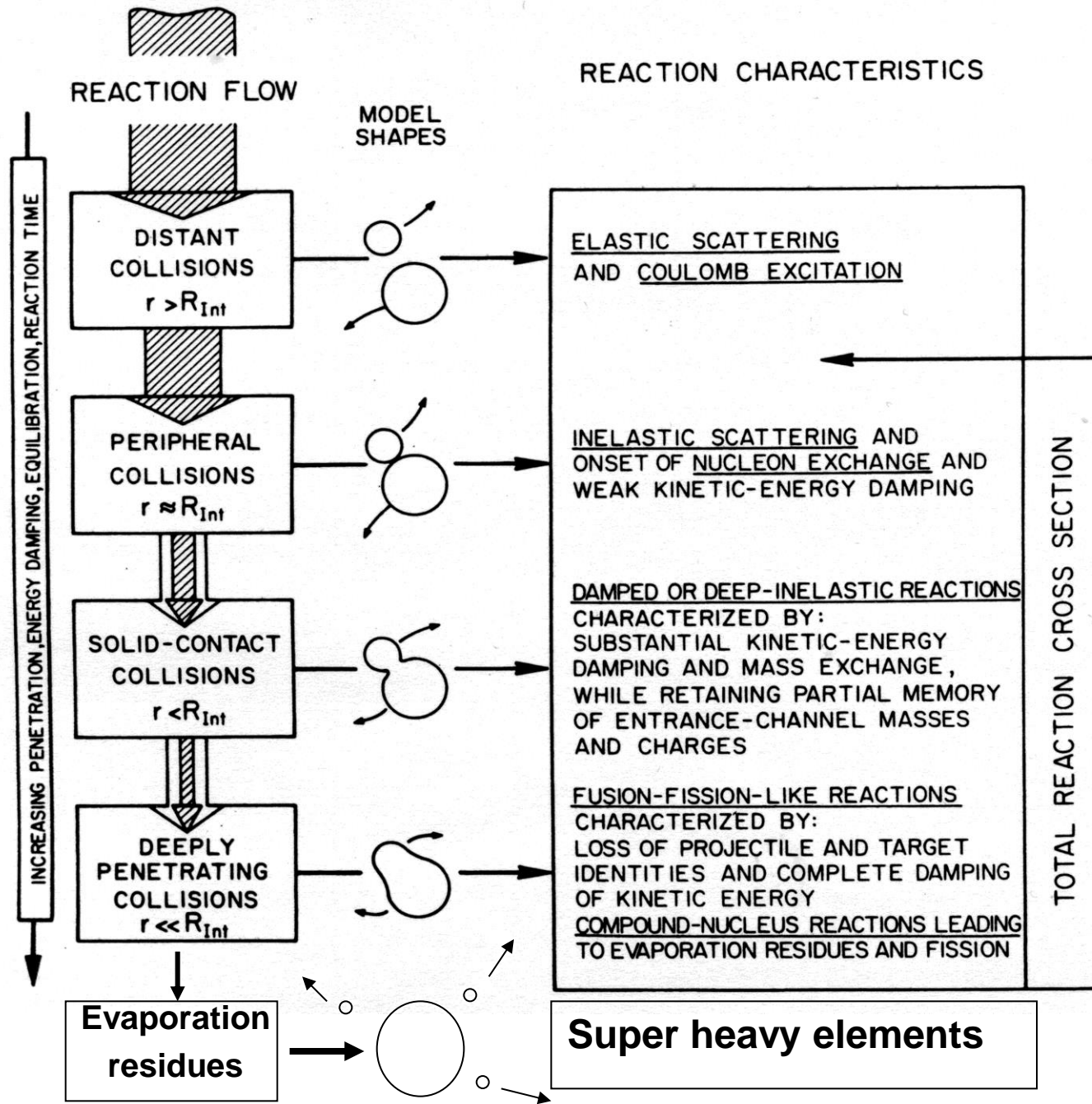
## Lecture III

<sup>1</sup>*Permanent position in Institute of Nuclear Physics, Tashkent, Uzbekistan*

# Content



- Introduction
- Main mechanisms of heavy ion collisions at low energies.
- Dinuclear system is a basic transition stage between entrance channel and formation of reaction products.
- Is it possible to control competition between quasifission and complete fusion in heavy ion collisions.
- Conclusions



# Enhancement and suppression of fusion in reactions forming heavy elements

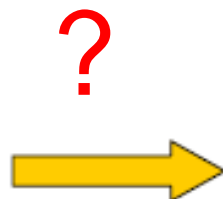
D.J. Hinde

Department of Nuclear Physics  
RSPHysSE  
Australian National University  
ACT 0200, Australia

FUSION06, San Servolo, Venezia, March 2006



capture



evaporation residue (ER)

$$\text{Yield of ER} = \sigma_{\text{capture}} \times P_{\text{compact nucleus}} \times W_{\text{survival}}$$

capture yield

× probability of compact nucleus formation (quasi fission competition)

× survival of ER against fission competition

Describe a framework to extract  $P_{\text{CN}}$  in a model-independent way

## Experimental study of $P_{CN}$

- Experimental method: “cross-bombardment”
  - same C.N., different projectile/target
  - match C.N. properties:  $E^*$ ,  $\ell$ -distribution
  - taking ratios of ER yields (  $\rightarrow P_{CN}$  )

Element ( $Z$ )

Neutron-richness ( $N$ )

Static deformation (compact contact shapes)

Expt: Hinde et al., Phys.Rev.Lett. 74 (1995) 1295; Trotta et al., EPJ 25 Suppl.1(2005) 615; Mitsuoka et al., Phys Rev C65 (2002) 054608

Shell effects (PES, diabatic dynamics)

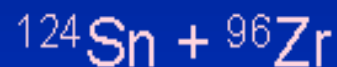
# Experimental study of the difference in the fusion mechanism in reactions leading to the same compound nucleus

Element (Z)

Z=90

Heavier, more fissile element Th – data (ANU)

earlier data



Hinde et al., Phys. Rev. Lett 89(2002)272701

Vermeulen et al. Z.Phys. A 318 (1984)157

Sahm et al., Nucl.Phys. A441(1985)316

Satou et al., Phys. Rev. C 65(2002)054602

Sahm et al., Nucl.Phys. A441(1985)316

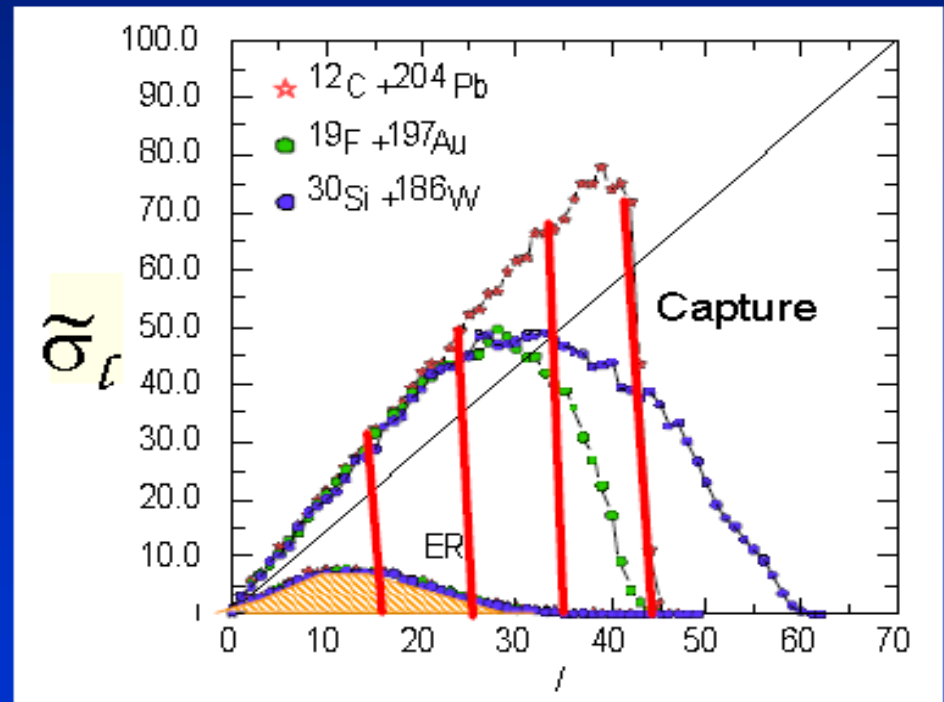
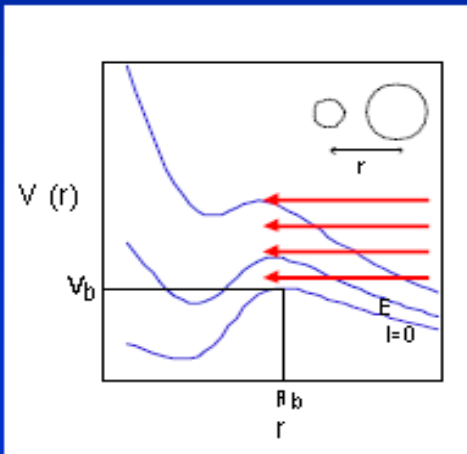
# Partial cross capture sections

$$\sigma_{ER}(E) = \pi \chi^2 \sum_{l=0}^{\infty} (2l+1) T_l(E) (1 - P_f(l, E^*)) P_{CN}$$

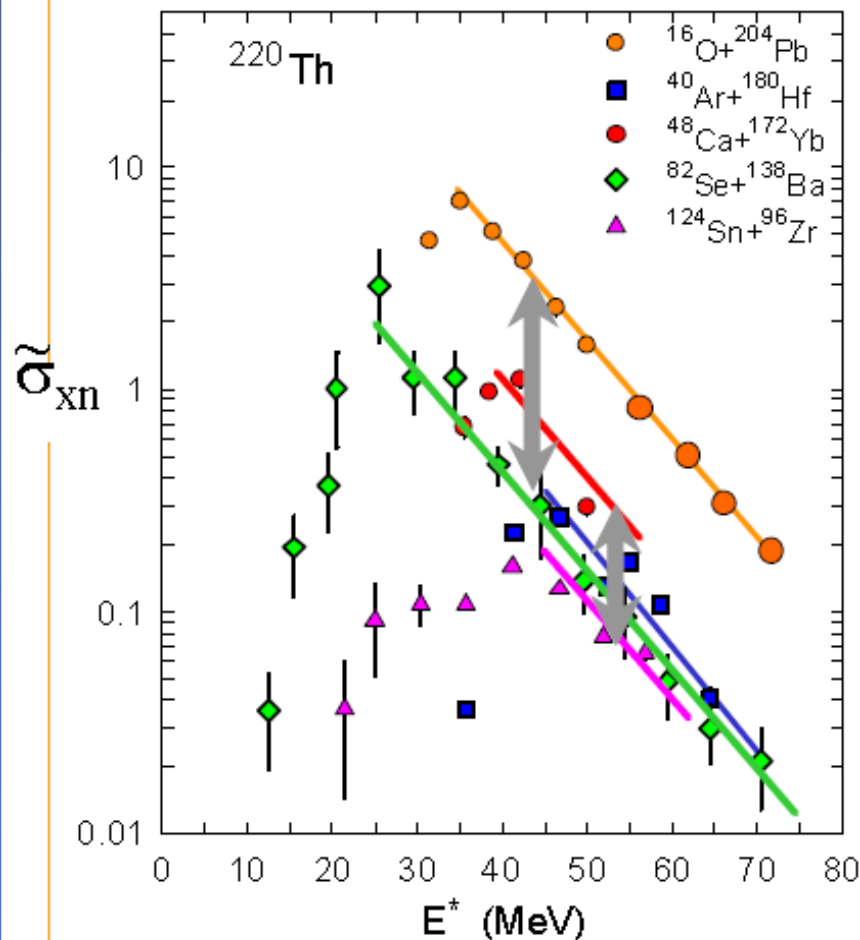
$$\tilde{\sigma}_{ER}(E) = \sum_{l=0}^{\infty} (2l+1) (1 - P_f(l, E^*)) P_{CN}$$

$P_f$ : statistical fission probability

$P_f \rightarrow 1$  for high ang. mom.







Hinde, Dasgupta, Mukherjee Phys. Rev. Lett. 89 (2002) 272701

Z=90

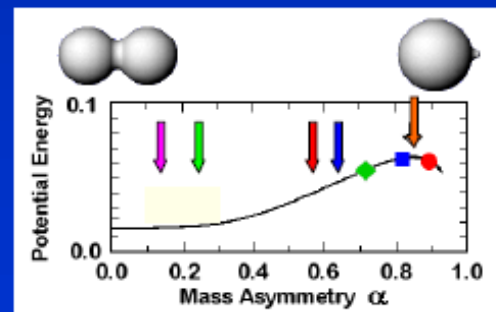
More mass-symmetric reactions:

$P_{xn}$  only ~10% of that for  $^{16}\text{O}$

Weaker dependence on mass asymmetry for more symmetric reactions

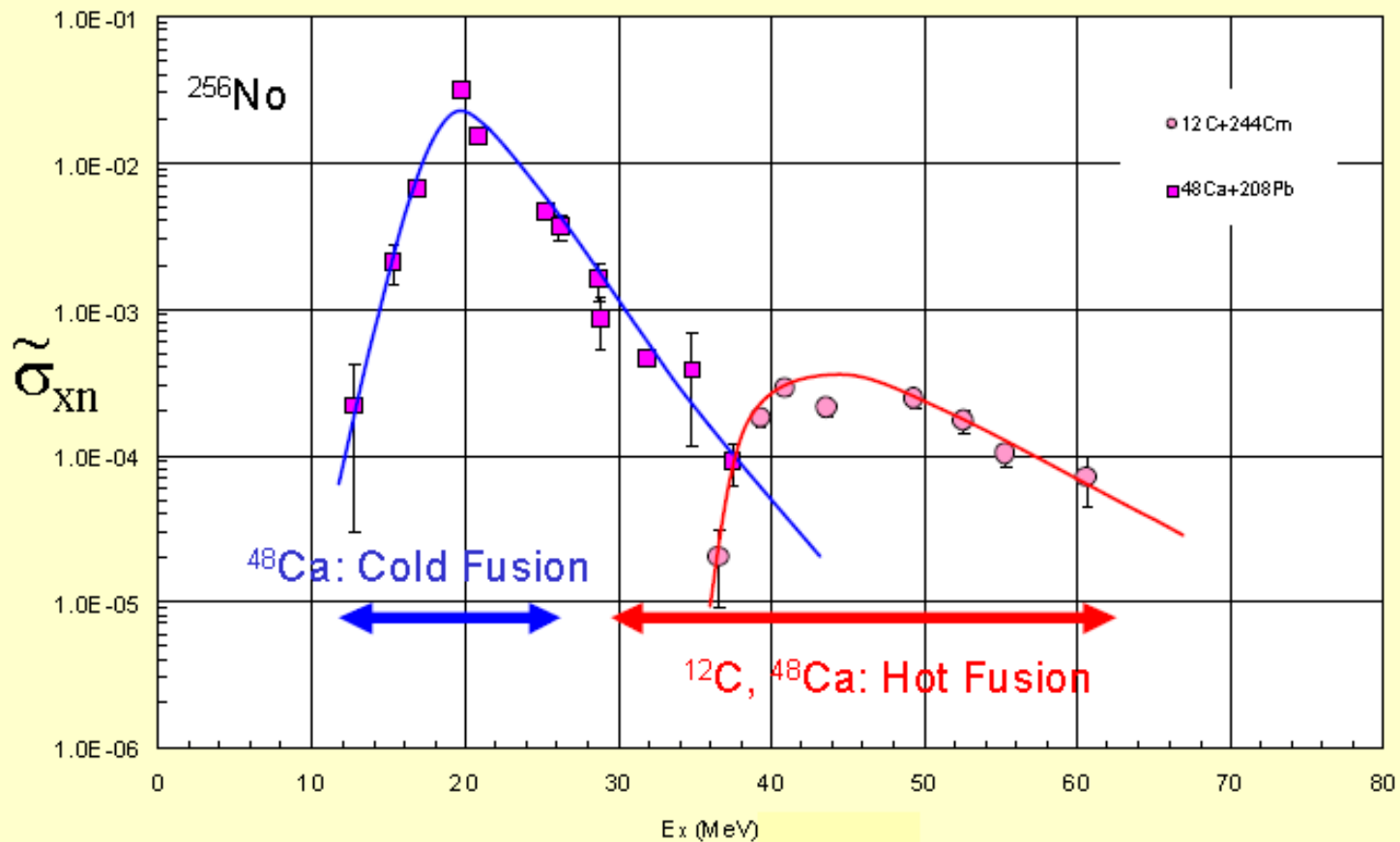
$P_{xn} \sim \text{constant}$  - independent of energy - no extra push

Qualitative relationship with Businaro-Gallone peak: mass-asymmetry evolution seems important



# Difference in formation of the evaporation residues in “hot” and “cold” fusion reactions.

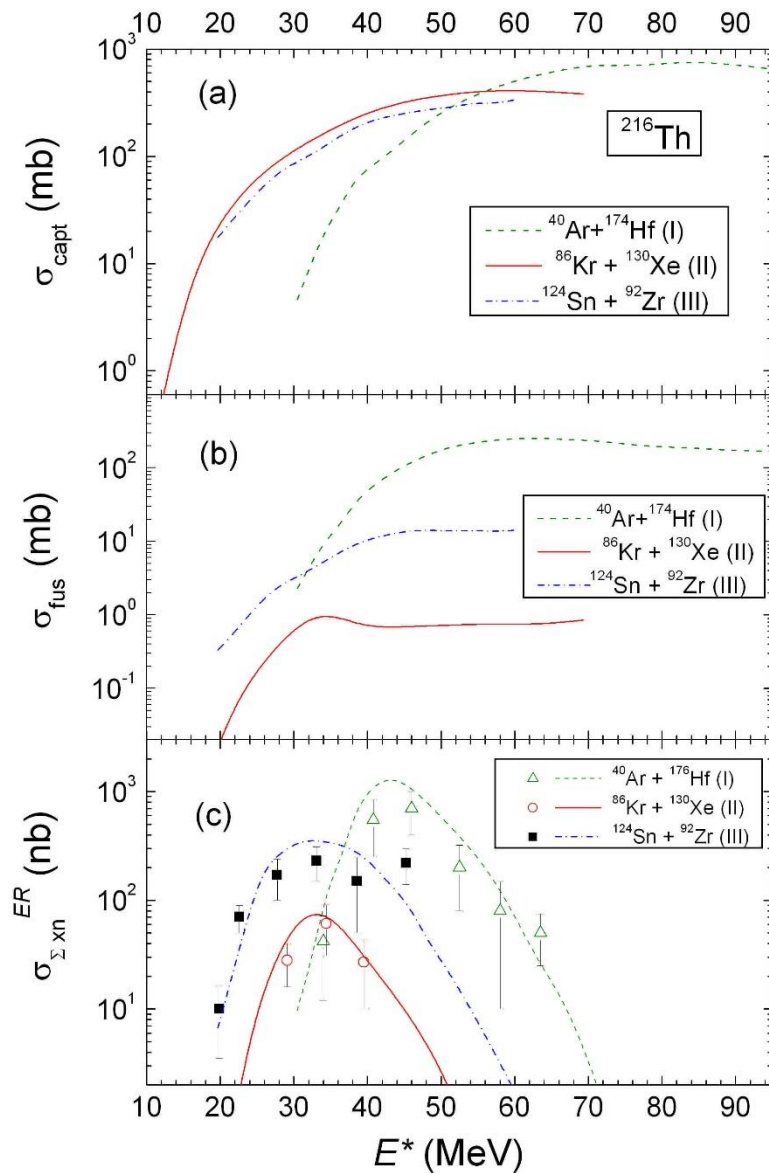
Reactions forming  $^{256}\text{No}$  – with  $^{12}\text{C}$  and  $^{48}\text{Ca}$  projectiles



## CONCLUSIONS

Entrance channel conditions dramatically affect evolution to compact CN (quasi-fission competition), and thus heavy element yields

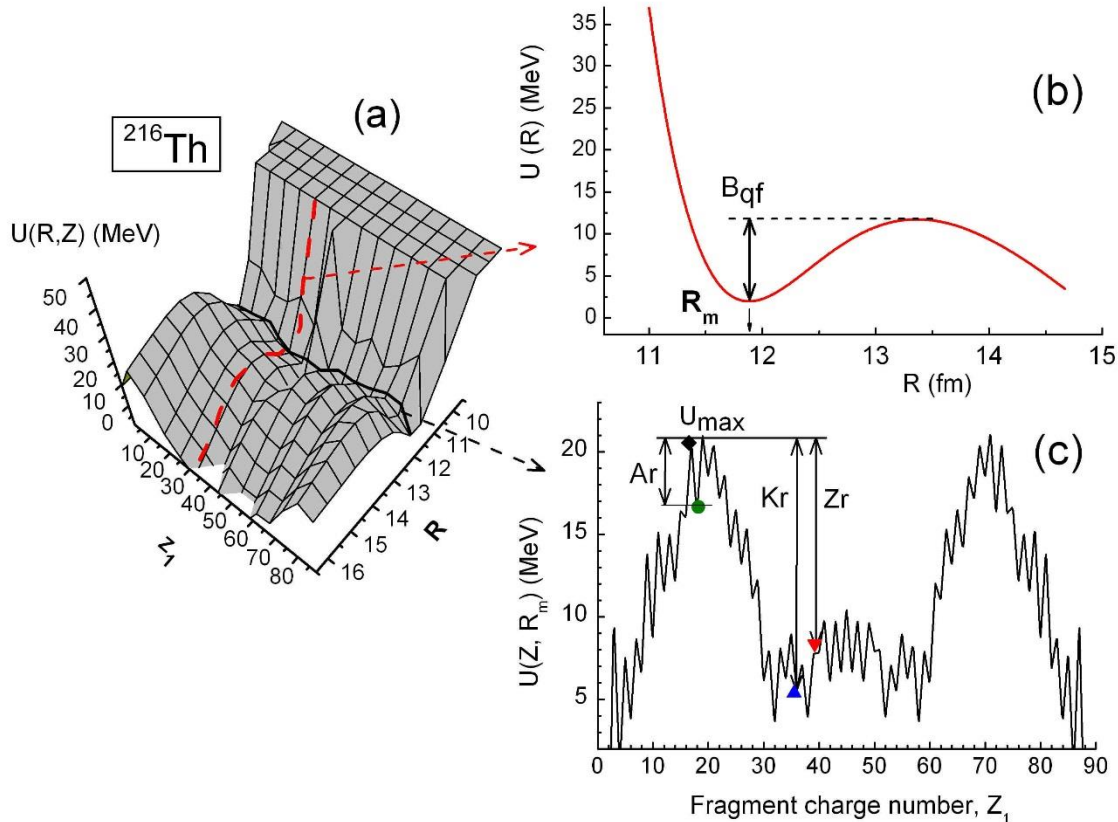
- See inhibition of ER yields even for quite mass-asymmetric reactions
- Mass-asymmetry larger than B-G peak is favourable
- Neutron-richness of composite system can be very important
- Special cases show large enhancement in yield due to closed shells
- Some existing results are not yet understood
- Existing models should be tested by calculating  $P_{xn}$  for these experimental data for  $Z=88,90,102$  !!!



The role of the entrance channel and shell structure of reactants at formation of the evaporation residues in reactions leading to the same compound nucleus  $^{216}\text{Th}$ :

- Capture
- Complete fusion
- Evaporation residues cross sections.

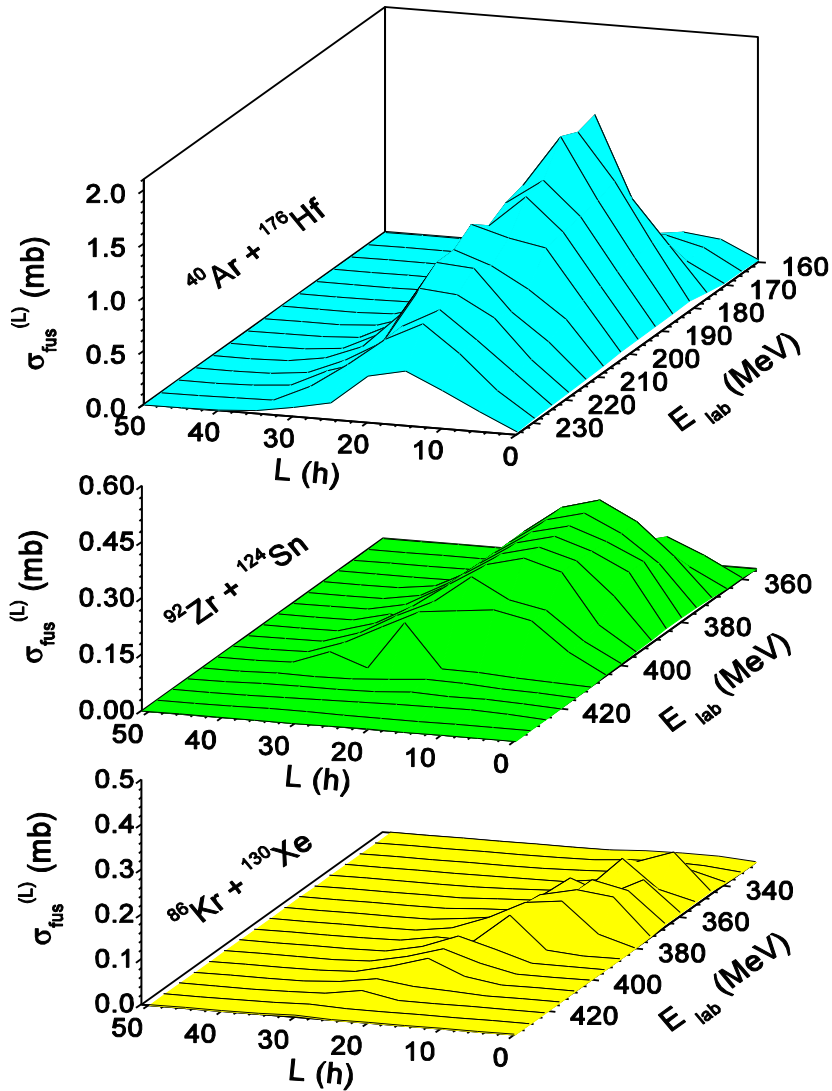
Driving potential  $U_{\text{driving}}(c)$  for reactions  $^{40}\text{Ar}+^{172}\text{Hf}$ ,  $^{86}\text{Kr}+^{130}\text{Xe}$ ,  $^{124}\text{Sn}+^{92}\text{Zr}$  leading to formation of compound nucleus  $^{216}\text{Th}$  :



Due to peculiarities of shell structure  
 $B_{\text{fus}}(\text{Kr}) > B_{\text{fus}}(\text{Kr})$   
 and, consequently,

$$\sigma_{\text{fus}}(\text{Kr}+\text{Xe}) < \sigma_{\text{fus}}(\text{Zr}+\text{Sn})$$

$$U_{\text{driving}} = B_1 + B_2 - B_{(1+2)} + V(R)$$



Angular momentum distribution for the complete fusion  $\sigma_{\text{fus}}^{(L)}(E_{\text{lab}})$  as a function of momentum and and beam energy for reactions leading to formation of  $^{216}\text{Th}$ .

G. Fazio, et al., Journal of the Physical Society of Japan 388, 2509 (2003).

# Classification of the nuclear reactions in heavy ion collisions

Early studies of reaction mechanisms between heavy ions have shown that, in a Wilczynski diagram, a definite evolution towards negative scattering angles with increasing energy loss is present, so that the scattering angle was used as an estimate of the interaction time. As usual three regions can be distinguished:

- (i) the elastic or quasi-elastic component,
- (ii) the partially damped region where the nuclear forces bend the trajectories toward smaller scattering angles and
- (iii) the fully relaxed component, where negative angle scattering (or orbiting), fusion-fission and symmetric fragmentation may occur.

# Partial cross sections of compound nucleus (CN), fusion-like (FL), damped (D), quasielastic (QE), Coulomb excitation (CE) and elastic (EL)

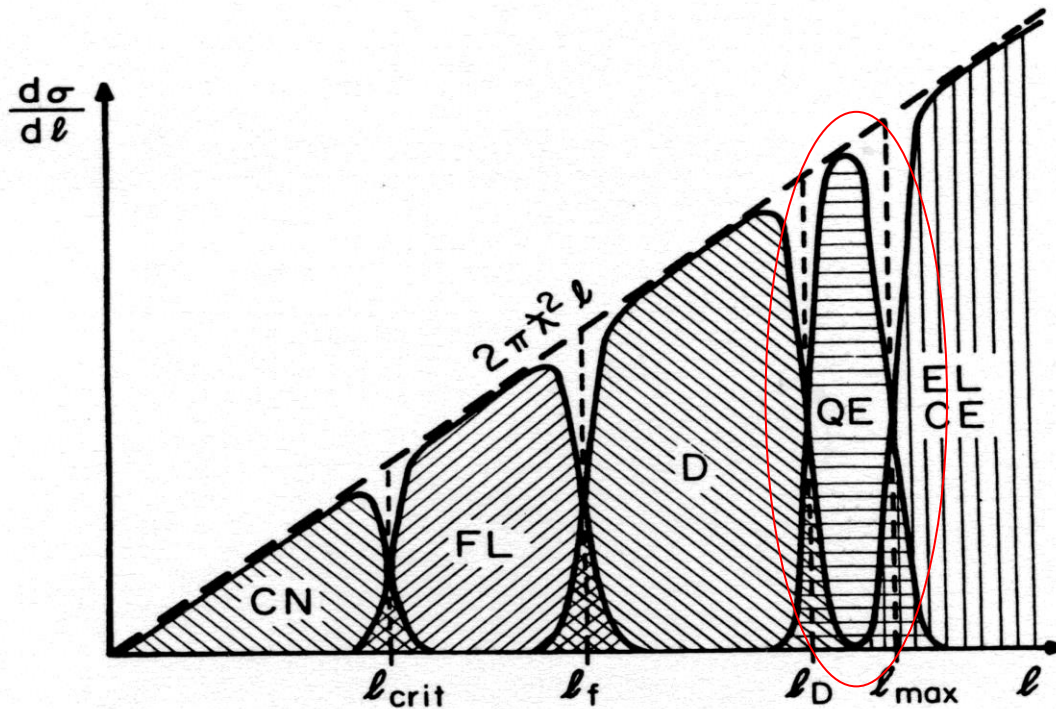


**Figure 39.** Schematic illustration of the  $l$  dependence of the partial cross section for compound-nucleus (CN), fusion-like (FL), damped (D), quasielastic (QE), Coulomb-excitation (CE), and elastic (EL) processes. The long-dashed line represents the geometrical partial cross section  $d\sigma/dl = 2\pi\lambda^2 l$ . Vertical dashed lines indicate the extensions of the various  $l$  windows in a sharp cutoff model with the characteristic  $l$  values noted at the abscissa. Hatched areas represent the diffuse  $l$  windows assumed in a smooth cutoff model.



# Partial cross sections of compound nucleus (CN), fusion-like (FL), damped (D), quasielastic (QE), Coulomb excitation (CE) and elastic (EL)

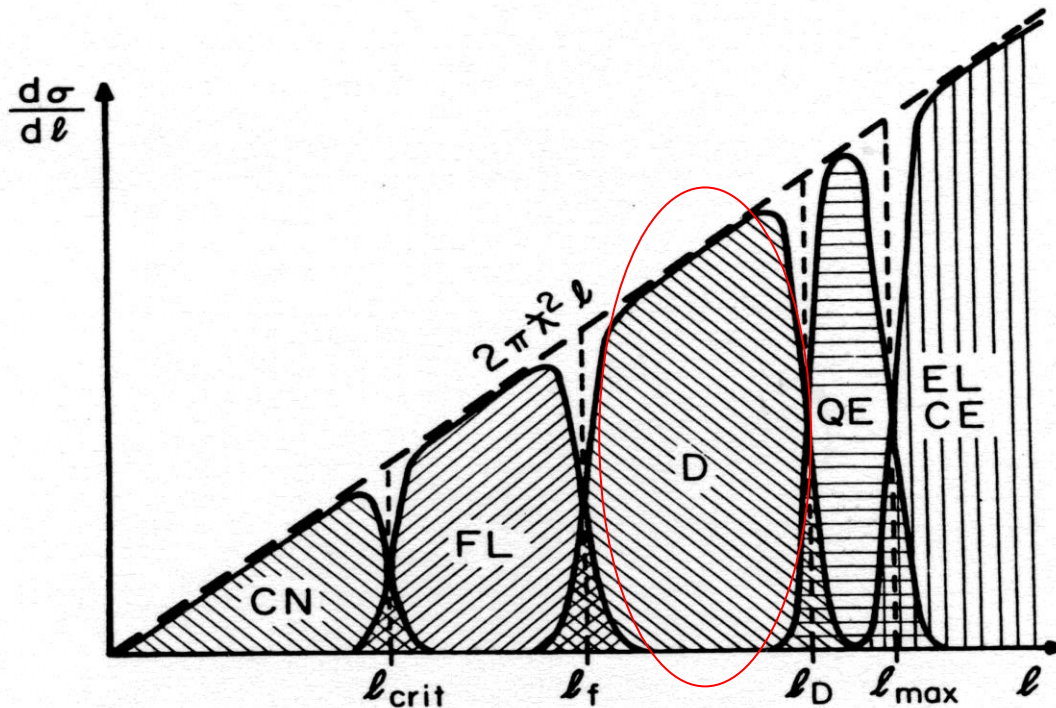
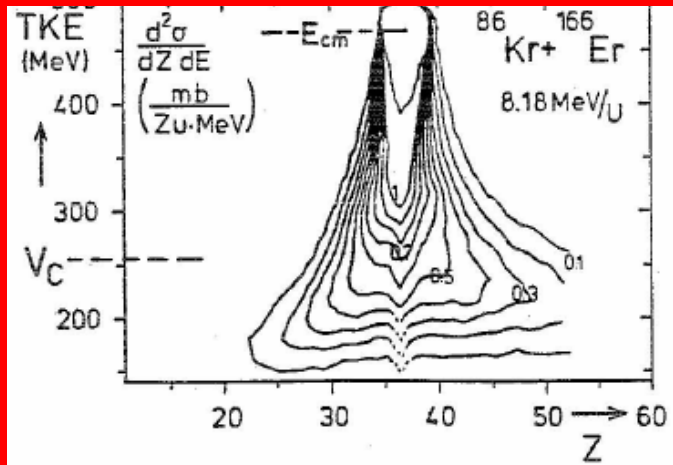


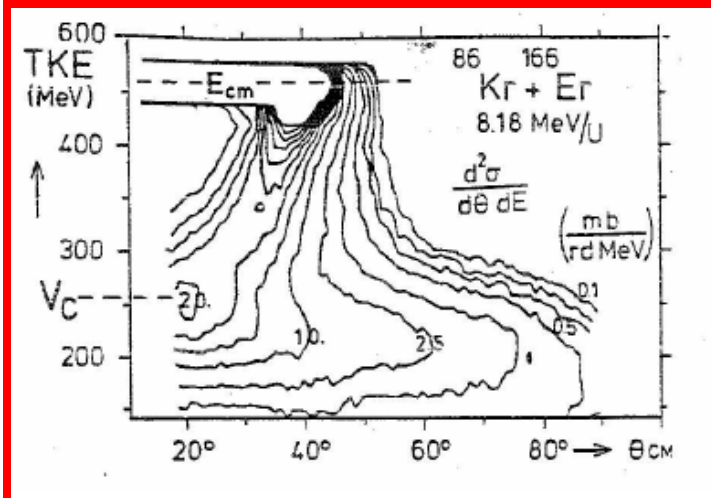
**Figure 39.** Schematic illustration of the  $l$  dependence of the partial cross section for compound-nucleus (CN), fusion-like (FL), damped (D), quasielastic (QE), Coulomb-excitation (CE), and elastic (EL) processes. The long-dashed line represents the geometrical partial cross section  $d\sigma/dl = 2\pi\lambda^2 l$ . Vertical dashed lines indicate the extensions of the various  $l$  windows in a sharp cutoff model with the characteristic  $l$  values noted at the abscissa. Hatched areas represent the diffuse  $l$  windows assumed in a smooth cutoff model.

# Deep inelastic collisions : macroscopic view

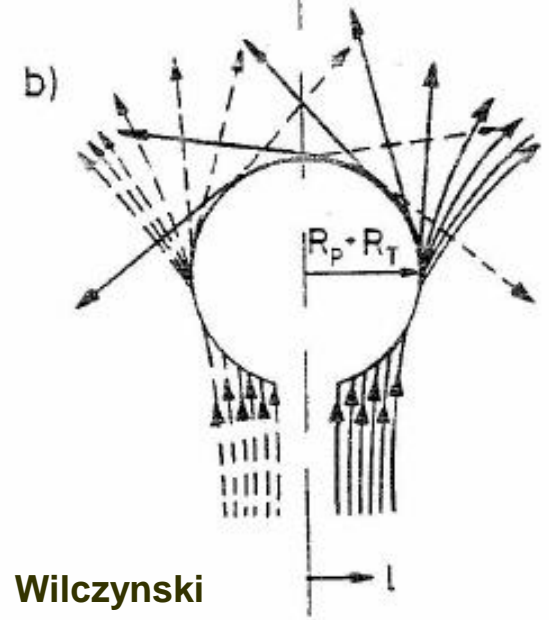
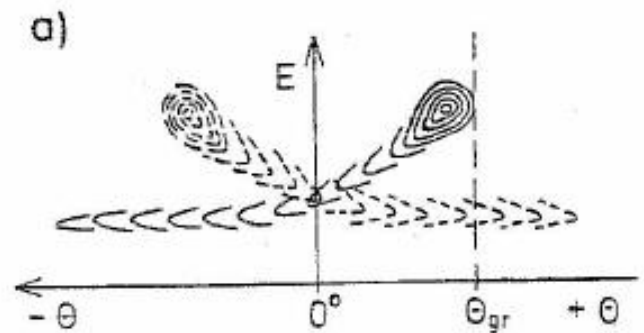
## diffusion effects on nucleons



## angular dependence of energy loss

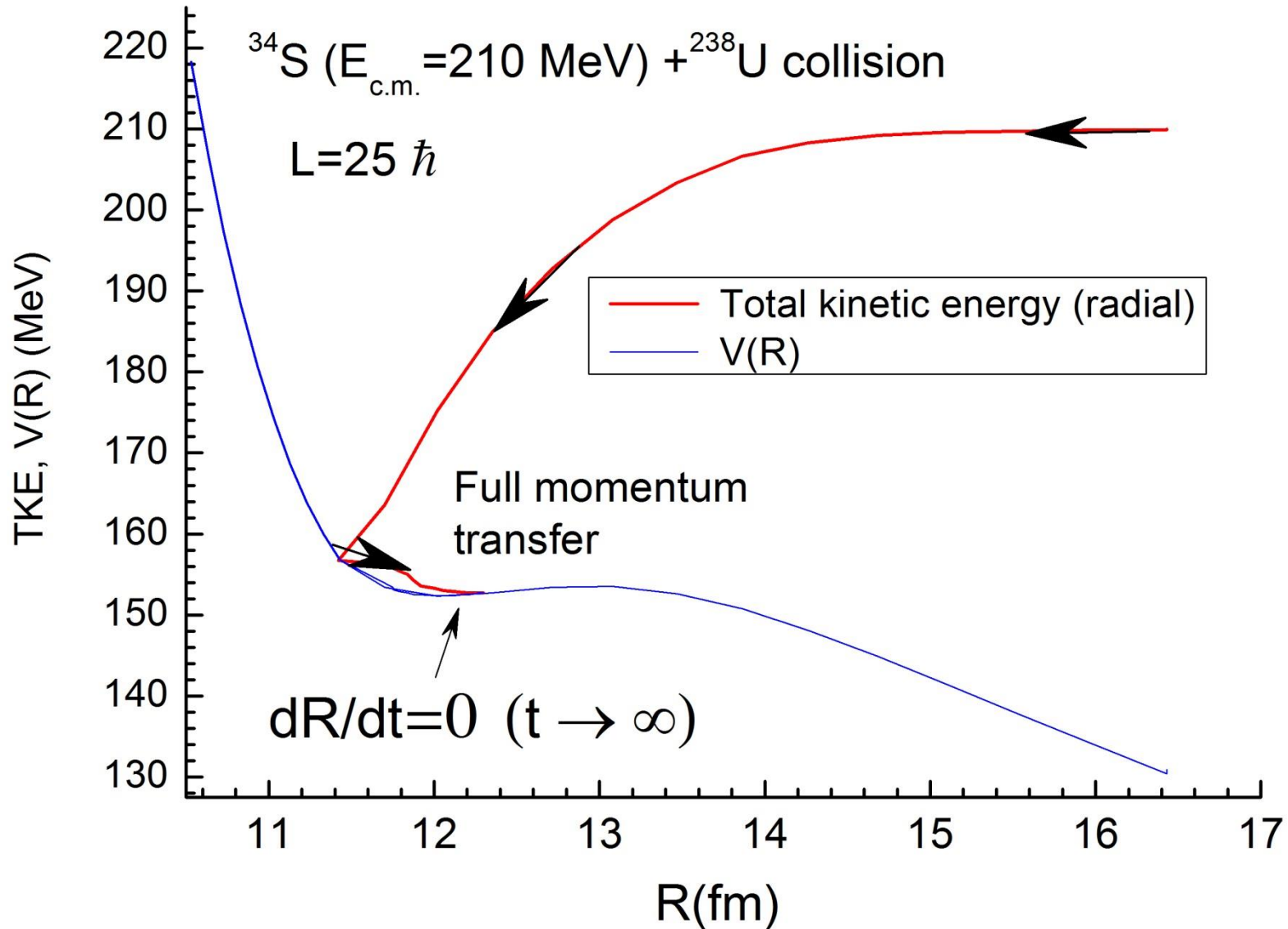


## concept of dinuclear system

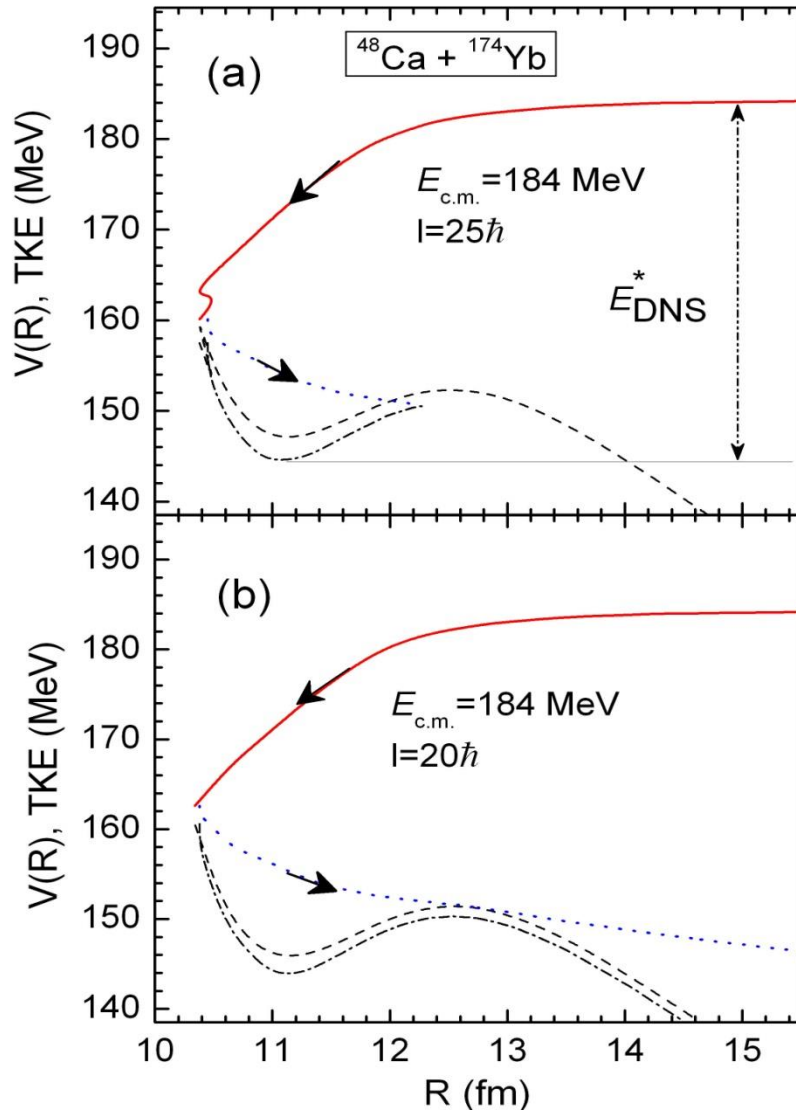


Wilczynski

# Capture event is full momentum transfer in the radial motion of colliding nuclei



# Difference between classical paths of the capture and deep inelastic collisions



TKE-total kinetic energy  
 $V(R)$  – nucleus-nucleus potential

$E_{\text{DNS}}^*$  – excitation energy of double nuclear system

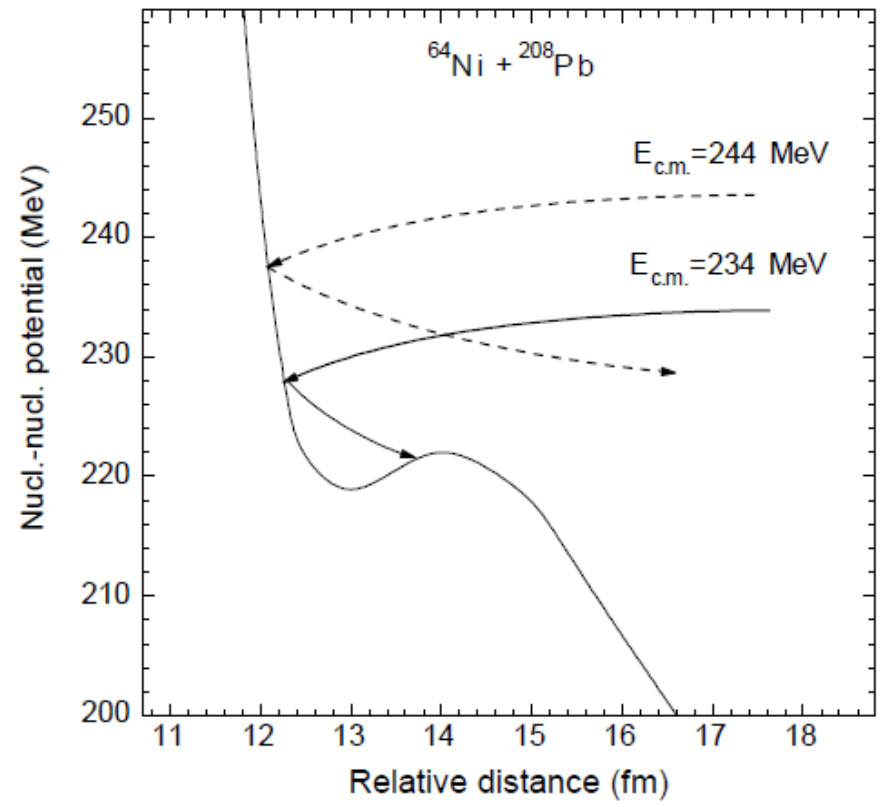
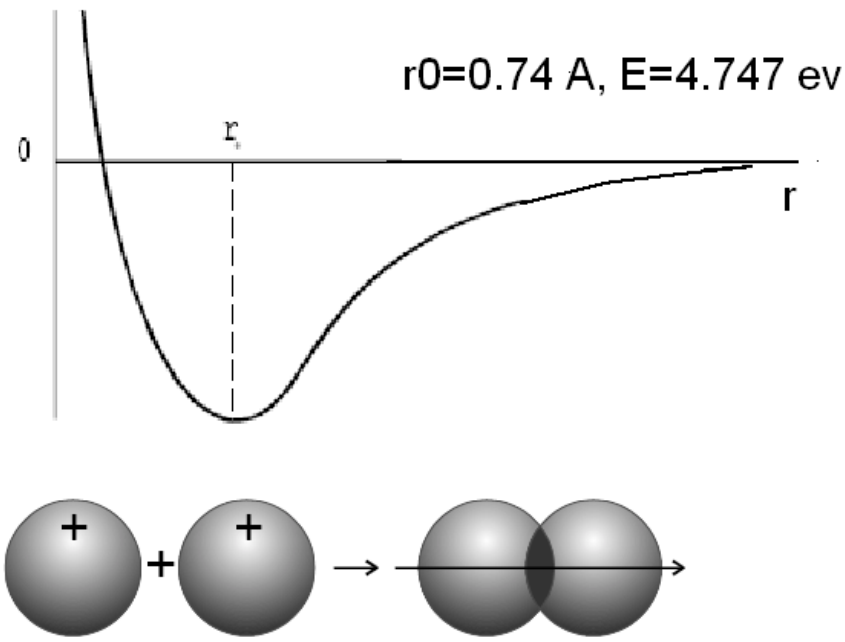
Full momentum transfer reactions

Capture=Fusion+Quasifission +Fast fission

Fusion=Fission+Evaporation residues

Fission >> Evaporation residues 20

# Interaction potential of the two hydrogen atoms H + H



- In the nucleus-nucleus interaction between nuclei of dinuclear system, their neutrons play the same role as the “valent” electrons in atomic interaction similar  $H + H \Rightarrow H_2$  molecule .
- Beam energy and strength of the radial friction forces determines capture probability, when  $E_{c.m.} > V_{Coulomb}$  . About  $V(R)$  we discuss later...

# Equations of motion used to find capture of projectile by target

$$\mu(R) \frac{d\dot{R}}{dt} + \gamma_R(R) \dot{R}(t) = - \frac{\partial V(R)}{\partial R} - \dot{R}^2 \frac{\partial \mu(R)}{\partial R}$$

$$L_0 = J_R \dot{\theta} + J_1 \dot{\theta}_1 + J_2 \dot{\theta}_2 ,$$

$$\frac{dL}{dt} = \gamma_\theta(R) R(t) \left[ \dot{\theta} R(t) - \dot{\theta}_1 R_{1eff} - \dot{\theta}_2 R_{2eff} \right]$$

$$E_{rot} = \frac{J_R \theta^2}{2} + \frac{J_1 \theta_1^2}{2} + \frac{J_2 \theta_2^2}{2}$$

## Nucleus-nucleus interaction potential

$$V_C(R, \alpha_1, \alpha_2) = \frac{Z_1 Z_2}{R} e^2 + \frac{Z_1 Z_2}{R^3} e^2 \left\{ \left( \frac{9}{20\pi} \right)^{1/2} \sum_{i=1}^2 R_{0i}^2 \beta_2^{(i)} P_2(\cos \alpha_i) + \frac{3}{7\pi} \sum_{i=1}^2 R_{0i}^2 \left[ \beta_2^{(i)} P_2(\cos \alpha_i) \right]^2 \right\}$$

$$V_{nucl}(R, \alpha_1, \alpha_2) = \int \rho_1^{(0)}(\vec{r} - \vec{R}) f_{eff} \left[ \rho_1^{(0)} + \rho_2^{(0)} \right] \rho_2^{(0)}(\vec{r}) d^3 \vec{r}$$

$$\rho_i^{(0)}(\vec{r}, \vec{R}_i, \alpha_i, \theta_i, \beta_2^{(i)}) = \left\{ 1 + \exp \left[ \frac{|\vec{r} - \vec{R}_i(t)| - R_{oi} (1 + \beta_2^{(i)} Y_{20}(\theta_i, \alpha_i))}{a} \right] \right\}^{-1}.$$

$$V_{rot} = \hbar^2 \frac{l(l+1)}{2\mu [R(\alpha_1, \alpha_2)]^2 + J_1 + J_2}$$

# Constants of the effective nucleon-nucleon interaction (Migdal forces)

$$\begin{aligned}\varepsilon_{FK}^{(Z)} &= \varepsilon_F \left[ 1 - \frac{2}{3} (1 + 2f'_K) \frac{\langle N_K \rangle - \langle Z_K \rangle}{\langle A_K \rangle} \right], \\ \varepsilon_{FK}^{(N)} &= \varepsilon_F \left[ 1 + \frac{2}{3} (1 + 2f'_K) \frac{\langle N_K \rangle - \langle Z_K \rangle}{\langle A_K \rangle} \right],\end{aligned}\tag{A.14}$$

where  $\varepsilon_F = 37$  MeV,

$$\begin{aligned}f_K &= f_{\text{in}} - \frac{2}{\langle A_K \rangle^{1/3}} (f_{\text{in}} - f_{\text{ex}}), \\ f'_K &= f'_{\text{in}} - \frac{2}{\langle A_K \rangle^{1/3}} (f'_{\text{in}} - f'_{\text{ex}})\end{aligned}\tag{A.15}$$

and  $f_{\text{in}} = 0.09$ ,  $f'_{\text{in}} = 0.42$ ,  $f_{\text{ex}} = -2.59$ ,  $f'_{\text{ex}} = 0.54$ ,  $g = 0.7$  are the constants of the effective nucleon–nucleon interaction.

A.B. Migdal, *Theory of the Finite Fermi—Systems and Properties of Atomic Nuclei*, Moscow, Nauka, 1983.



# About matrix elements for nucleon exchange between nuclei of dinuclear system

$$g_{PT}(\mathbf{R}) = \int d\mathbf{r} \Psi_T^*(\mathbf{r}) \quad (3)$$

$$\times \left[ \frac{1}{2} \{ U_T(\mathbf{r}) + U_P(\mathbf{r} - \mathbf{R}) \} \right] \Psi_P(\mathbf{r} - \mathbf{R}),$$

$$g_{PT}(R) = \frac{(-1)^{m_r - 1/2}}{16\pi^3} [(2j_P + 1)$$

$$\times (2j_T + 1)]^{1/2} \sum_L i^L \left( j_T - \frac{1}{2}, j_P \frac{1}{2} \middle| L 0 \right)$$

$$\times (j_T - m_T, j_P m_P \middle| L 0) \int_0^\infty dp p^2 j_L(pR)$$

$$\times \left[ \left\{ \varepsilon_P - \frac{\hbar^2}{2m} p^2 \right\} + \left\{ \varepsilon_T - \frac{\hbar^2}{2m} p^2 \right\} \right] \varphi_{l_T}^*(p) \varphi_{l_P}(p).$$

Expressions for the friction coefficients

$$\gamma_R(R(t)) = \sum_{i,i'} \left| \frac{\partial V_{ii'}(R(t))}{\partial R} \right|^2 B_{ii'}^{(1)}(t), \quad (\text{B.1})$$

$$\gamma_\theta(R(t)) = \frac{1}{R^2} \sum_{i,i'} \left| \frac{\partial V_{ii'}(R(t))}{\partial \theta} \right|^2 B_{ii'}^{(1)}(t), \quad (\text{B.2})$$

and the dynamic contribution to the nucleus-nucleus potential

$$\delta V(R(t)) = \sum_{i,i'} \left| \frac{\partial V_{ii'}(R(t))}{\partial R} \right|^2 B_{ii'}^{(0)}(t), \quad (\text{B.3})$$

$$B_{ik}^{(n)}(t) = \frac{2}{\hbar} \int_0^t dt' (t - t')^n \exp\left(\frac{t' - t}{\tau_{ik}}\right) \\ \times \sin[\omega_{ik}(\mathbf{R}(t'))(t - t')] [\tilde{n}_k(t') - \tilde{n}_i(t')], \quad (\text{B.4})$$

$$\hbar\omega_{ik} = \epsilon_i + \Lambda_{ii} - \epsilon_k - \Lambda_{kk}. \quad (\text{B.5})$$

# Relaxation time of the occupation numbers of single-particle states

$$\frac{1}{\tau_i^{(\alpha)}} = \frac{\sqrt{2}\pi}{32\hbar\varepsilon_{F_K}^{(\alpha)}} \left[ (f_K - g)^2 + \frac{1}{2}(f_K + g)^2 \right] \\ \times \left[ \left( \pi T_K \right)^2 + \left( \tilde{\varepsilon}_i - \lambda_K^{(\alpha)} \right)^2 \right] \left[ 1 + \exp\left( \frac{\lambda_K^{(\alpha)} - \tilde{\varepsilon}_i}{T_K} \right) \right]^{-1}, \quad (\text{A.1})$$

where

$$T_K(t) = 3.46 \sqrt{\frac{E_K^*(t)}{\langle A_K(t) \rangle}} \quad (\text{A.2})$$

# Change of single-particle energies and transition matrix elements of nucleons

$$\tilde{\varepsilon}_P(\mathbf{R}(t)) = \varepsilon_P + \langle P | U_T(\mathbf{r}) | P \rangle,$$

$$\tilde{\varepsilon}_T(\mathbf{R}(t)) = \varepsilon_T + \langle T | U_P(\mathbf{r} - \mathbf{R}(t)) | T \rangle,$$

$$\chi_{PP'}^{(T)}(\mathbf{R}(t)) = \langle P | U_T(\mathbf{r}) | P' \rangle,$$

$$\chi_{TT'}^{(P)}(\mathbf{R}(t)) = \langle T | U_P(\mathbf{r} - \mathbf{R}(t)) | T' \rangle,$$

$$g_{PT}(\mathbf{R}(t)) = \frac{1}{2} \langle P | U_P(\mathbf{r} - \mathbf{R}(t)) + U_T(\mathbf{r}) | T \rangle.$$

$$P \equiv (n_P, j_P, l_P, m_P) \text{ and } \tilde{T} \equiv (n_T, j_T, l_T, \dot{m}_T)$$

# Partial cross sections of compound nucleus (CN), fusion-like (FL), damped (D), quasielastic (QE), Coulomb-excitation (CE), and elastic (EL) processes.

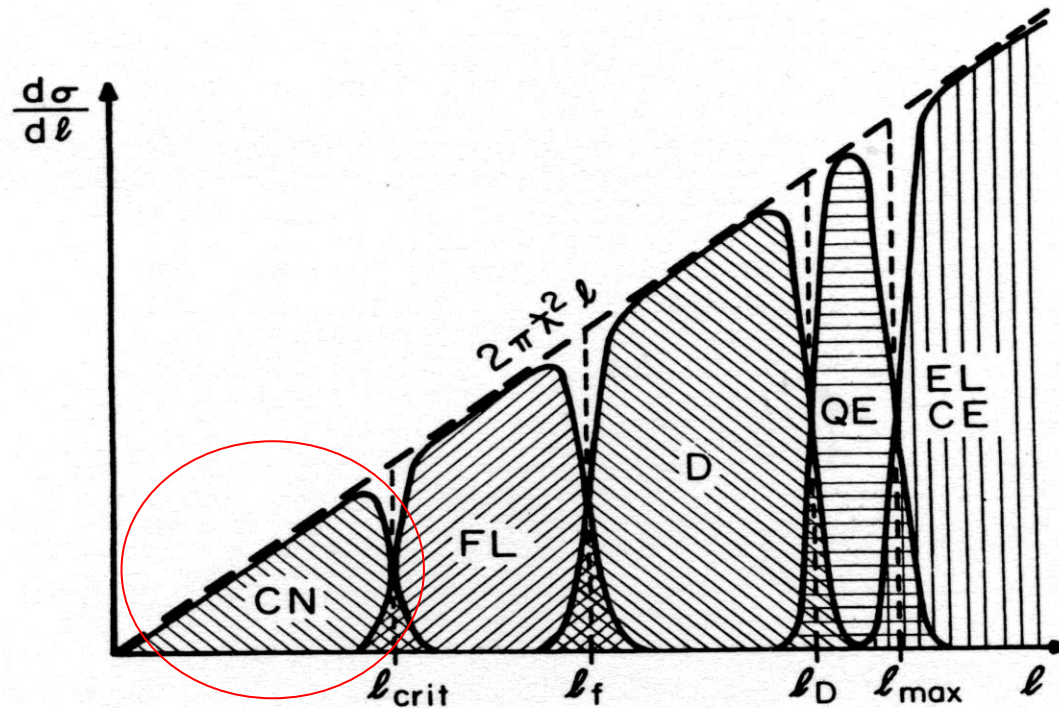
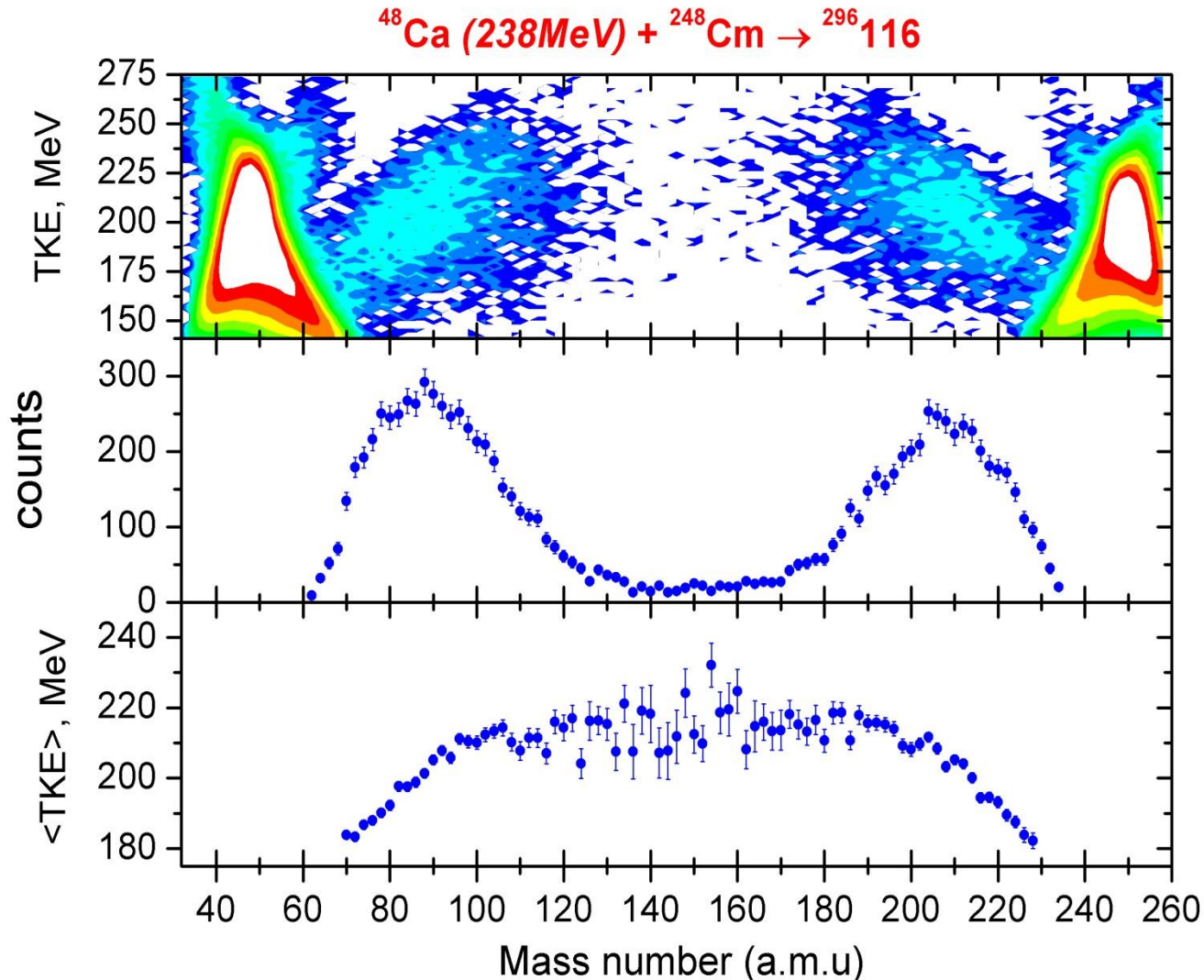


**Figure 39.** Schematic illustration of the  $l$  dependence of the partial cross section for compound-nucleus (CN), fusion-like (FL), damped (D), quasielastic (QE), Coulomb-excitation (CE), and elastic (EL) processes. The long-dashed line represents the geometrical partial cross section  $d\sigma/dl = 2\pi\lambda^2 l$ . Vertical dashed lines indicate the extensions of the various  $l$  windows in a sharp cutoff model with the characteristic  $l$  values noted at the abscissa. Hatched areas represent the diffuse  $l$  windows assumed in a smooth cutoff model.

Mass-energetic distribution of the binary products in heavy ion collisions. The N=126 and Z=82 magic numbers responsible for the maximum of quasifission fragments



# Competition between fusion-fission and quasifission processes in the $^{32}\text{S} + ^{184}\text{W}$ reaction

H. Q. Zhang,<sup>\*</sup> C. L. Zhang, C. J. Lin, Z. H. Liu, and F. Yang

*China Institute of Atomic Energy, Post Office Box 275, Beijing 102413, People's Republic of China*

A. K. Nasirov<sup>†</sup>

*Joint Institute for Nuclear Research, RU-141980 Dubna, Russia*

G. Mandaglio, M. Manganaro, and G. Giardina

*Dipartimento di Fisica dell' Università di Messina, 98166 Messina, and Istituto Nazionale di Fisica Nucleare, Sezione di Catania, Italy*

(Received 5 June 2009; revised manuscript received 21 February 2010; published 24 March 2010)

$$\sigma_{\text{ER}}(E) = \sum_{l=0}^{\infty} (2l + 1) \sigma_{\text{fus}}^{(l)}(E) W_{\text{sur}}(E, l). \quad (1)$$

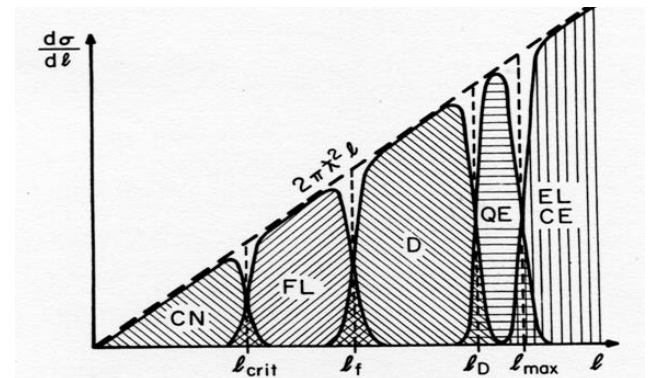
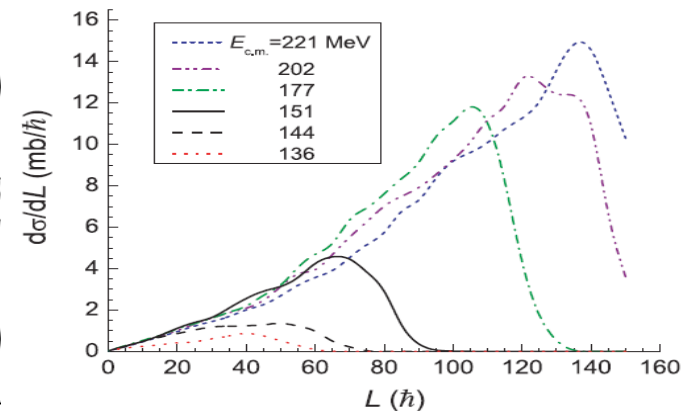
The entrance channel effects can be studied [16] by analyzing the partial fusion cross section  $\sigma_{\text{fus}}^{(l)}(E)$ , which is defined by the expression

$$\sigma_{\text{fus}}^{(l)}(E) = \sigma_{\text{capture}}^{(l)}(E) P_{\text{CN}}(E, l). \quad (2)$$

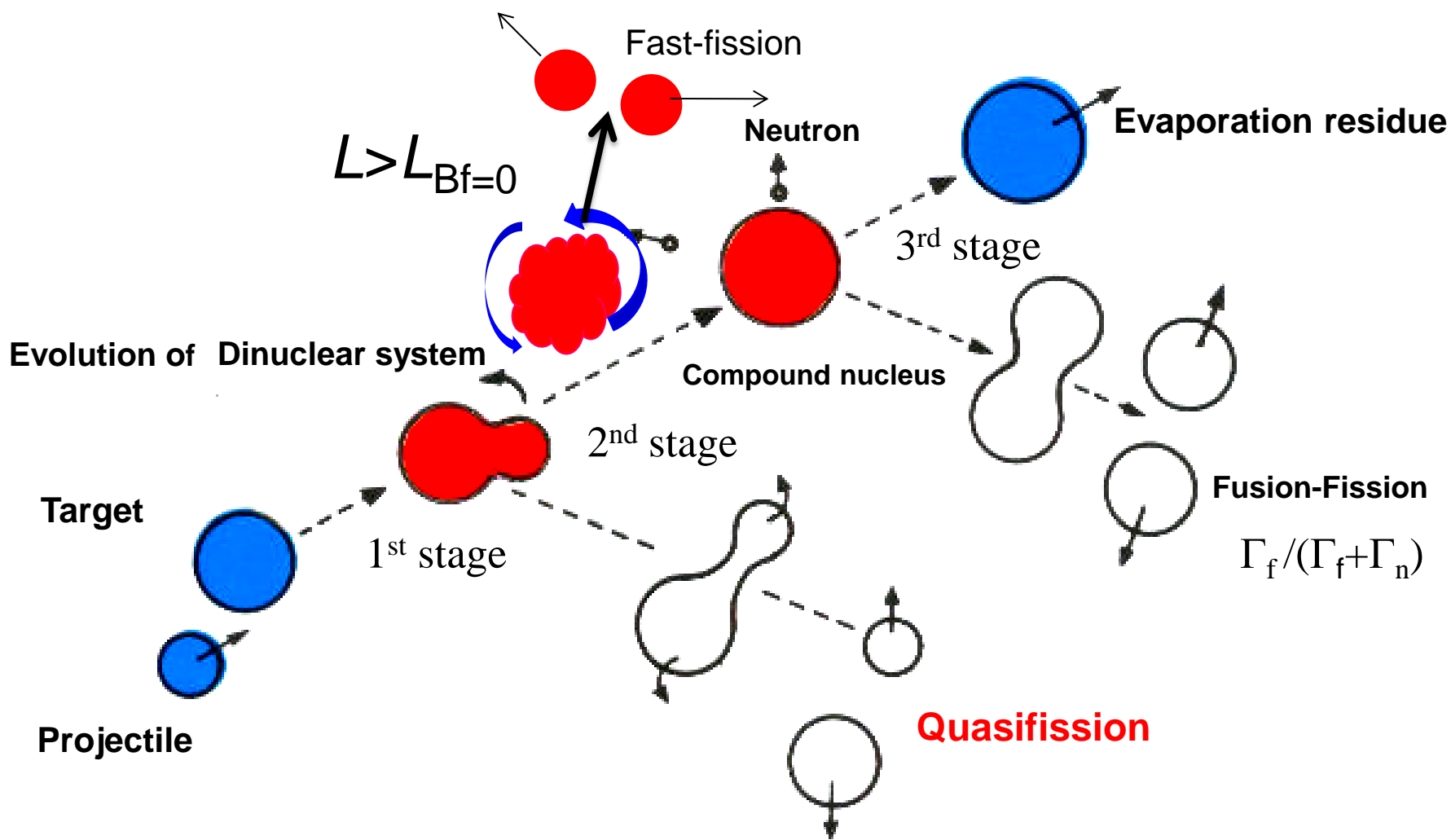
The theoretical cross section for capture includes the contributions of all fragment yields from full momentum transfer reactions:

$$\begin{aligned} \sigma_{\text{cap}}(E_{\text{c.m.}}) = & \sigma_{\text{ER}}(E_{\text{c.m.}}) + \sigma_{\text{f}}(E_{\text{c.m.}}) + \sigma_{\text{qf}}(E_{\text{c.m.}}) \\ & + \sigma_{\text{fast fission}}(E_{\text{c.m.}}), \end{aligned} \quad (3)$$

where  $\sigma_{\text{ER}}$ ,  $\sigma_{\text{f}}$ ,  $\sigma_{\text{qf}}$ , and  $\sigma_{\text{fast fission}}$  are the evaporation residue, fusion-fission, quasifission, and fast-fission cross sections, respectively.



For heavy systems, capture inside of the Coulomb barrier, i.e. formation of a dinuclear system is not the sufficient condition for fusion:

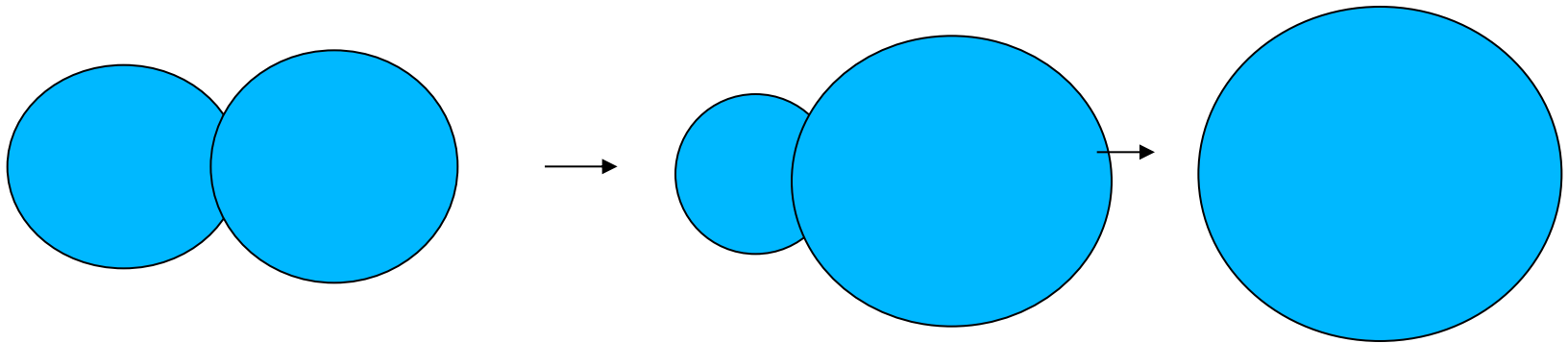


**Capture = Quasifission + Fast-fission + Fusion-Fission + Evaporation residues**



# Fusion of light nuclei

Light nuclei are fused similar drops of liquid Because Coulomb forces are not so strong relative to the nuclear forces and the surface tension energy is much large than shell correction in nuclei, Capture process is nearly equal to complete fusion: dinuclear system stahe is very short.



# Models of complete fusion with adiabatic and diabatic potentials

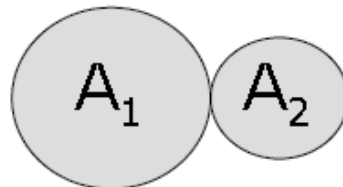
Two main collective coordinates are used for the description of the fusion process:

1. Relative internuclear distance  $R$
2. Mass asymmetry coordinate  $\eta$  for transfer

Idea of Volkov (Dubna) to describe fusion reactions with the dinuclear system concept:

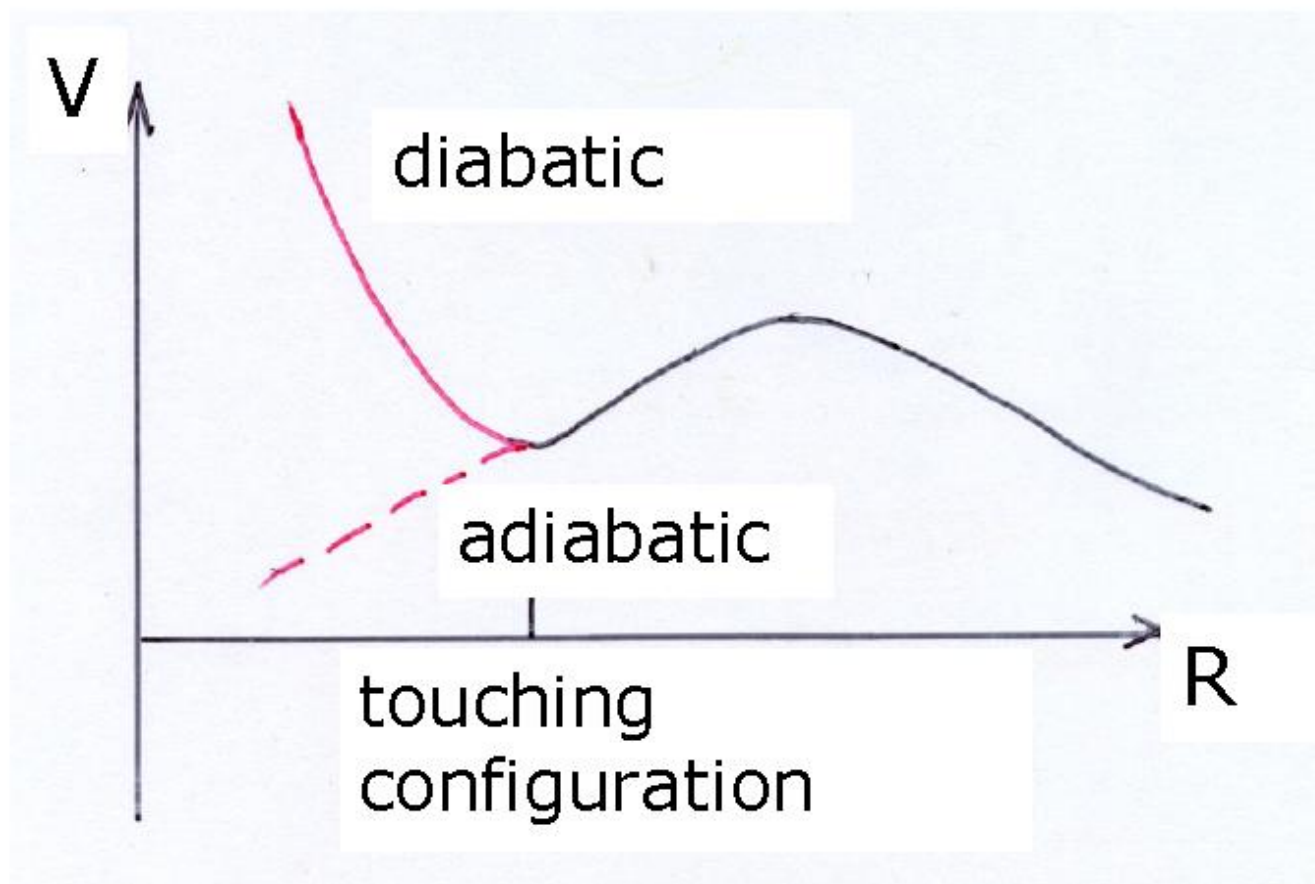
Fusion is assumed as a **transfer of nucleons** (or clusters) from the lighter nucleus to the heavier one in a dinuclear configuration.

This process is describable with the mass asymmetry coordinate  $\eta = (A_1 - A_2) / (A_1 + A_2)$ .



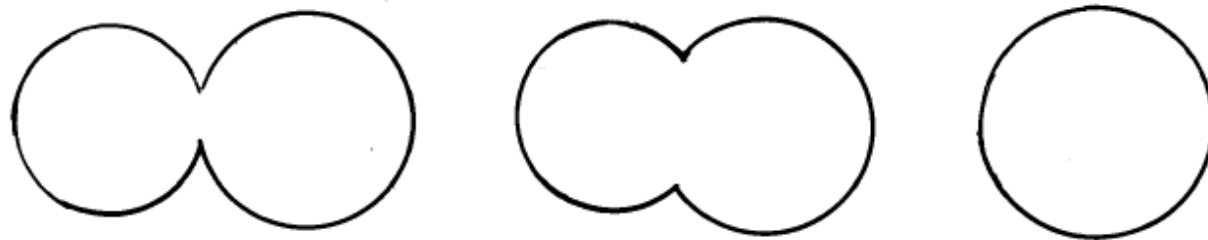
If  $A_1$  or  $A_2$  get small, then  $|\eta| \rightarrow 1$  and the system fuses.

Description of fusion dynamics depends strongly whether adiabatic or diabatic potential energy surfaces are assumed.



## a) Models using adiabatic potentials

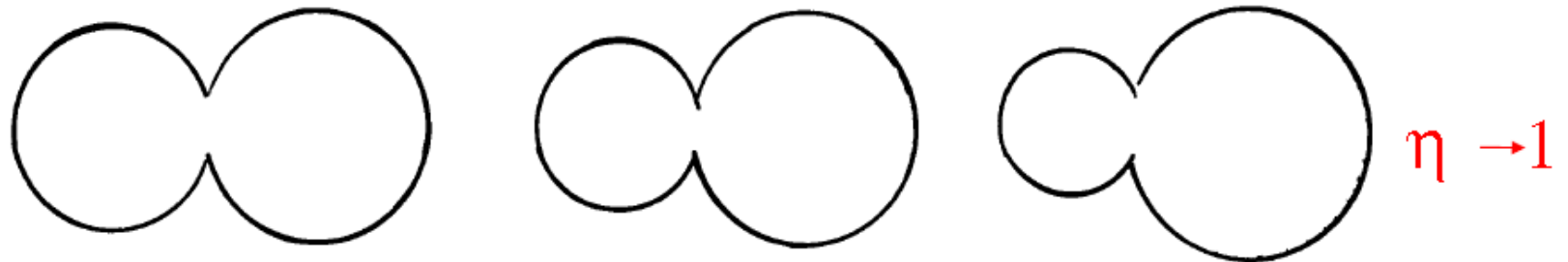
Minimization of potential energy, essentially adiabatic dynamics in the internuclear distance, nuclei melt together.



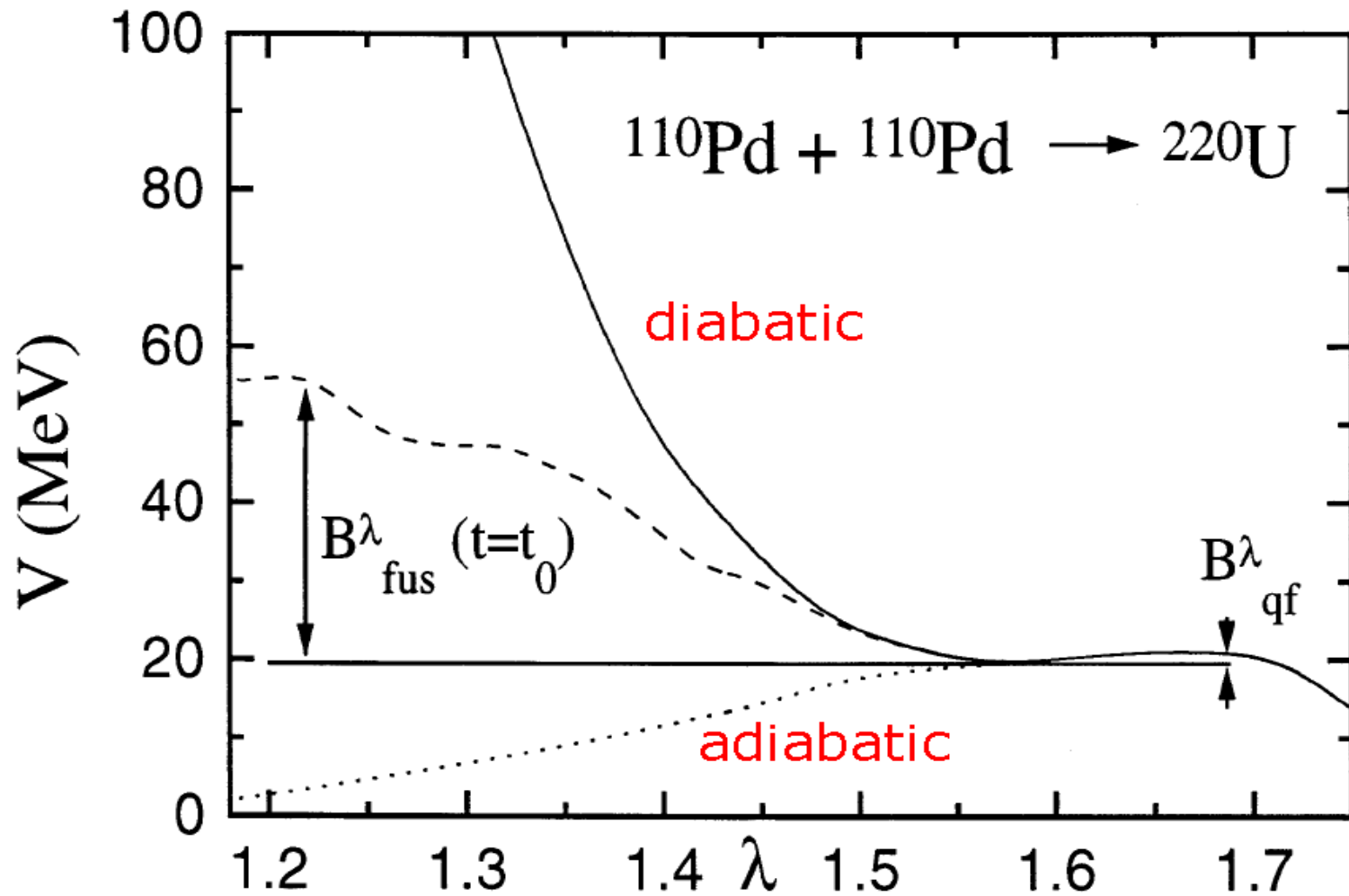
Large probabilities of fusion for producing nuclei with similar projectile and target nuclei.

## b) Dinuclear system (DNS) concept

Fusion by transfer of nucleons between the nuclei (idea of V. Volkov, also von Oertzen), mainly dynamics in mass asymmetry degree of freedom, use of diabatic potentials, e.g. calculated with the diabatic two-center shell model.

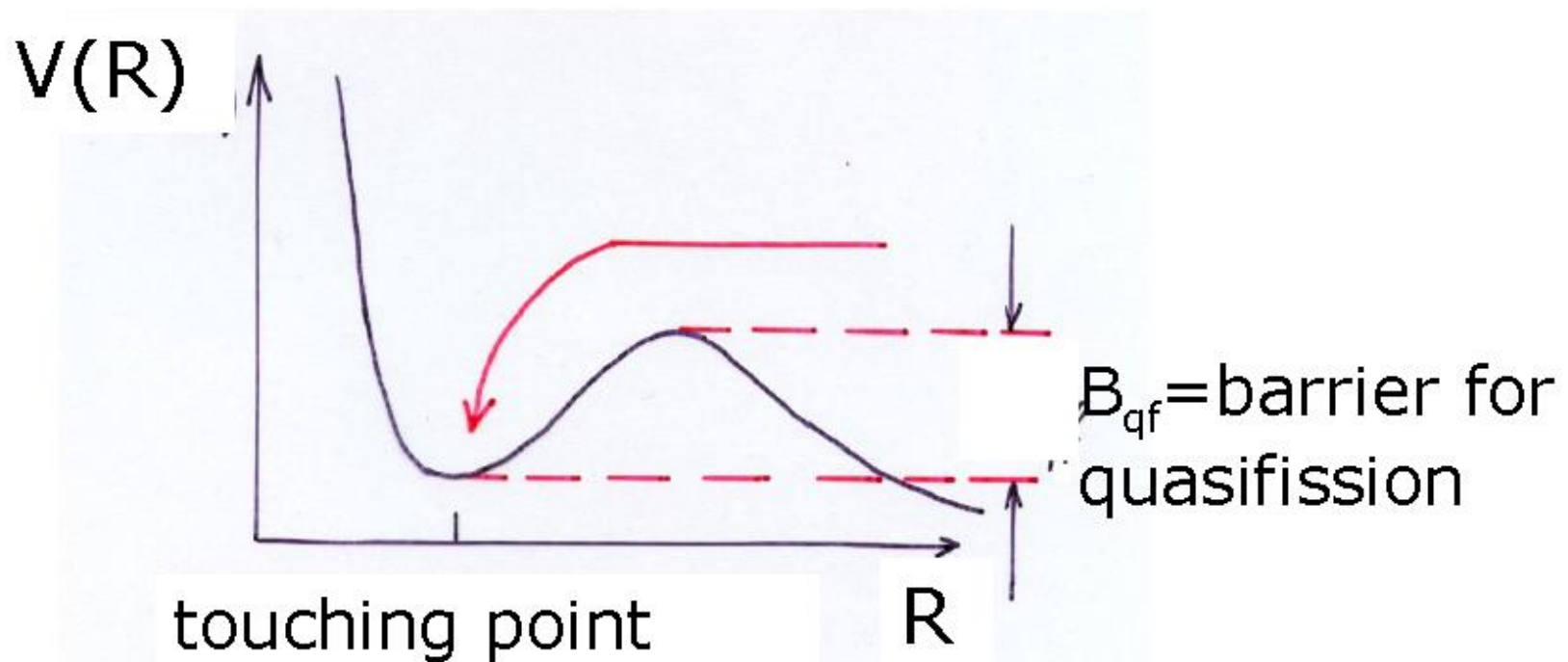


# Hindrance to complete fusion in the symmetric reactions.



a) Partial capture cross section  $\sigma_{\text{cap}}$

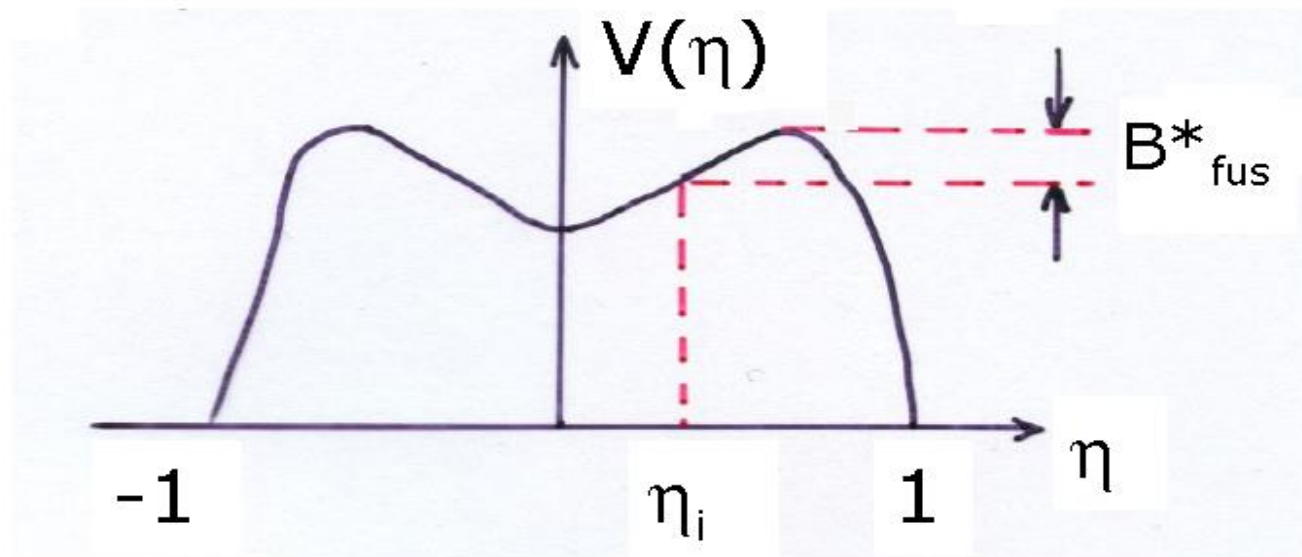
Dinuclear system is formed at the initial stage of the reaction, kinetic energy is transferred into potential and excitation energy.



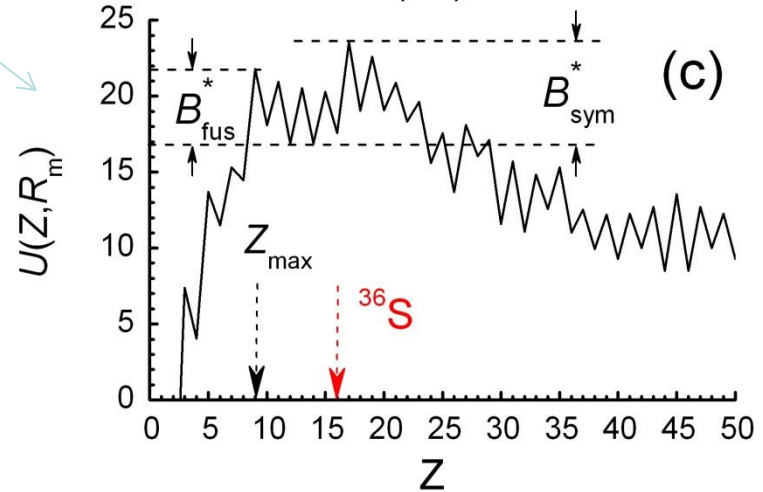
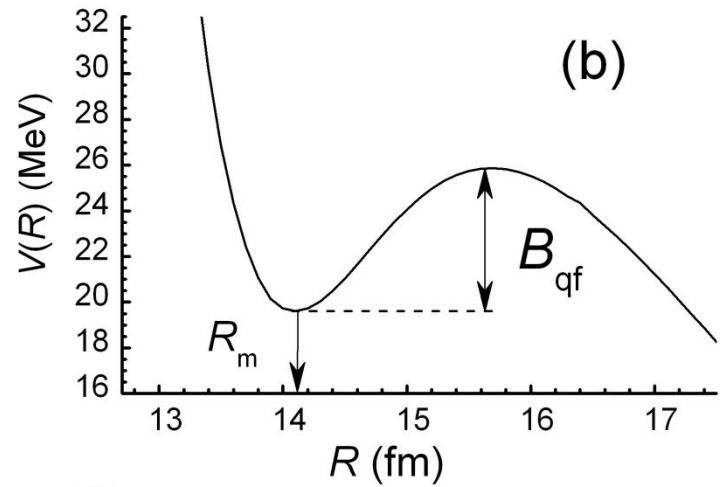
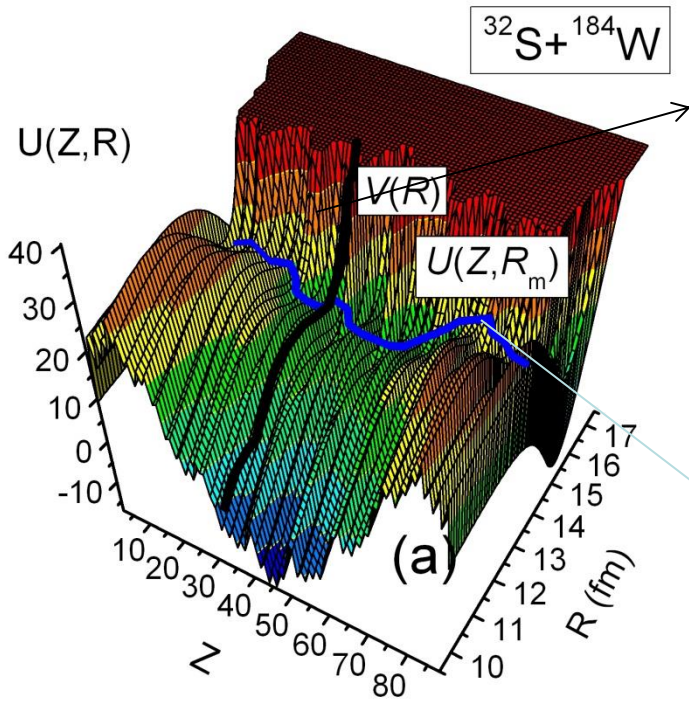


## b) Probability for complete fusion $P_{CN}$

DNS evolves in mass asymmetry coordinate by diffusion processes toward fusion and in the relative coordinate toward the decay of the dinuclear system which is quasifission.



$B_{fus}^*$  = inner fusion barrier



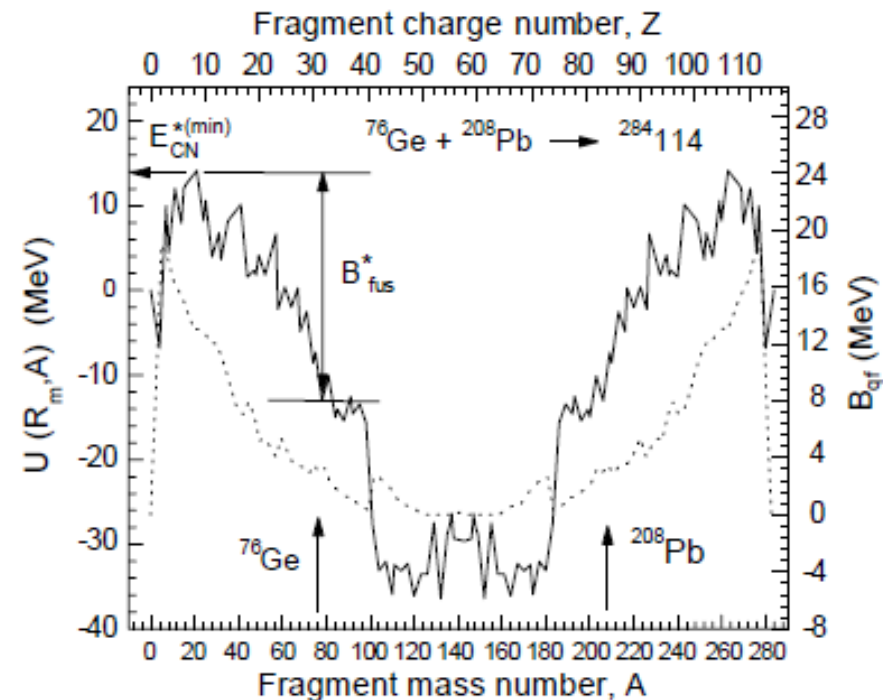
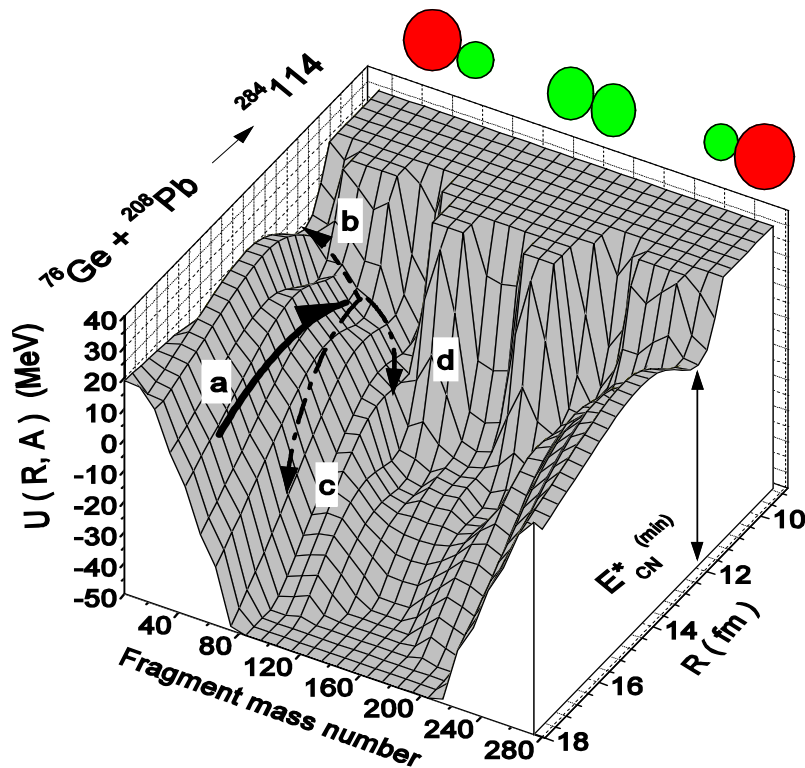
$$U(R, Z, A) = V(R, Z, A) + Q_{gg}(Z, A)$$

$$U_{dr}(R_{\min}, Z, A) = U(R = R_{\min}, Z, A) \quad [8]$$

$$Q_{gg}(Z, A) = B_1(Z_1, A_1) + B_2(Z_2, A_2) - B_{CN}(Z_{tot}, A_{tot})$$

$Q_{gg}$  – balance of reaction energy     $B$  – binding energy

# Potential energy surface of dinuclear



**a-** entrance channel;  
**b-** fusion channel;  
**c** and **d** are quasifission channels

G. Giardina, S. Hofmann, A.I. Muminov, and A.K. Nasirov,  
 Eur. Phys. J. A **8**, 205–216 (2000)

$$U_{dr}(A, Z, \beta_1, \beta_2) = B_1 + B_2 + V(A, Z, \beta_1; \beta_2; R) - B_{CN} - V_{CN}(L)$$

## Nucleus-nucleus interaction potential

$$V(R, Z, A, l, \beta) = V_{nuc}(R, A, \beta) + V_{coul}(R, Z, \beta) + V_{rot}(R, l, \beta)$$

$V_{nuc}$  – nuclear part

$V_{coul}$  – coulomb part

$V_{rot}$  – rotational energy

$R$  – distance between centers of two nuclei

$Z$  – charge number,  $A$  – mass number

$\beta$  – deformation parameter

$l$  – angular momentum of nucleus

$$V(R, Z, A) = V_{nuc}(R, A) + V_{coul}(R, Z)$$

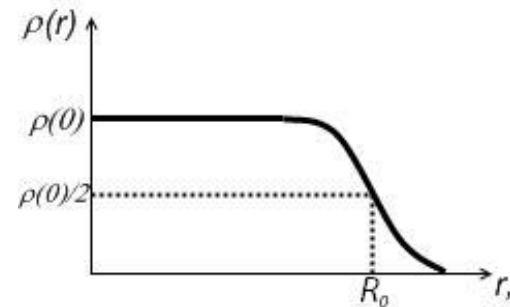
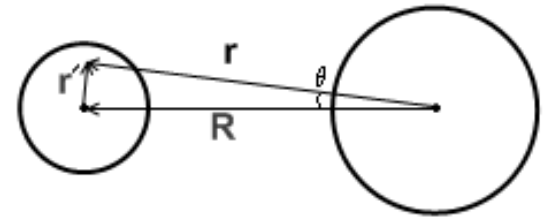
As nucleus-nucleus potential used  
double folding potential

$$V_{nuc}(R) = \int \rho_1(r') f_{eff}[\rho(r, r')] \rho_2(r) dr$$

$\mathbf{r}' = \mathbf{r} - \mathbf{R}$       $\rho_i$  – density function of  $i$  – nucleus

As  $\rho$  used the **Fermi distribution**:

$$\rho(r) = \frac{\rho_0}{1 + \exp\left(\frac{r - R_0}{a}\right)}$$



$$f_{eff}[\rho(\mathbf{r}, \mathbf{R})] = C \left[ f_{in} + (f_{ex} - f_{in}) \frac{\rho_0 - \rho(r, r')}{\rho_0} \right] - \text{effective nucleon-nucleon potential}$$

$$\rho(r, r') = \rho_1(r) + \rho_2(r') \quad R_0 = r_0 A^{1/3} - \text{nuclear radius, } \rho(R_0) = \rho_0 / 2$$

$$f_{in} = 0.09, f_{ex} = -2.59 - \text{constants of effective nucleon-nucleon potential}$$

$$C = 300 \text{ MeV} \cdot \text{fm}^3 - \text{interaction coefficient} \quad r_0 = 1.16 \div 1.18 \text{ fm}$$

$$\rho_0 = 0.17 \text{ fm}^{-3} - \text{density in center of nucleus}$$

$$a = 0.54 \text{ fm} - \text{diffuseness parameter}$$

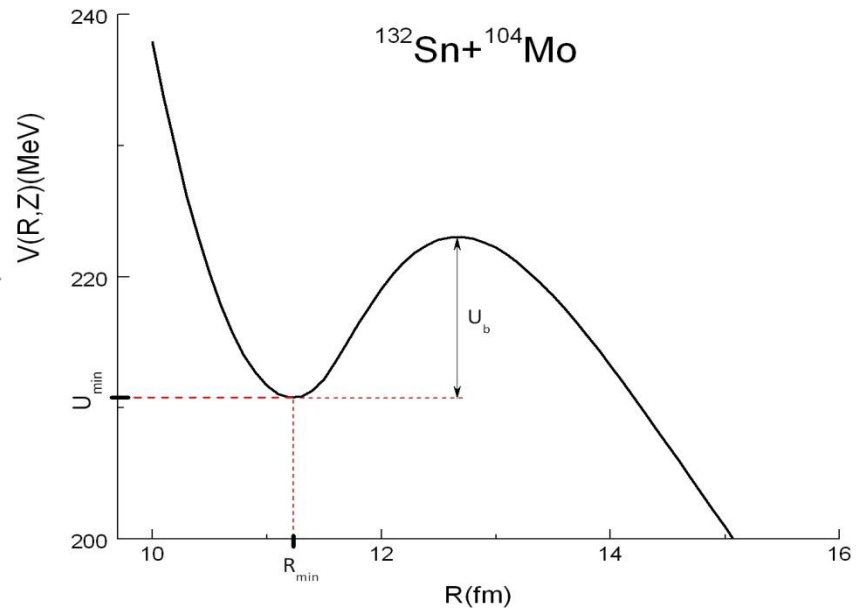
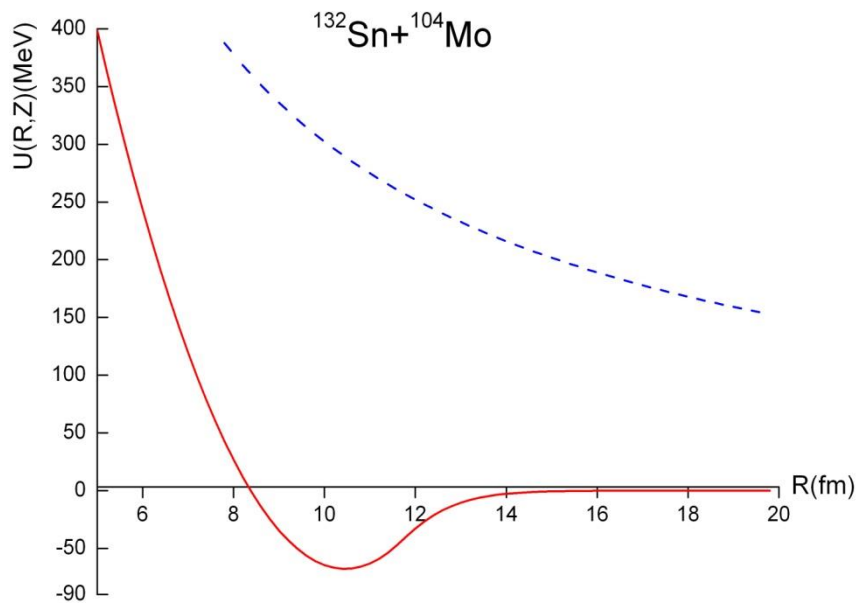
$$V_{nuc}(R) = \int \frac{\rho_0}{1 + \exp\left(\frac{r' - R_{01}}{a}\right)} C \left[ f_{in} + (f_{ex} - f_{in}) \frac{\rho_0 - \rho(r, r')}{\rho_0} \right] \frac{\rho_0}{1 + \exp\left(\frac{r - R_{02}}{a}\right)} d\mathbf{r}$$

$$V_{nuc}(R) = 2\pi\rho_0^2 C \int_0^R r^2 dr \int_0^\pi \frac{\left[ f_{in} + (f_{ex} - f_{in}) \frac{\rho_0 - \rho(r, r')}{\rho_0} \right]}{\left[ 1 + \exp\left(\frac{r' - R_{01}}{a}\right) \right] \left[ 1 + \exp\left(\frac{r - R_{02}}{a}\right) \right]} \sin\theta d\theta$$

Coulomb potential is of this form:

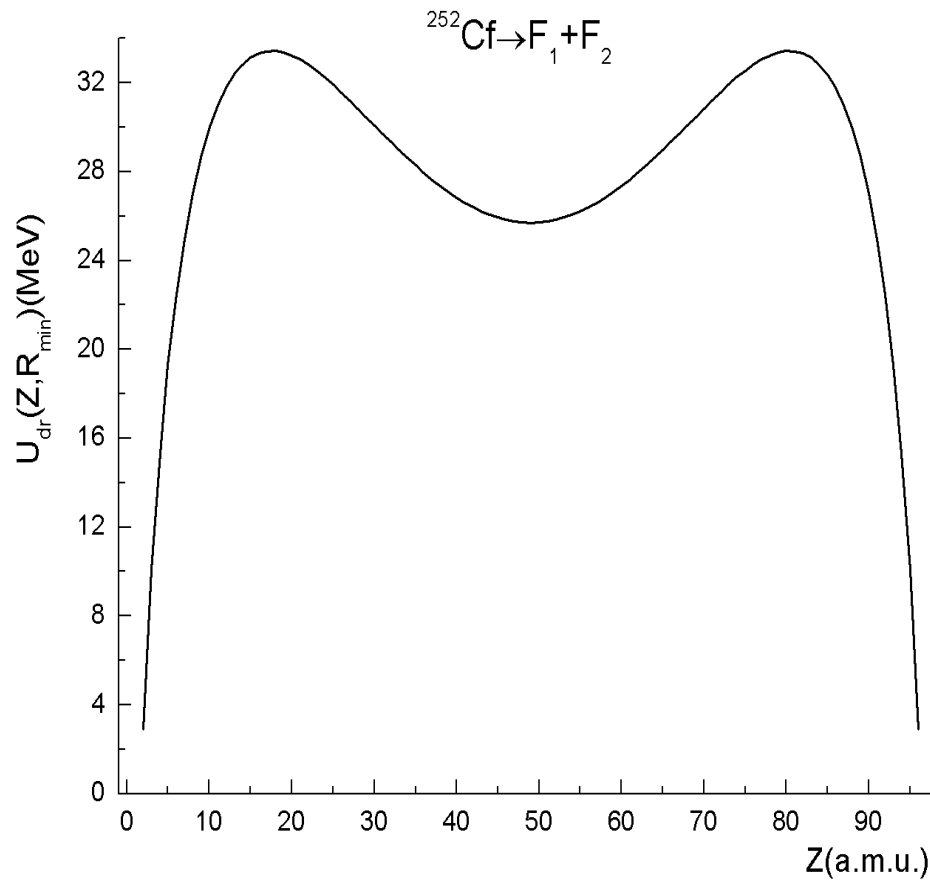
$$V_{coul}(R, Z_1, Z_2)[MeV] = 1.44 \frac{Z_1 Z_2}{R[fm]}$$

Thereby, we obtain following pictures for nucleus-nucleus potential:

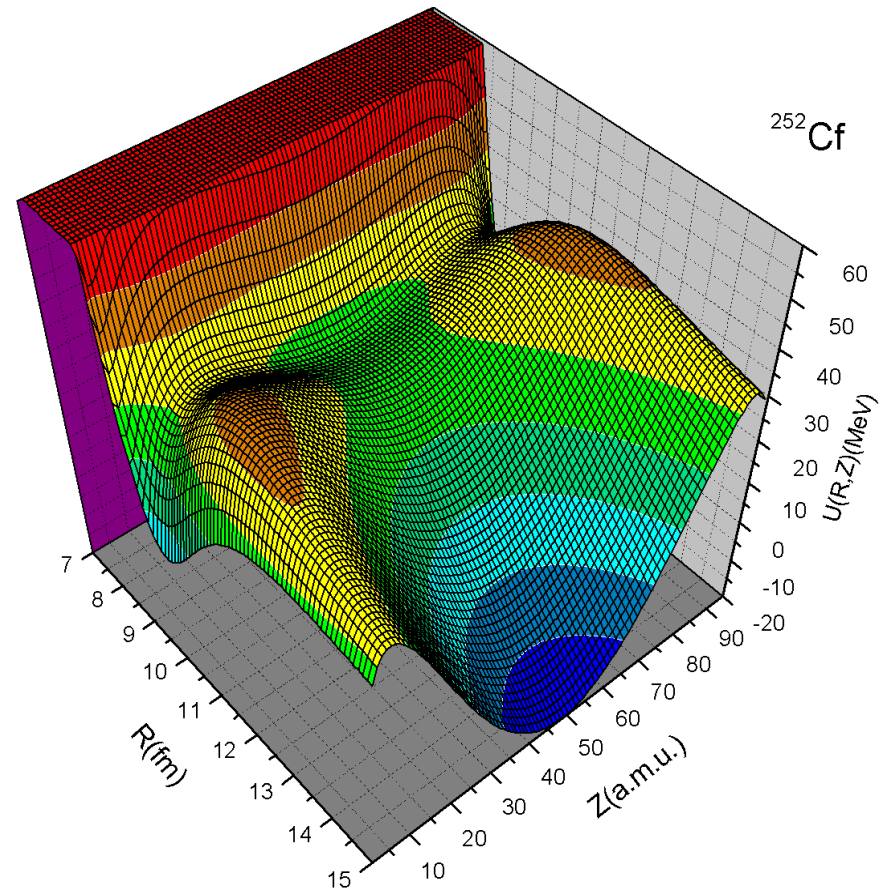


# Results of calculation

Driving potential for  $^{252}\text{Cf}(\text{sf})$   
within liquid drop model

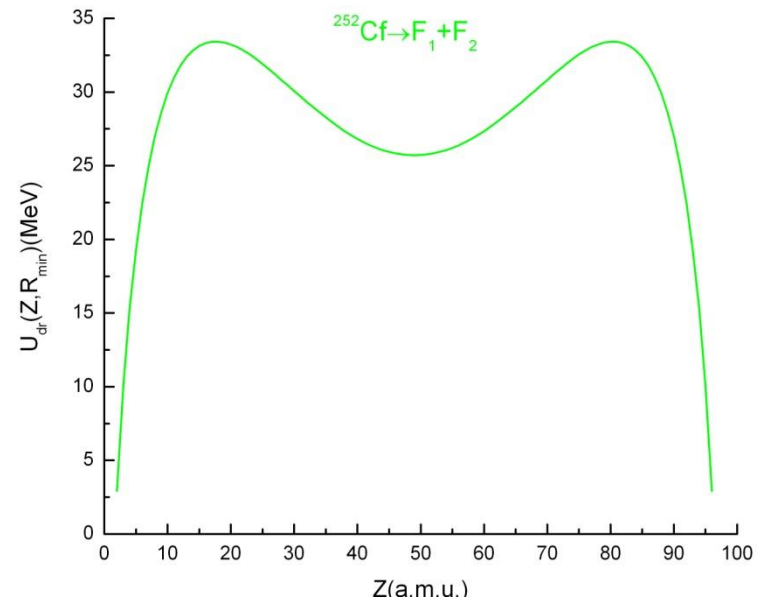
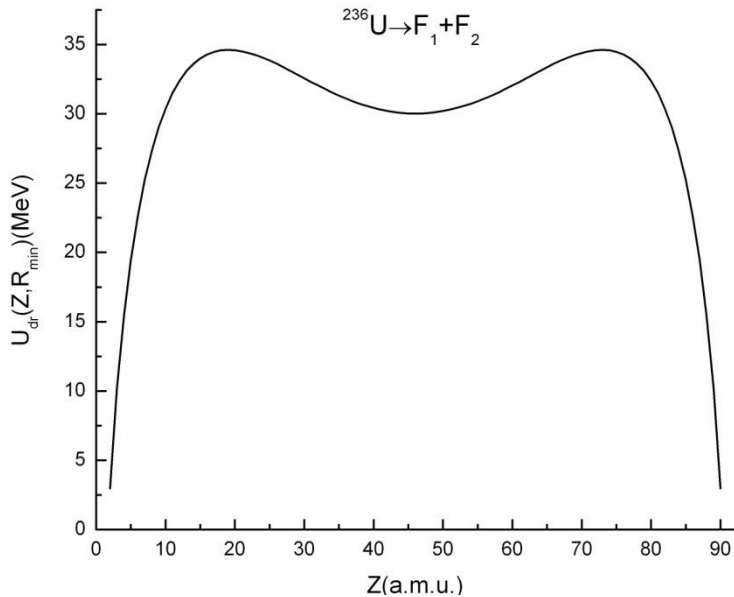
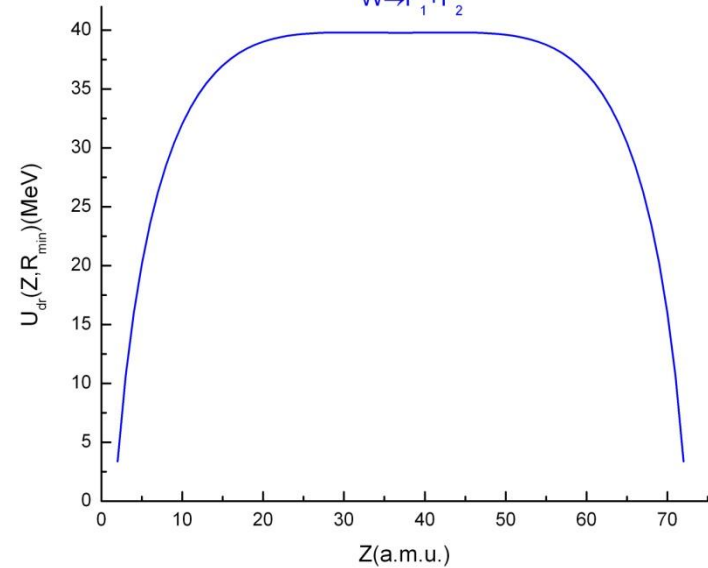
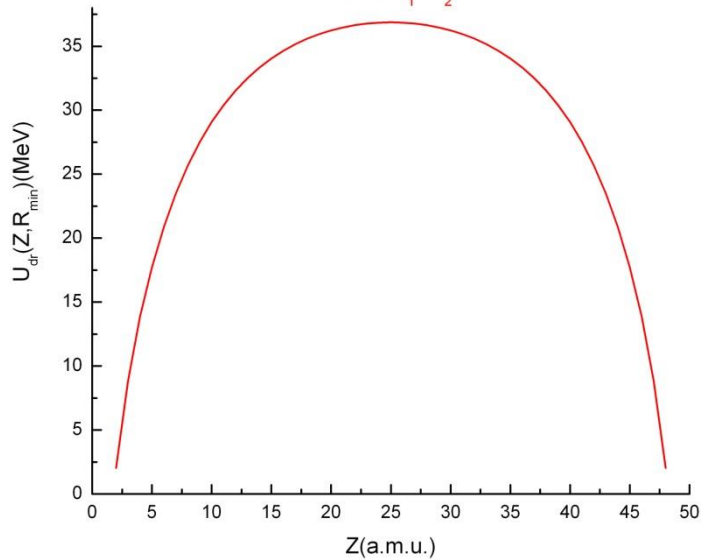


Potential energy surface for  
 $^{252}\text{Cf}(\text{sf})$  within liquid drop model



# Driving potential within the liquid drop model

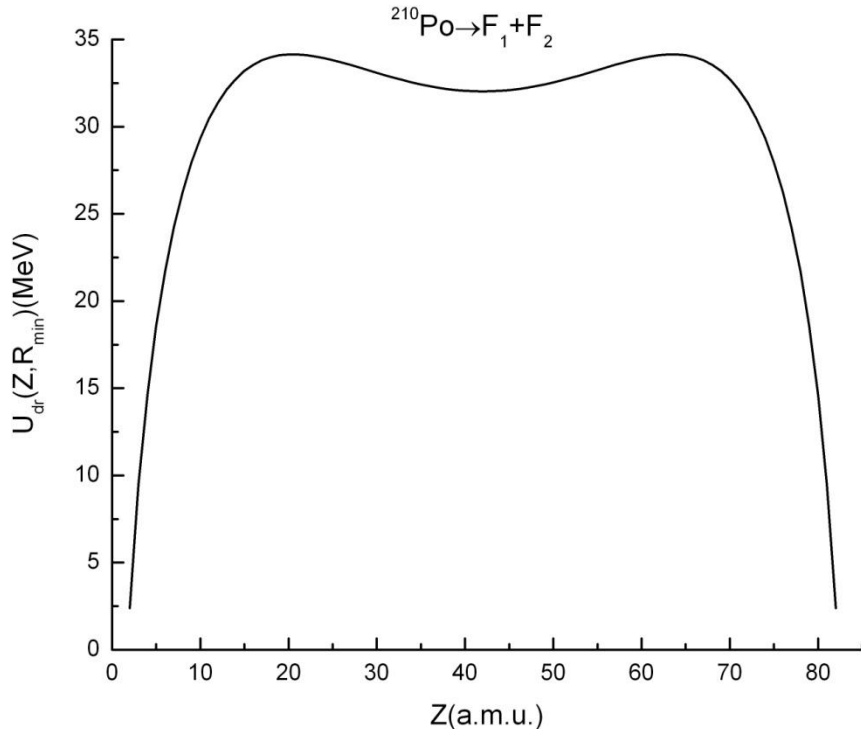
for  $^{120}\text{Sn}$ ,  $^{190}\text{W}$ ,  $^{236}\text{U}$  and  $^{252}\text{Cf}$   
 $^{120}\text{Sn} \rightarrow F_1 + F_2$        $^{190}\text{W} \rightarrow F_1 + F_2$





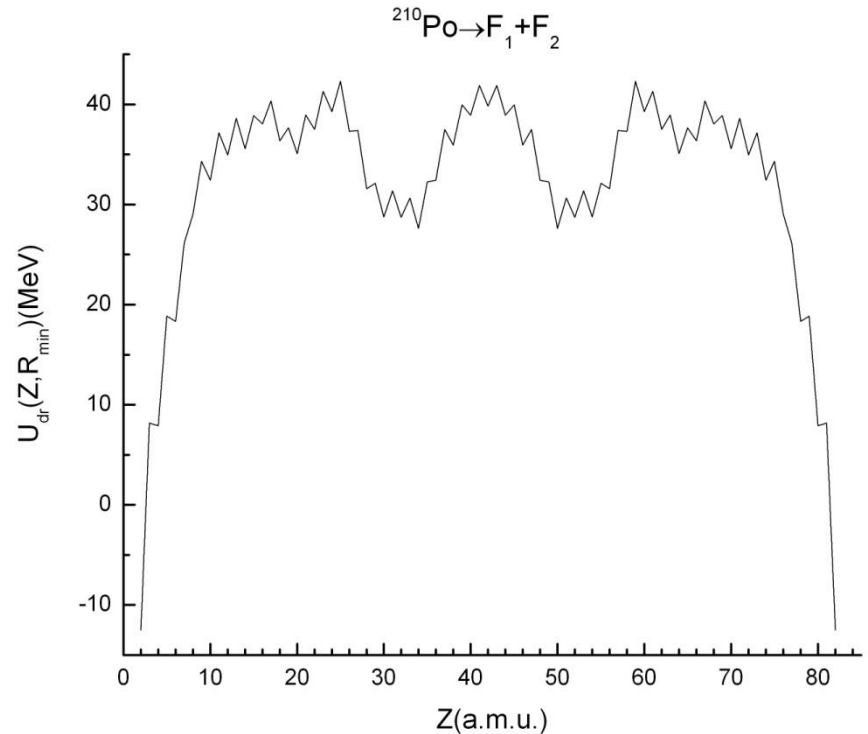
# Role of the shell effects in fission

*Driving potential for  $^{210}\text{Po}$   
within liquid drop model*



*symmetrical fission  
channel is energetically preferable*

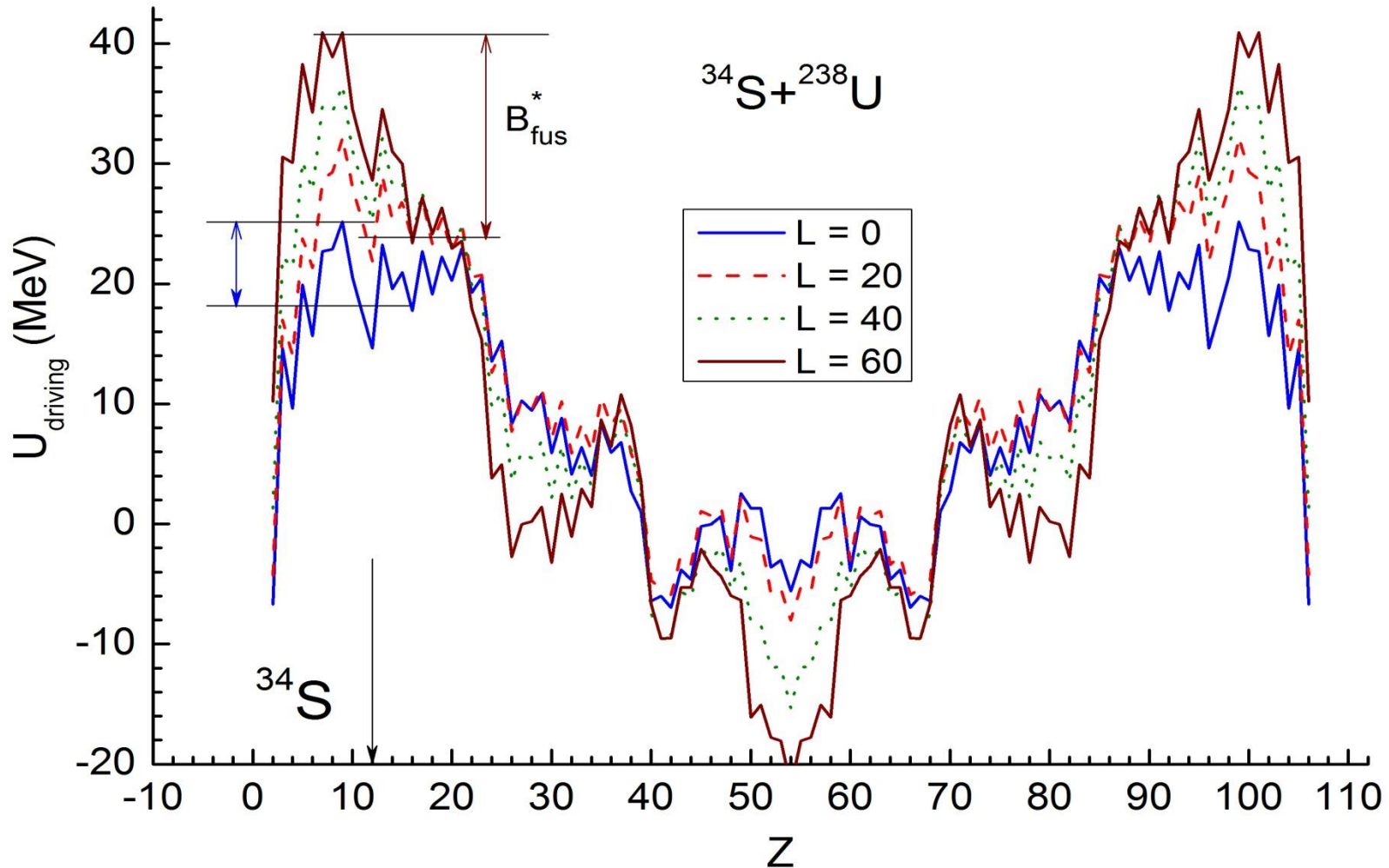
*Driving potential for  $^{210}\text{Po}$   
with shell effects*



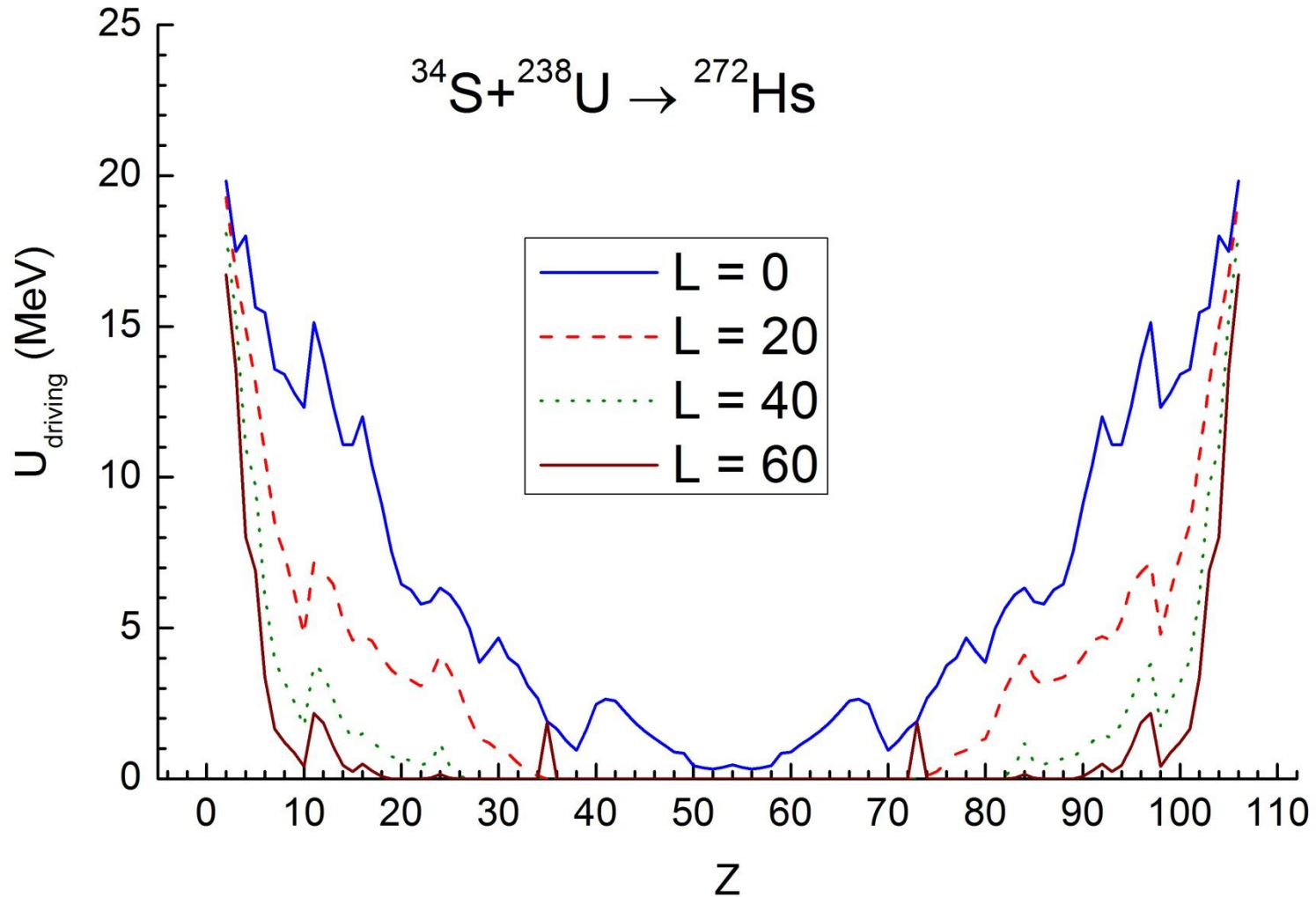
*asymmetrical fission  
channel is energetically preferable*

In experiment [9] observed symmetrical fission of  $^{210}\text{Po}$  in  $^{209}\text{Bi}(p, f)$  reaction at proton's energy 36 MeV

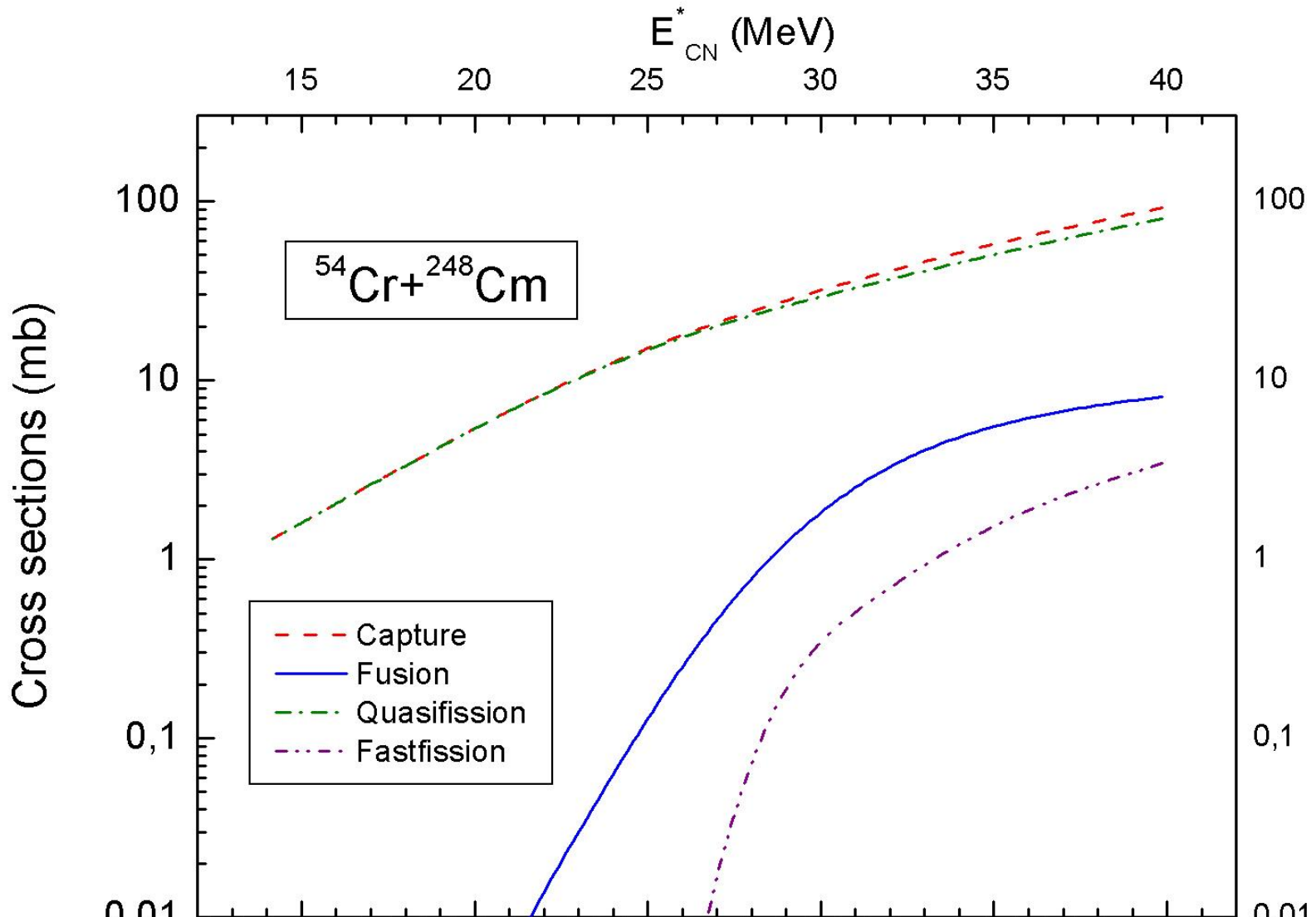
Dependence of the driving potential for the dinuclear system formed in  $^{34}\text{S}+^{238}\text{U}$  reaction on the orbital angular momentum  $L=[b \times p]$ .  $b$ -impact parameter,  $p$  is momentum



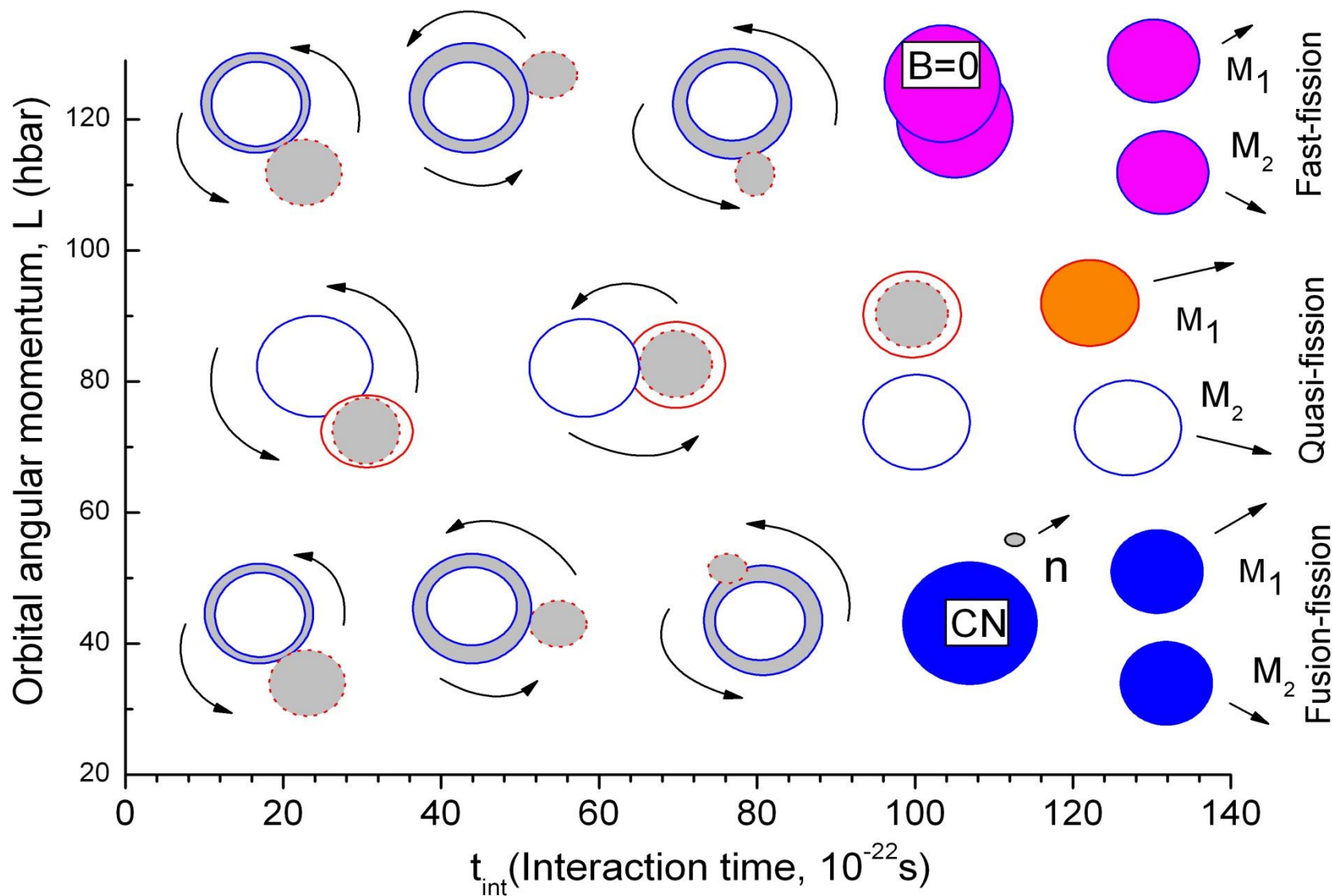
Dependence of the quasifission barrier for the dinuclear system formed in  $^{34}\text{S}+^{238}\text{U}$  reaction on the orbital angular momentum  $L=[b \times p]$ .  $b$ -impact parameter,  $p$  is momentum



# Capture, quasifission, complete fusion and fast fission cross sections



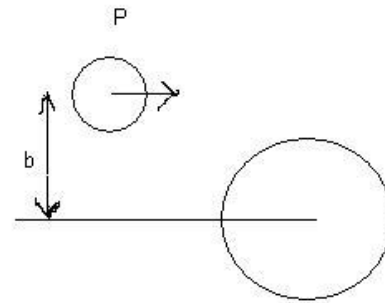
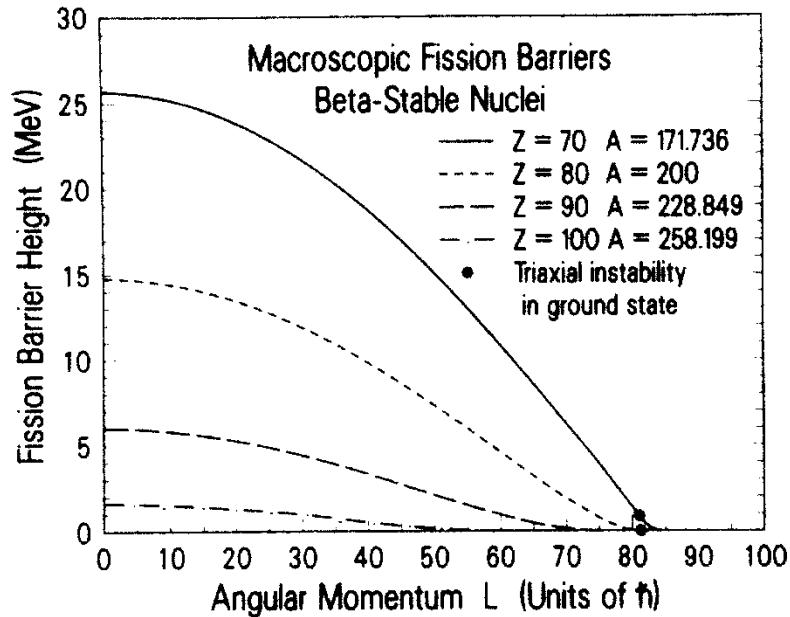
# Reaction mechanisms following after capture: fast-fission, quasi-fission and fusion-fission.



# Fast-fission of the mononucleus

33

## MACROSCOPIC MODEL (



$$L_{fus} > L > L_{fis.bar}$$

FIG. 10. Same as Fig. 9 for  $Z=70$  to 100. There are no solid points for  $Z=90$  and  $Z=100$  since no triaxial ground states exist for these nuclei.

# Calculation of P<sub>CN</sub>

$$P_{CN}^{(Z)} \approx \frac{\Gamma_{fus}^{(Z)}}{\Gamma_{gf}^{(Z)} + \Gamma_{fus}^{(Z)} + \Gamma_{sym}^{(Z)}}. \quad (12)$$

Here, the complete fusion process is considered as the evolution of the DNS along the mass asymmetry axis overcoming  $B_{fus}^{*(Z)}$  (a saddle point between  $Z = 0$  and  $Z = Z_P$ ) and ending in the region around  $Z = 0$  or  $Z = Z_{tot}$  (Fig. 1b). The evolution of the DNS in the direction of the symmetric configuration increases the number of events leading to quasifission of more symmetric masses. This kind of channels are taken into account by the term  $\Gamma_{sym}^{(Z)}$ . The widths of these "decays" leading to quasifission and complete fusion can be presented by the formula of the width of usual fission [28]:

$$\Gamma_i^{(Z)} = \frac{\rho(E_{DNS}^{*(Z)} - B_i^{(Z)})}{2\pi\rho(E_{DNS}^{*(Z)})} T(Z) \left(1 - \exp\left[-(B_i^{(Z)} - E_{DNS}^{*(Z)})/T(Z)\right]\right), \quad (13)$$

Calculation of fusion hindrance  
which is related to competition  
with quasifission.



# About description of the events of the synthesis of superheavy elements



The measured evaporation cross section can be described by the formula:

$$\sigma_{ER}(E^*) = \sum_{\ell=0}^{\ell=\ell_f} \sigma_{\text{cap}}(E_{\text{c.m.}}, \ell) P_{\text{CN}}(E^*, \ell) W_{\text{surv}}(E^*, \ell)$$

where

$$\sigma_{\text{fus}}(E_{\text{c.m.}}, \ell) = \sigma_{\text{cap}}(E_{\text{c.m.}}, \ell) P_{\text{CN}}(E^*, \ell)$$

is considered as the cross section of compound nucleus formation;  $W_{\text{surv}}$  is the survival probability of the heated and rotating nucleus. The smallness of  $P_{\text{CN}}$  means hindrance to fusion caused by huge contribution of quasifission process:

$$\sigma_{\text{qfis}}(E_{\text{c.m.}}, \ell) = \sigma_{\text{cap}}(E_{\text{c.m.}}, \ell) (1 - P_{\text{CN}}(E^*, \ell))$$

# Calculation of the competition between complete fusion and quasifission: $P_{CN}(E_{DNS}, L)$

$$P_{CN}(E_{DNS}^*, \ell) = \sum_{Z_{sym}}^{Z_{max}} Y_Z(E_{DNS}^*, \ell) P_{CN}^{(Z)}(E_{DNS}^*, \ell)$$

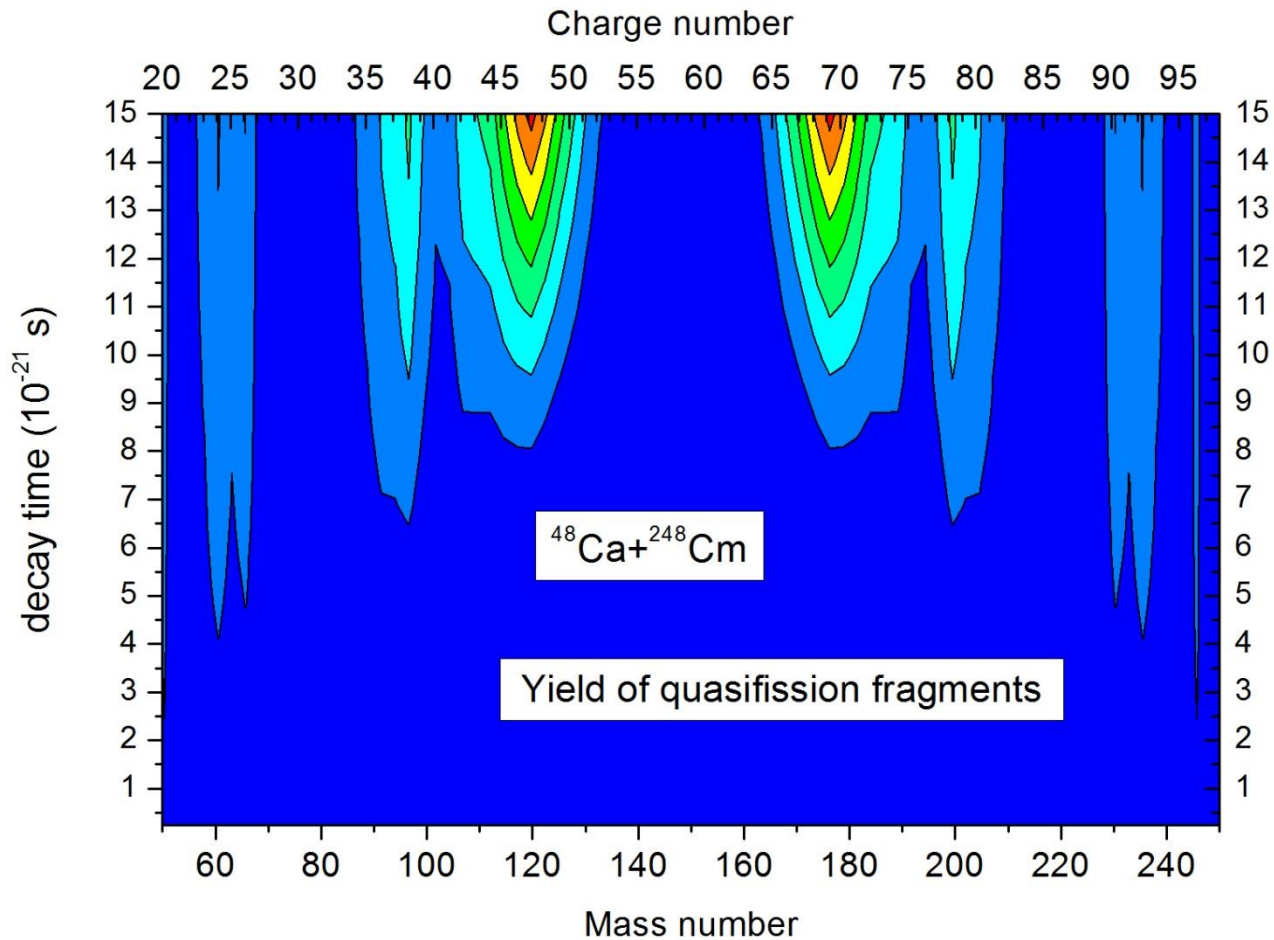
where

$$P_{CN}^{(Z)}(E_{DNS}^*, \ell) = \frac{\rho(E_{DNS}^*(Z) - B_{fus}^*(Z), \ell)}{\rho(E_{DNS}^*(Z) - B_{fus}^*(Z), \ell) + \rho(E_{DNS}^*(Z) - B_{qf}^*(Z), \ell) + \rho(E_{DNS}^*(Z) - B_{sym}^*(Z), \ell)}$$

$$\begin{aligned} \frac{\partial}{\partial t} Y_Z(E_Z^*, \ell, t) &= \Delta_{Z+1}^{(-)} Y_{Z+1}(E_Z^*, \ell, t) + \Delta_{Z-1}^{(+)} Y_{Z-1}(E_Z^*, \ell, t) \\ &\quad - (\Delta_Z^{(-)} + \Delta_Z^{(+)} + \Lambda_Z^{qf}) Y_Z(E_Z^*, \ell, t) \end{aligned}$$

for  $Z = 2, 3, \dots, Z_{tot} - 2$

# Calculation of the yield of quasifission fragments



# Nucleon transfer coefficients for evolution of the charge asymmetry of dinuclear system

$$\Delta_Z^{(\pm)} = \frac{1}{\Delta t} \sum_{P_z, T_z} |g_{P_z T_z}|^2 n_{T_z(P_z)}(t) (1 - n_{T_z(P_z)}(t)) W_{P_z T_z}(\Delta t) / (\varepsilon_{P_z} - \varepsilon_{T_z})^2$$

$$W_{P T_z}(\Delta t) = (1 + e^{-2(\Gamma_{P_z} + \Gamma_{T_z})\Delta t/\hbar} - 2 \cdot e^{-2(\Gamma_{P_z} + \Gamma_{T_z})\Delta t/\hbar} \cos((\varepsilon_{P_z} - \varepsilon_{T_z})\Delta t/\hbar))$$

$$\frac{1}{\tau_i^{(\alpha)}} = \frac{\sqrt{2}\pi}{32\hbar\varepsilon_{F_K}^{(\alpha)}} \left[ (f_K - g)^2 + \frac{1}{2}(f_K + g)^2 \right]$$

$$\times \left[ (\pi T_K)^2 + (\tilde{\varepsilon}_i - \lambda_K^{(\alpha)})^2 \right] \left[ 1 + \exp\left(\frac{\lambda_K^{(\alpha)} - \tilde{\varepsilon}_i}{T_K}\right) \right]^{-1}, \quad (\text{A.1})$$

where

$$\Gamma_i = \hbar/\tau_i \quad T_K(t) = 3.46 \sqrt{\frac{E_K^*(t)}{\langle A_K(t) \rangle}} \quad (\text{A.2})$$

# What is questionable in fusion reactions ?



Dynamics of complete fusion and role of the entrance channel in formation of heavy ion collision reactions are questionable or they have different interpretation still now.

For example,

-- what mechanism is fusion makes the main contribution to formation of compound nucleus: increasing the neck between interacting nucleus or multinucleon transfer at relatively restricted neck size?

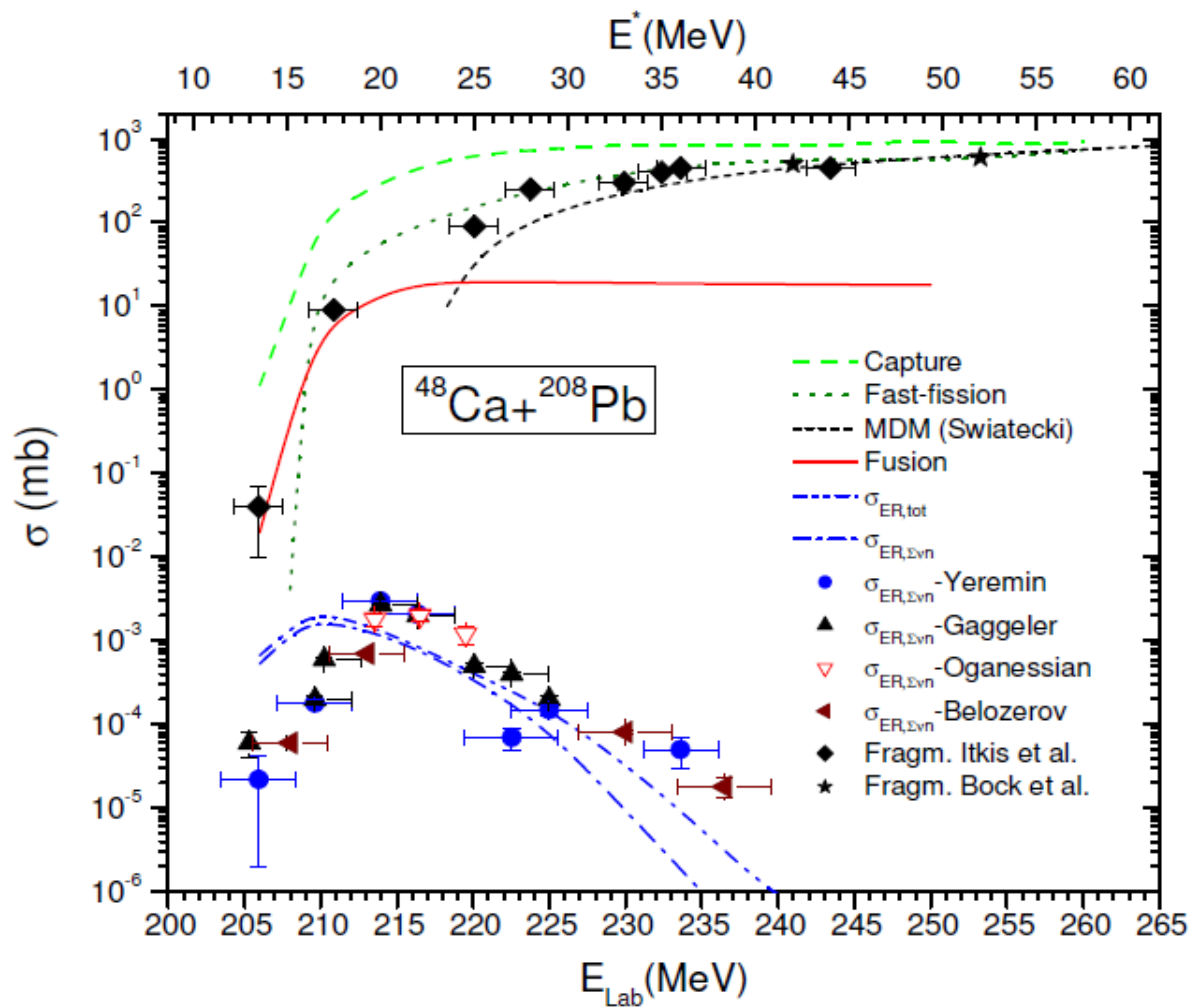
-- details of angular momentum distribution of dinuclear system and compound nucleus which determines the angular distribution of reaction products, cross sections of evaporation residue, fusion-fission and quasifission products;

-- separation of fusion-fission fragments from the quasifission and fast-fission products;

-- distribution of the excitation energy between different degrees of freedom, as well as between reaction products. There are exp.results showing evaporation residues at  $E^* > 100$  MeV.

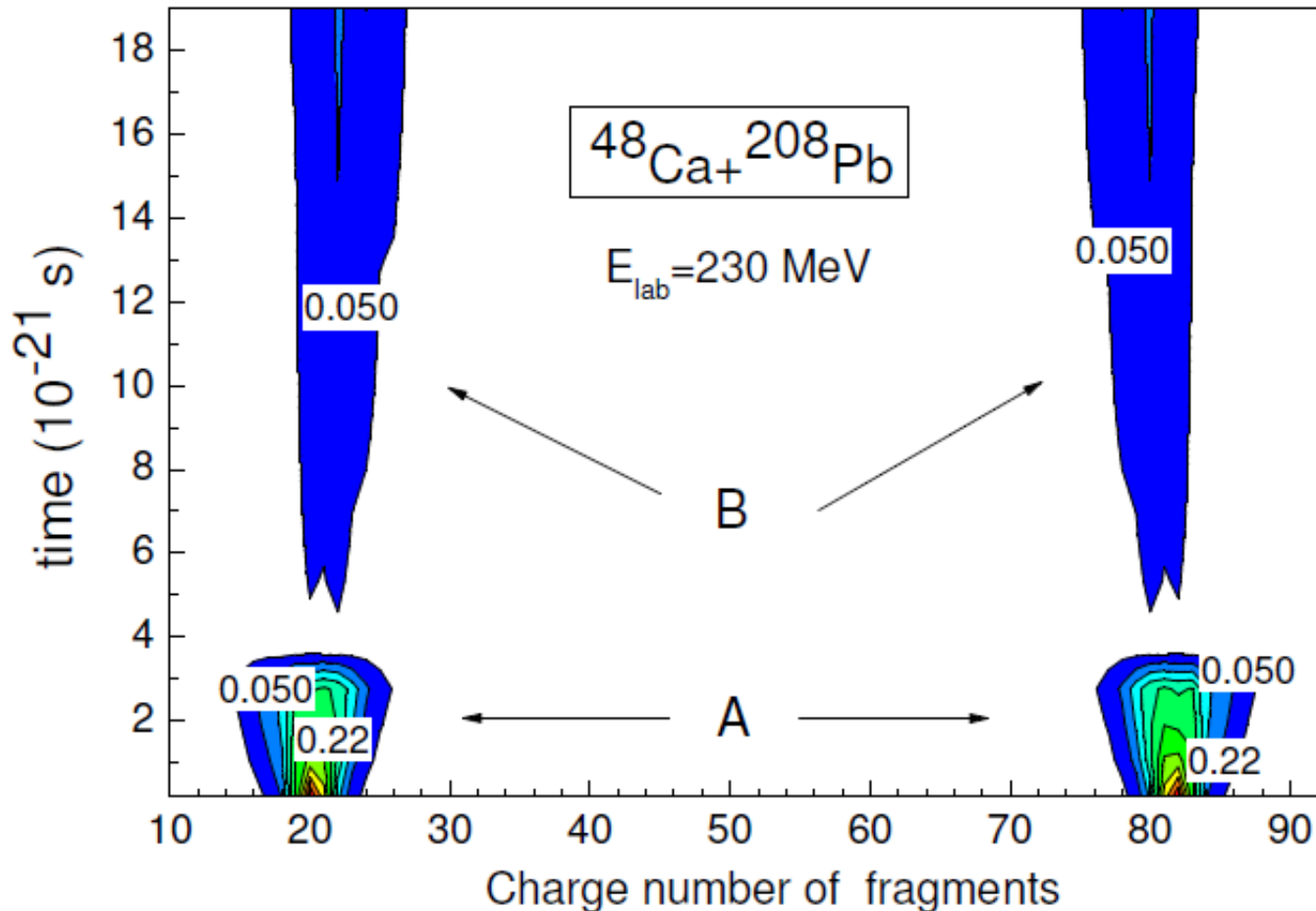
### 3. Yield of quasifission products as a function of shell structure

Comparison of the theoretical and experimental results obtained for the  $^{48}\text{Ca}+^{208}\text{Pb}$  reaction. Theoretical values of capture, fast fission, and fusion excitation functions are presented by dashed, dotted, and solid lines, respectively. Capture cross-section calculated by Swiatecki's dynamical model is shown by short-dashed line.



G. Fazio et al., (DNS model)  
 Modern Physics Letters A  
 Vol. 20, No. 6 (2005) p.391  
 M. G. Itkis et al., in Proc. of  
 the Symposium on Nuclear  
 Cluster, 2002, Rauscholzhausen  
 Germany, eds. R. V. Jolos and  
 W. Scheid (EP Systema, 2003),  
 p. 315;  
 Acta Phys. Hung. A19, 9 (2004).  
 (Experiment)

Yield of quafission products is hidden by products of the deep-inelastic collision in case of collision of two double magic nuclei,  $^{48}\text{Ca}$  and  $^{208}\text{Pb}$ .

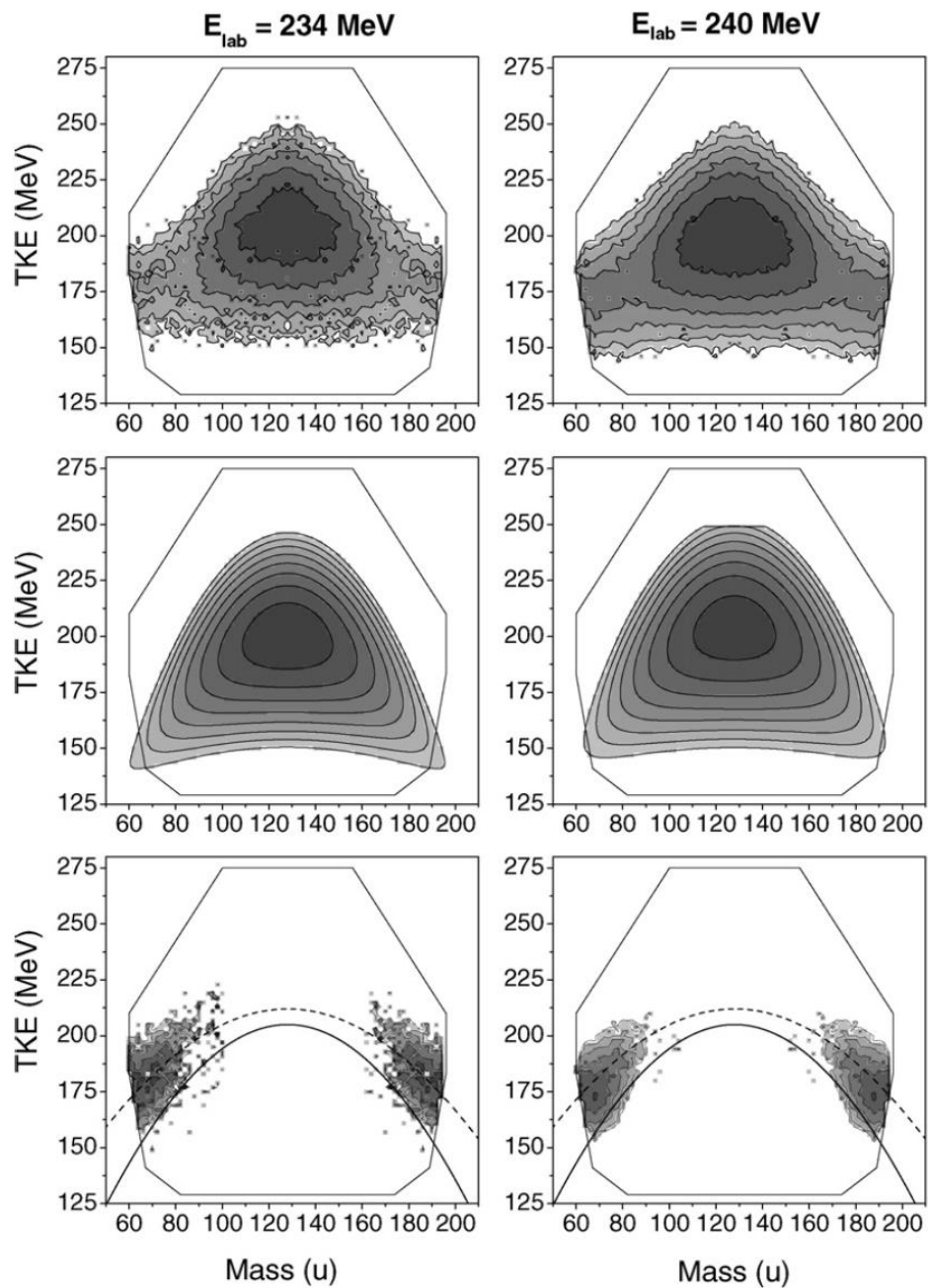


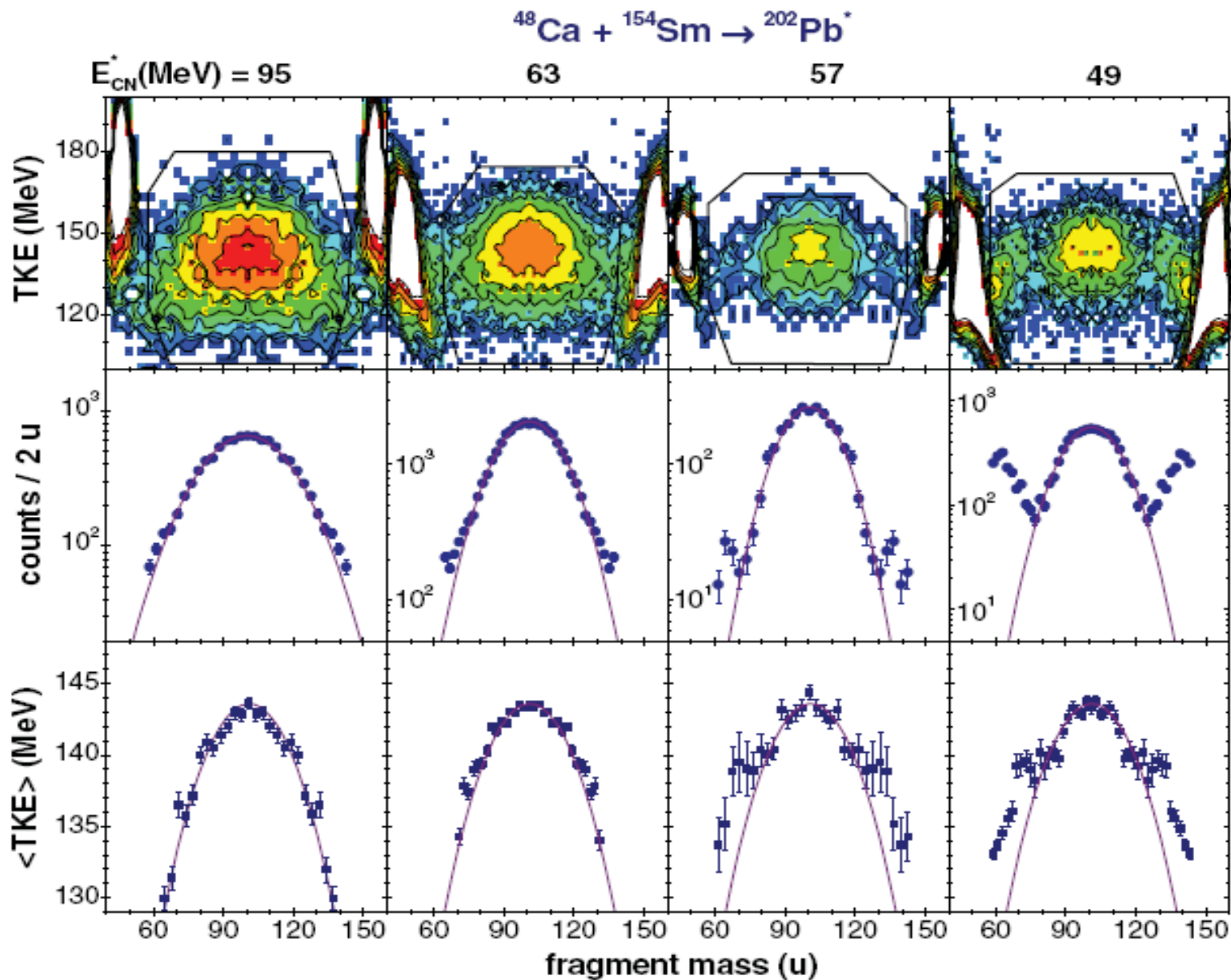
G. Fazio et al., (DNS model) *Modern Physics Letters A* Vol. 20, No. 6 (2005) p.391

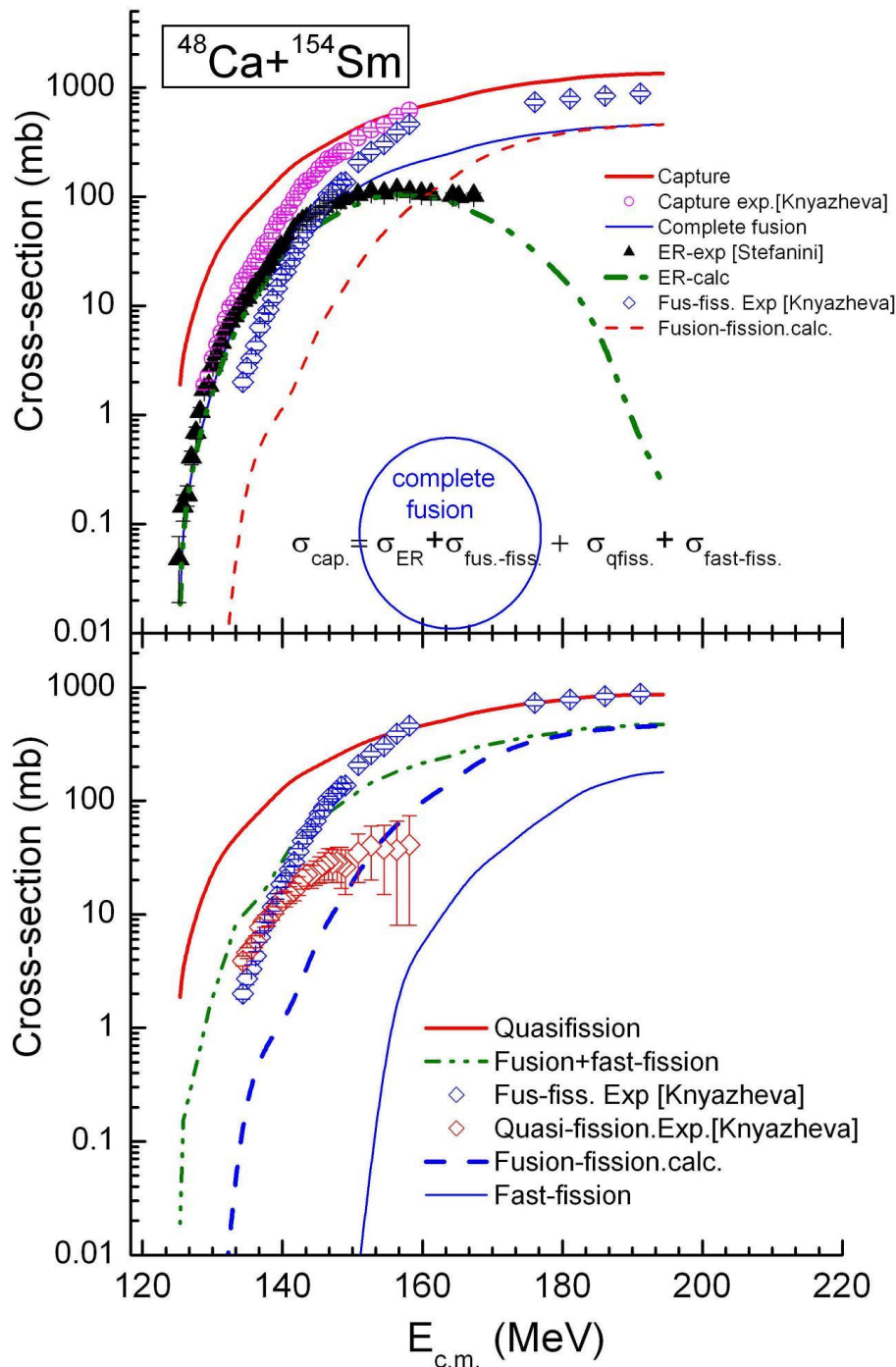
M. G. Itkis et al., in Proc. of the Symposium on Nuclear Cluster, 2002, Rauscholzhausen, Germany, eds. R. V. Jolos and W. Scheid (EP Systema, 2003), p. 315;

*Acta Phys. Hung.* A19. 9 (2004). (Experiment)









Comparison of the capture, fusion-fission and quasifission cross sections obtained in this work with data from experiments

***Knyazheva G.N. et al. Phys. Rev. C 2007. Vol. 75. –P. 064602(13).***

and evaporation residues

***Stefanini A.M. et al.***

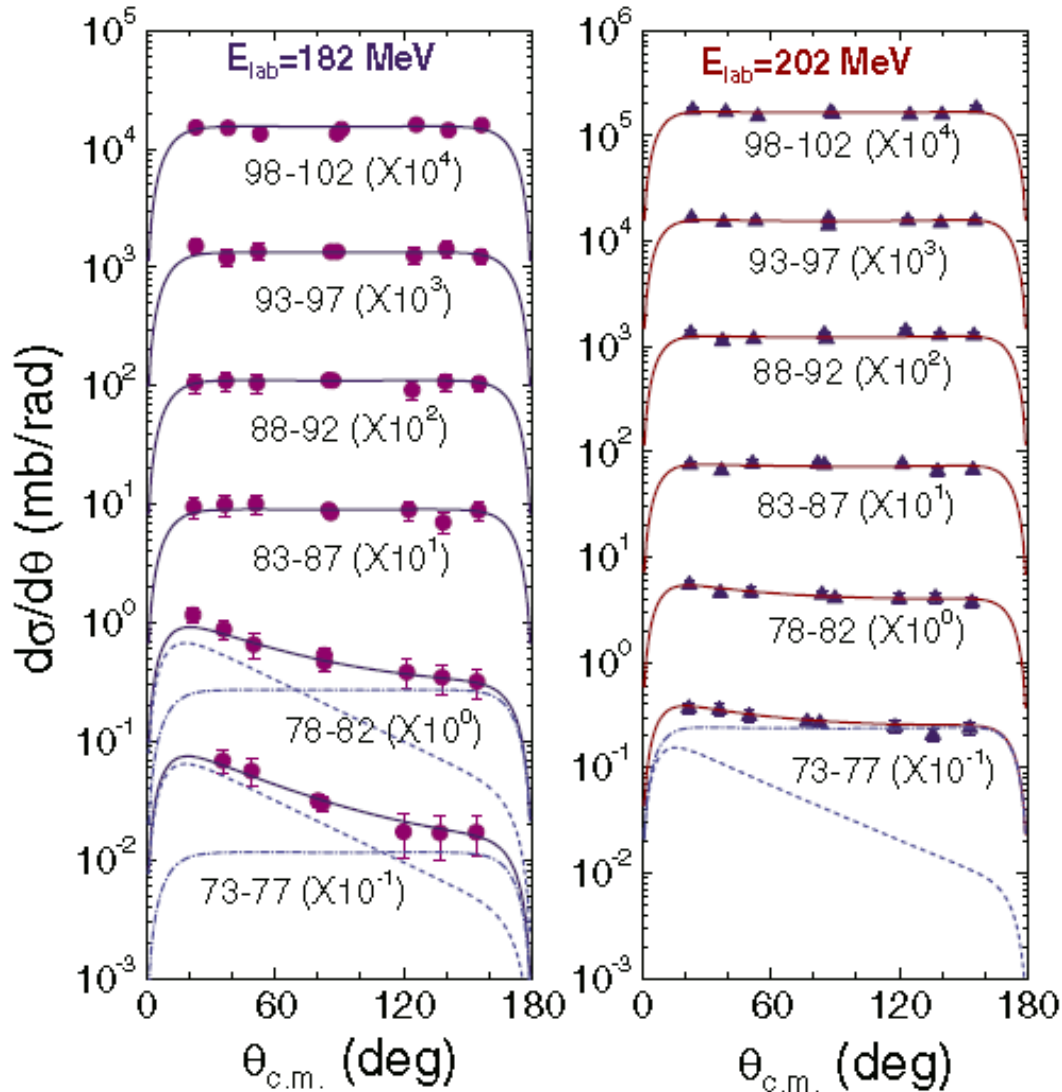
***Eur. Phys. J. A –2005. Vol. 23. –P.473***

## Experimental estimation of the capture and fusion-fission cross sections

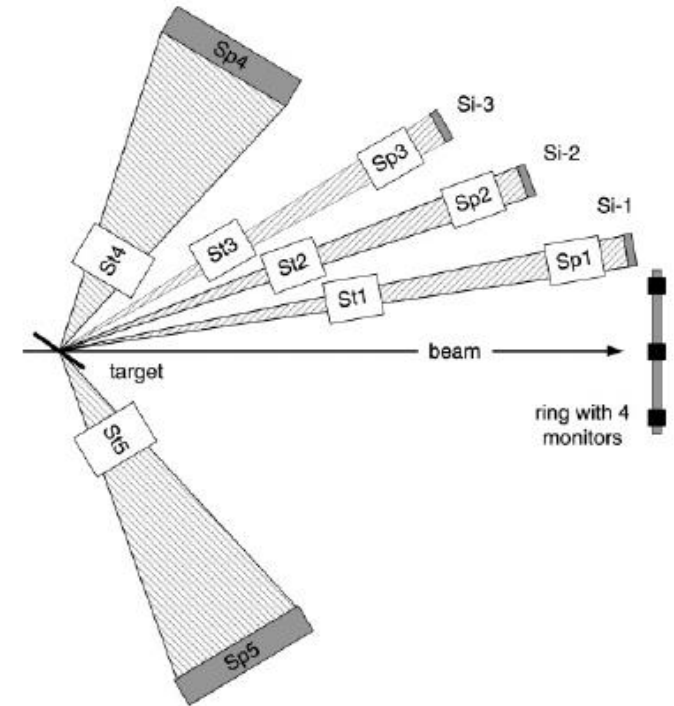
Angular distributions for different fragment masses were derived attempting to find experimental evidence for the QF nature of the mass-asymmetric “shoulders” observed in  $^{48}\text{Ca}+^{154}\text{Sm}$  (see Fig. 3). In Figs. 8 and 9 the angular distributions for the selected mass bins of fission-like fragments are shown. The width of each mass bin is 5 amu (mainly determined by statistics and mass resolution). The solid curves are fits to the experimental data given by the expression similar to the one proposed in [13]

$$\frac{d\sigma}{d\theta} = 2\pi \sin\theta \{a + b \exp[\gamma(\theta - \pi/2)]\} W(\theta), \quad (7)$$

Angular distribution of the mass symmetric reaction products  
(experimental)



Setup CORSET to measure mass, energy and angular distributions of the mass symmetric reaction products

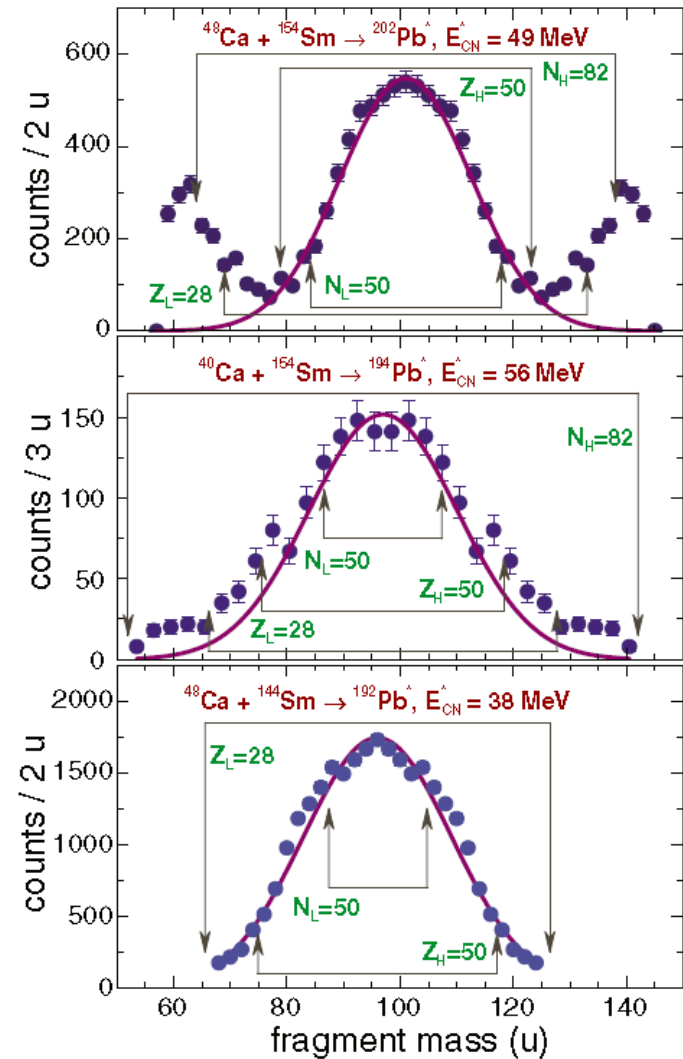
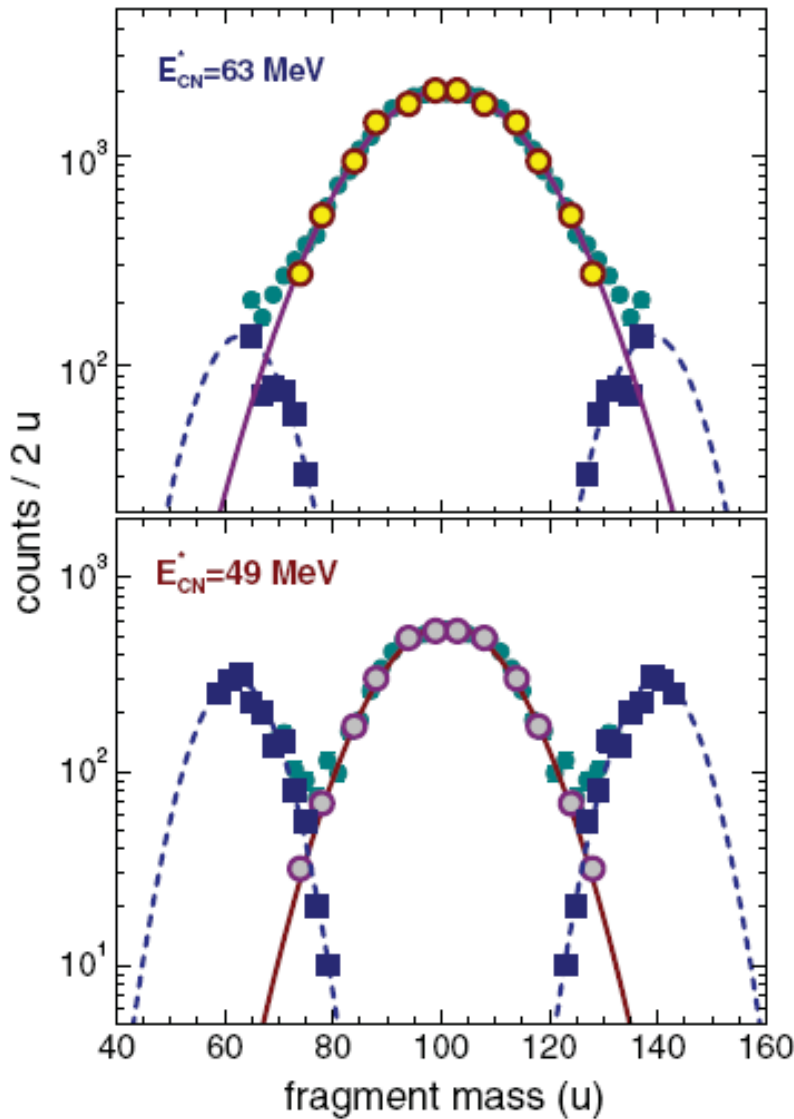


$$W(\theta) = \sum_{I=0}^{\infty} (2I+1) T_I \sum_{K=-I}^I (2I+1) |d_{0K}^I(\theta)|^2 / 2 \\ \times \exp[-K^2/2K_0^2(I)] / \sum_{K=-I}^I \exp[-K^2/2K_0^2(I)],$$

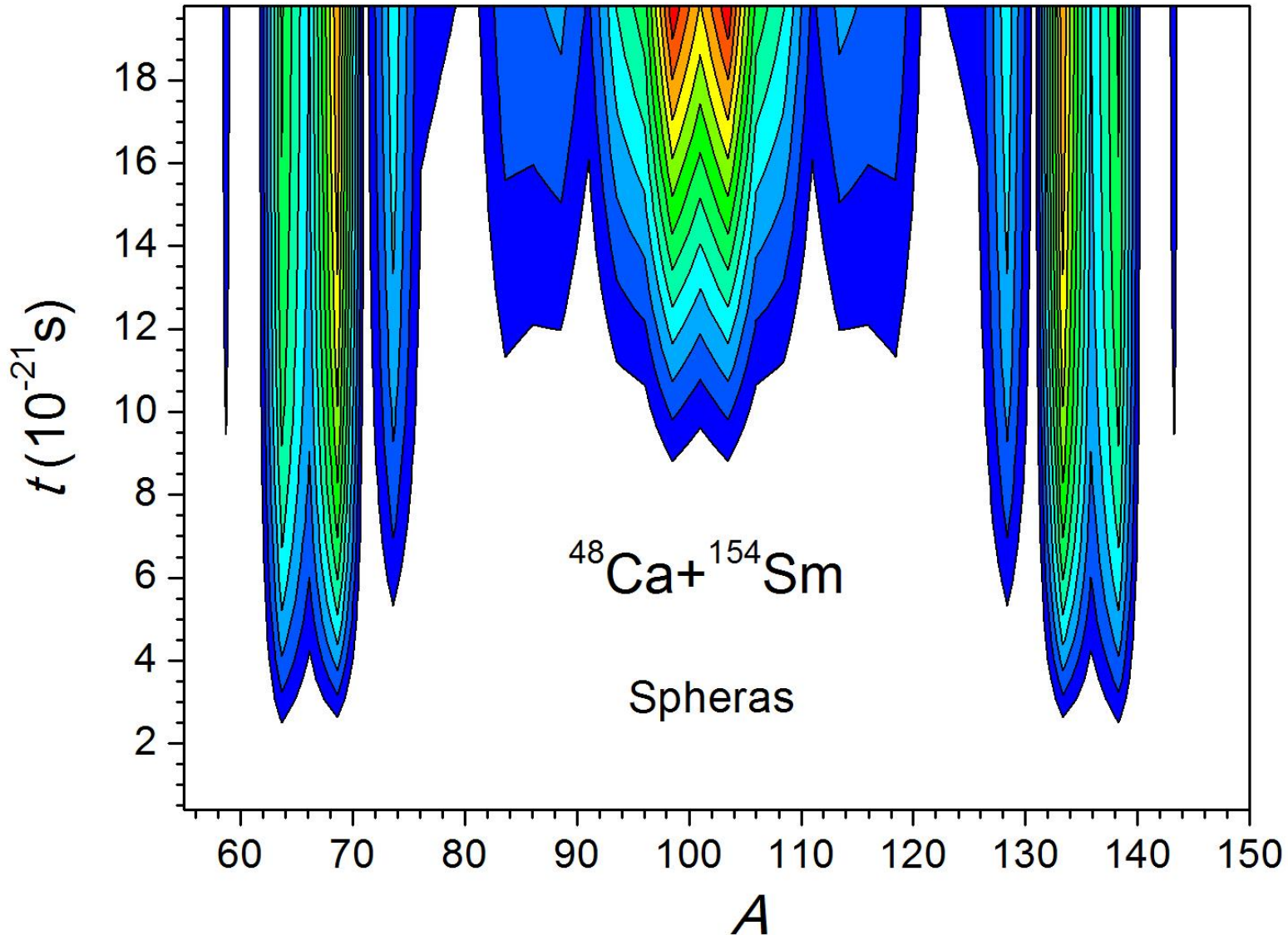
$$K_0 = J_{\text{eff}} T / \hbar$$

$$\sigma_M^2 = (98.1 \pm 15.1) T + (0.05 \pm 0.01) \langle I^2 \rangle.$$

# Overlap of yields of binary fragments coming from of fusion fission and quasifission channels of reaction

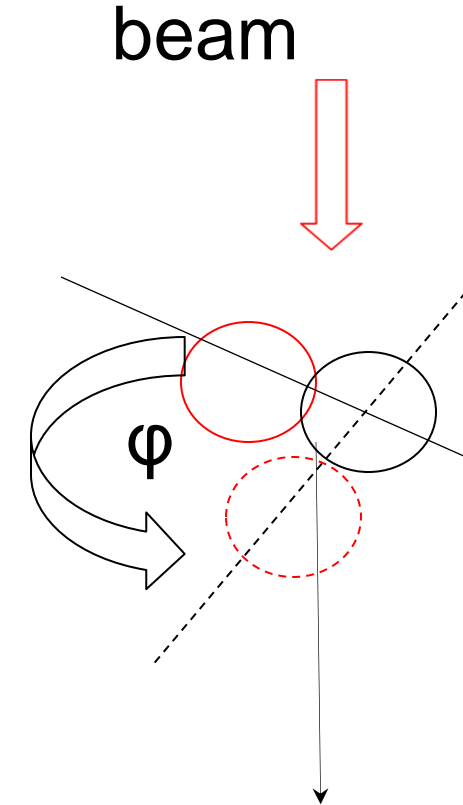
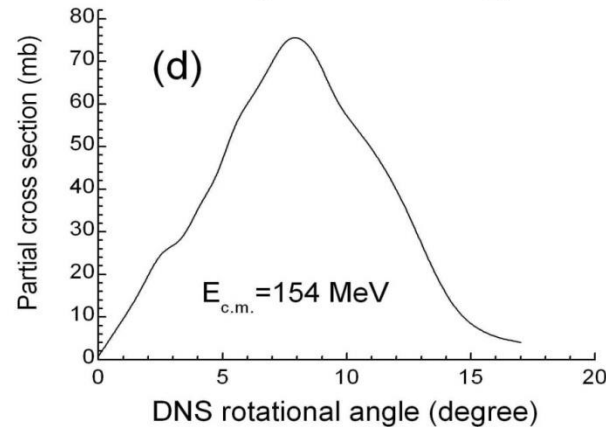
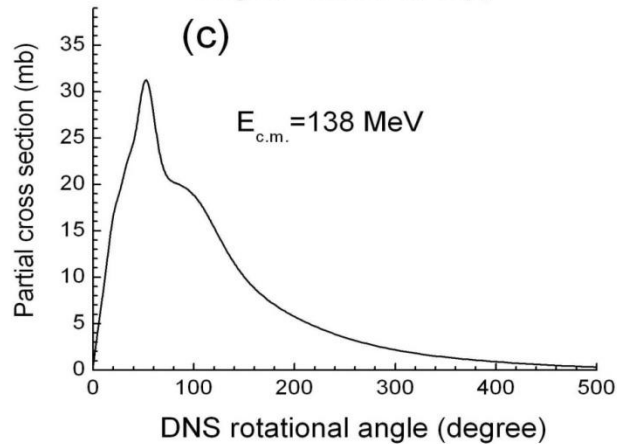
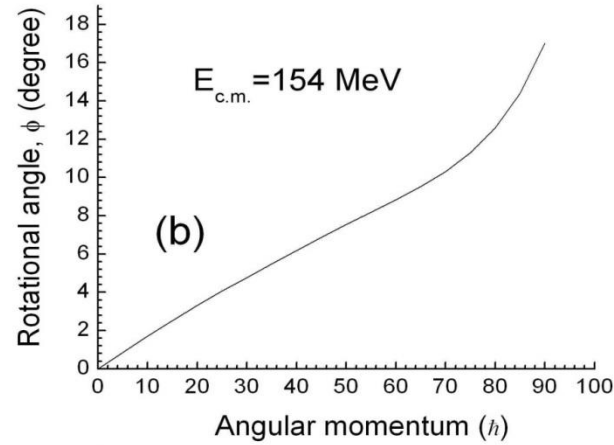
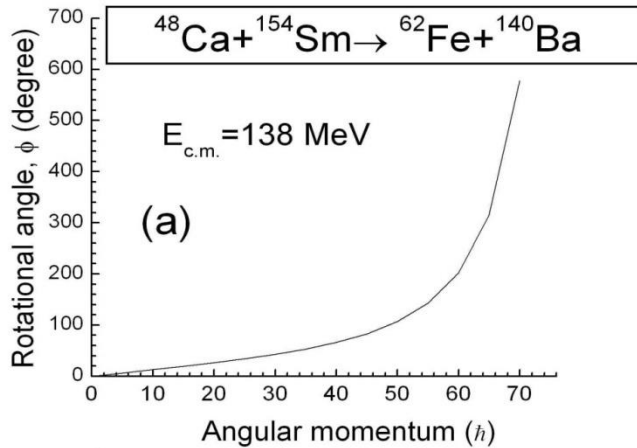


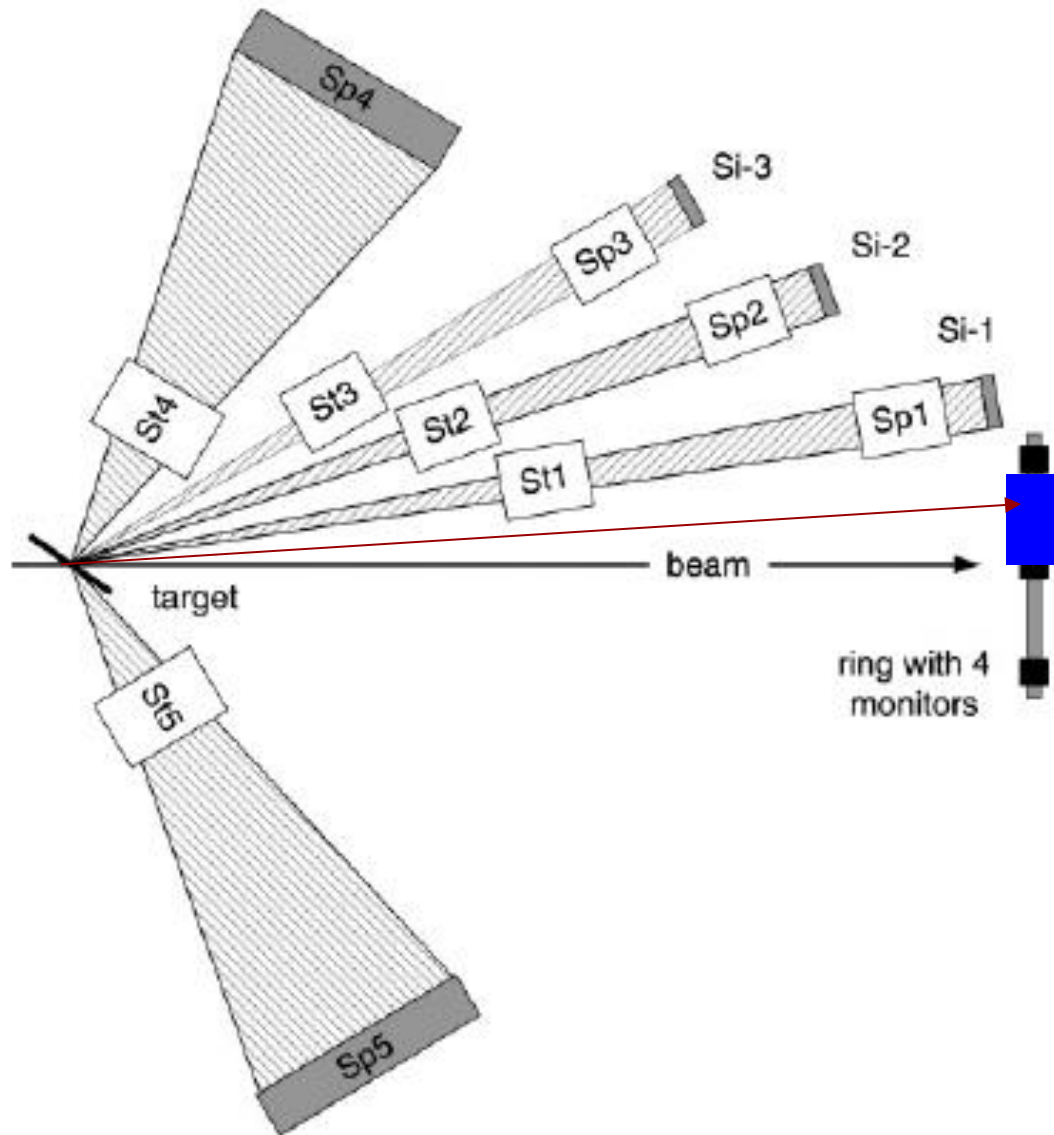
# Evolution of the mass distribution of quasifission fragments

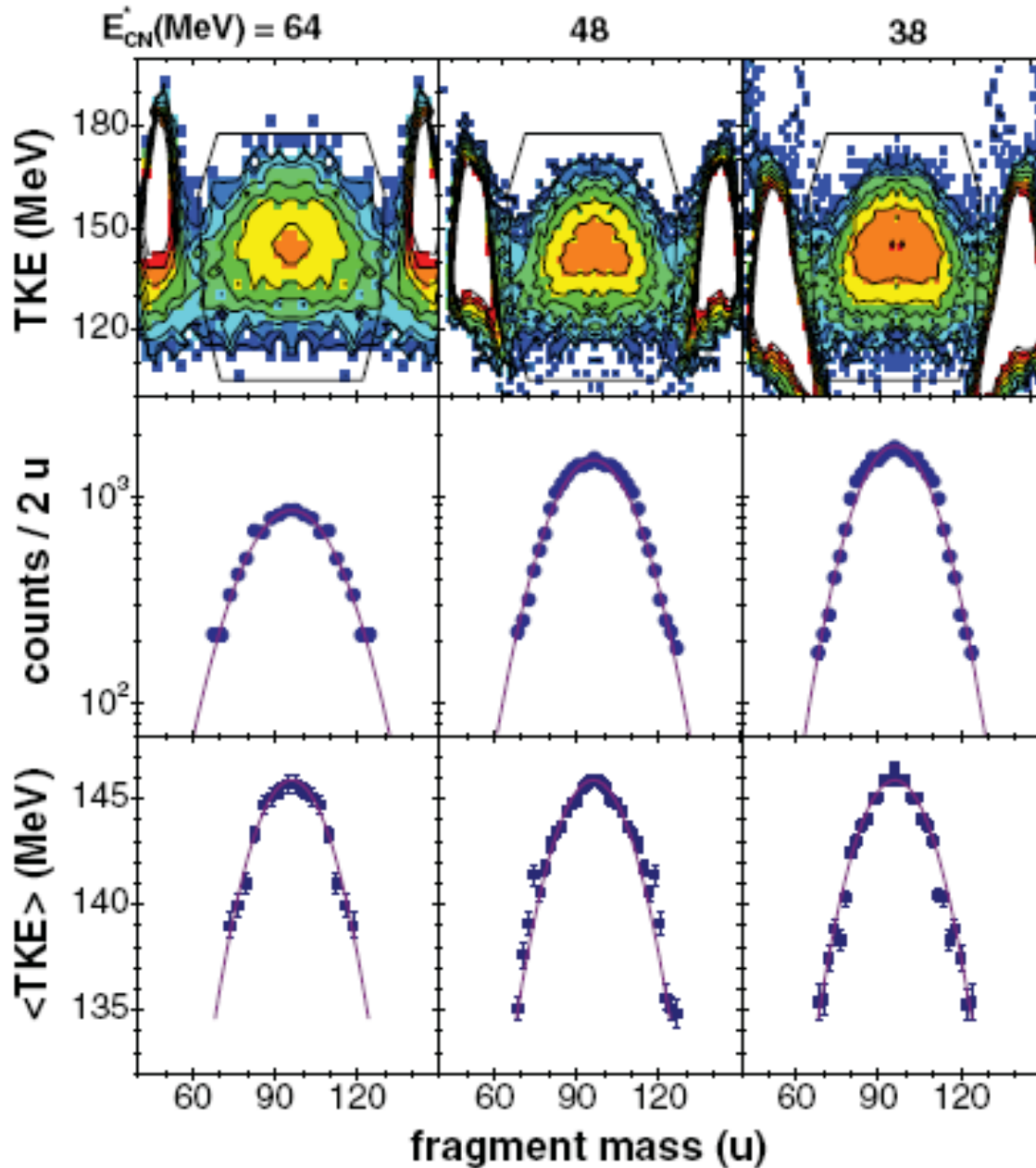




# The rotational angle of the dinuclear system as a function of the orbital angular momentum (a) and (b), and angular distribution of the yield of quasifission fragments (c) and (d)







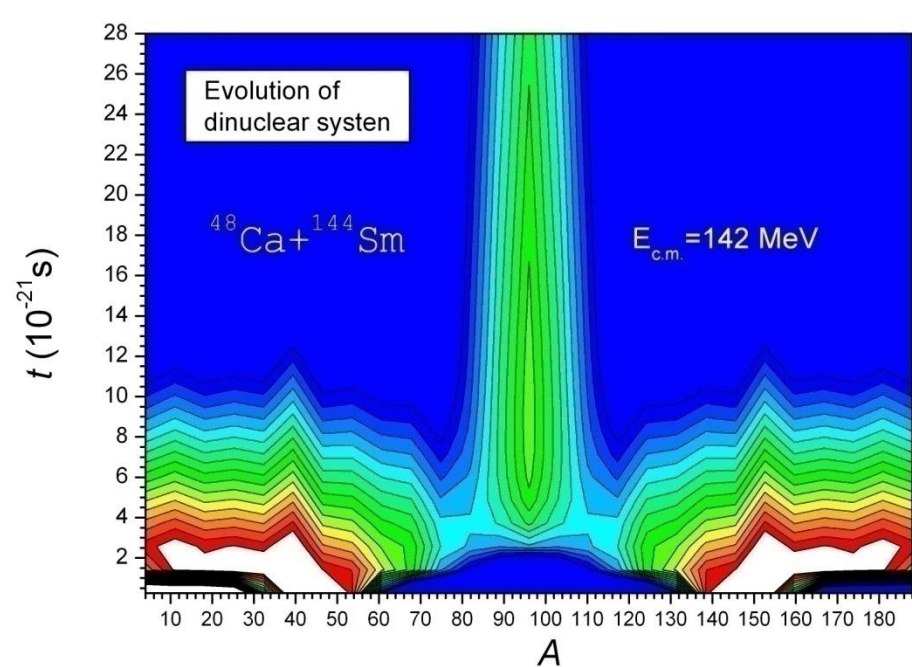
$$\text{TKE} = K_1 + K_2$$

$$P(M_1, M_2, \text{TKE})$$

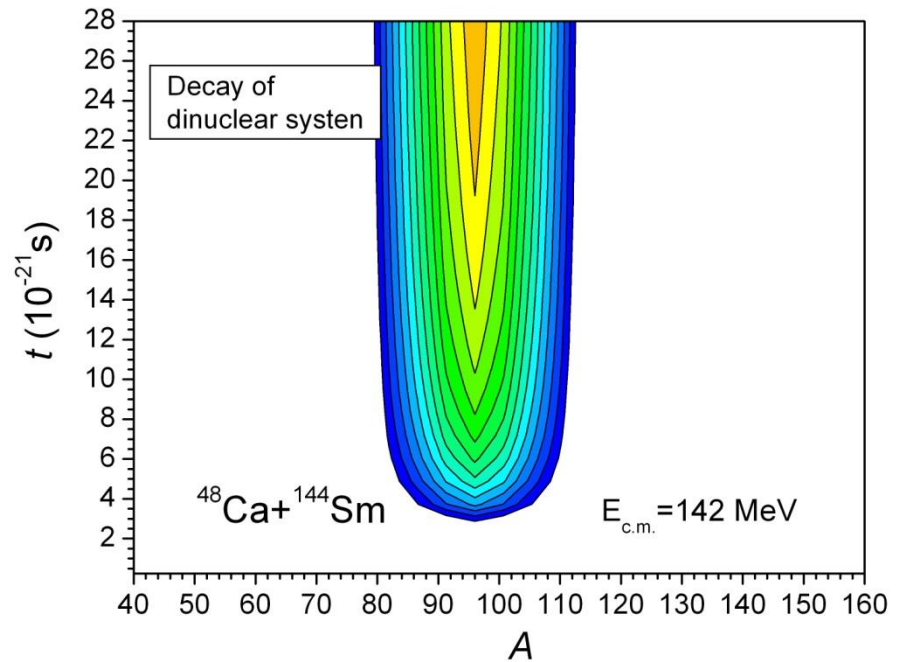
$$P(M_1, M_2) = \sum P(M_1, M_2, \text{TKE})$$

$$\langle \text{TKE} \rangle = \frac{\sum \text{TKE} P(M_1, M_2, \text{TKE})}{\sum P(M_1, M_2, \text{TKE})}$$

# Explanation of the lack of quasifission fragment yields at the expected place of mass distribution in the $^{48}\text{Ca}+^{144}\text{Sm}$ reaction

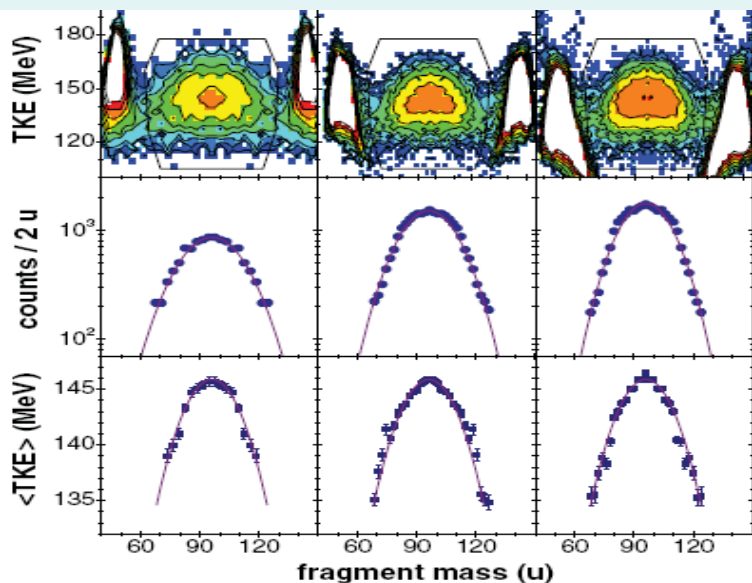


Evolution of dinuclear system



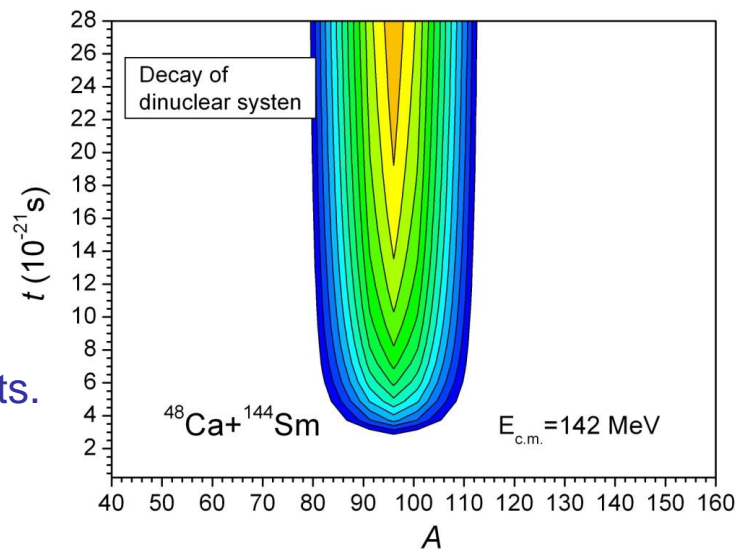
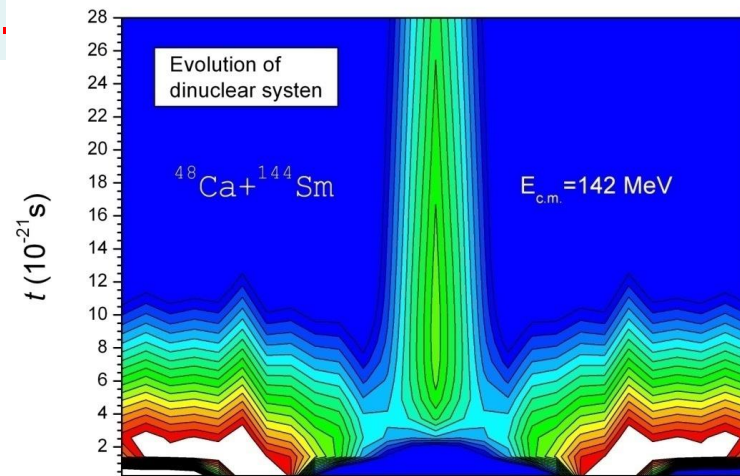
Decay of dinuclear system

Assumption about the yield of quasifission products appears only between mass symmetric region ( $A_{\text{tot}}/2 \pm 20$ ) and initial projectile and target mass region can lead to incorrect conclusion about reaction mechanism.

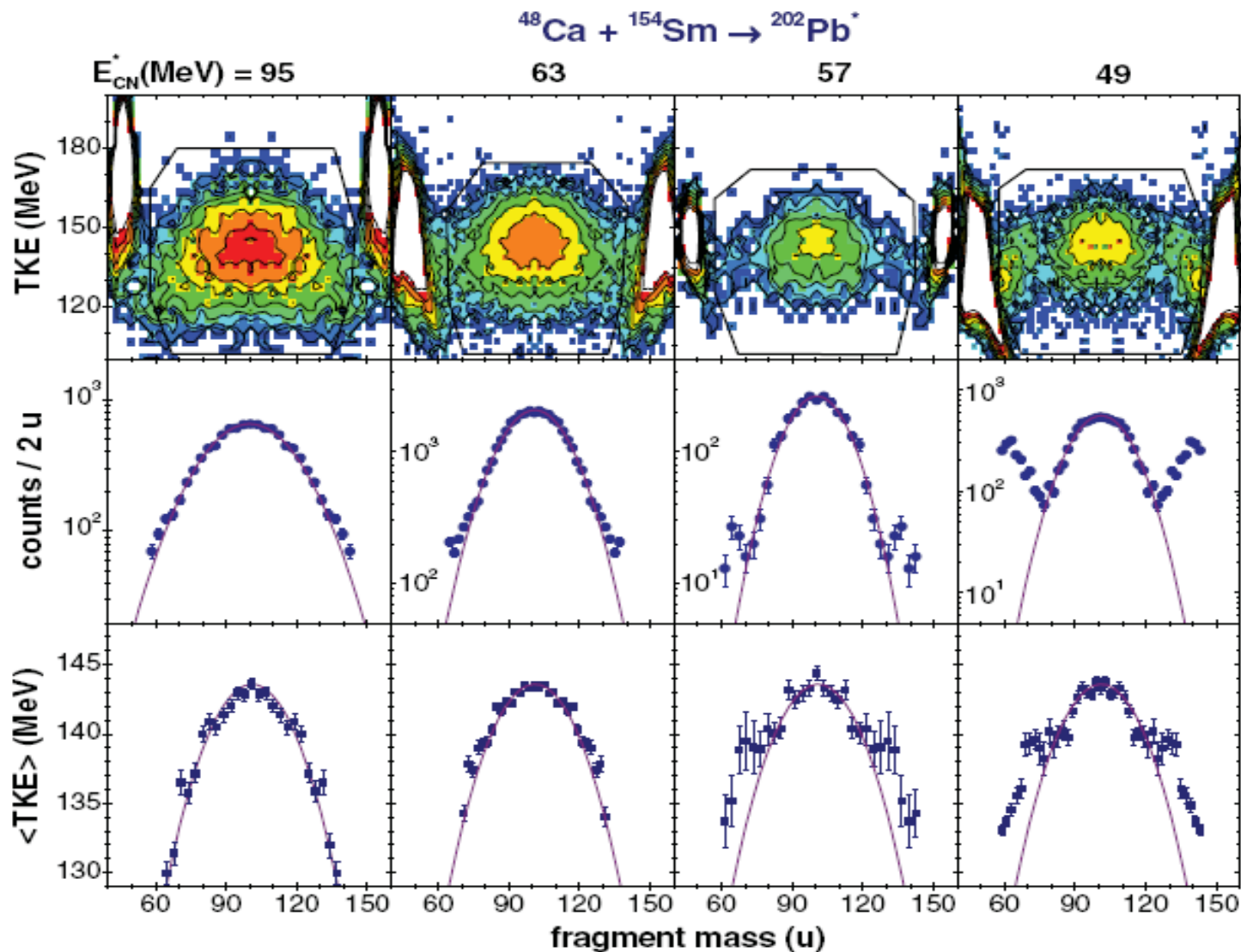


Knyazheva G.N. et al. Phys. Rev. C 75, 064602(2007).

Due to shell effects and behavior of the quasifission barrier as a function of the mass asymmetry, yield of quasifission occurs mainly from mass symmetric region which strongly overlap with the fusion-fission products. Counting the quasifission products as the fusion-fission products lead to overestimation of the experimental fusion cross section. This circumstance causes confusing at theoretical analysis.

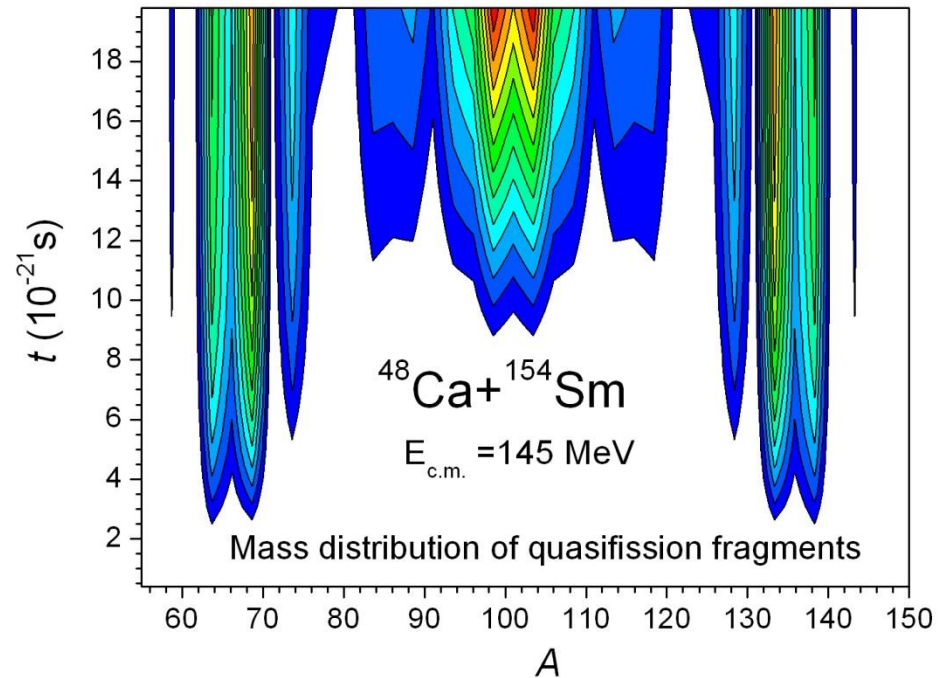
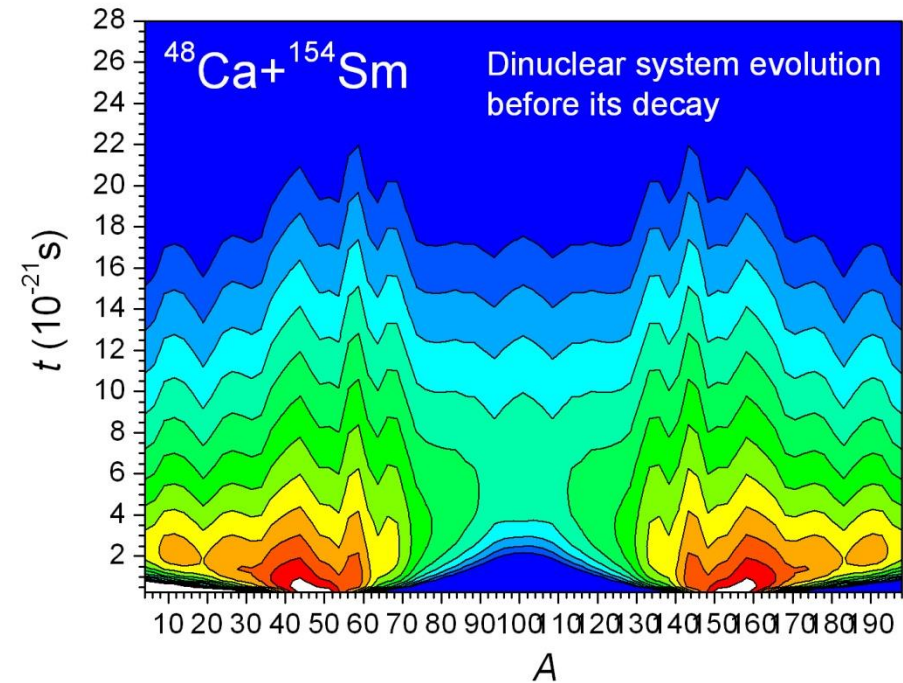


# “Disappearance” of the quasifission products in the yield of reaction products.



*Knyazheva G.N. et al. Phys. Rev. C 75, 064602(2007).*

Evolution of mass distributions of in the dinuclear system formed in the  $^{48}\text{Ca}+^{154}\text{Sm}$  reaction (left panel) and quasifission products at its decay (right panel) .



# Calculation of the charge distribution in the dinuclear system

$$\begin{aligned} \frac{\partial}{\partial t} Y_Z(E_Z^*, \ell, t) = & \Delta_{Z+1}^{(-)} Y_{Z+1}(E_Z^*, \ell, t) + \Delta_{Z-1}^{(+)} Y_{Z-1}(E_Z^*, \ell, t) \\ & - (\Delta_Z^{(-)} + \Delta_Z^{(+)} + \Lambda_Z^{\text{qf}}) Y_Z(E_Z^*, \ell, t), \quad \text{for } Z = 2, 3, \dots, Z_{\text{tot}} - 2. \end{aligned} \quad (6)$$

Here, the transition coefficients of multinucleon transfer are calculated as in Ref. 18

$$\Delta_Z^{(\pm)} = \frac{1}{\Delta t} \sum_{P,T} |g_{PT}^{(Z)}|^2 n_{T,P}^{(Z)}(t) (1 - n_{P,T}^{(Z)}(t)) \frac{\sin^2(\Delta t(\tilde{\epsilon}_{P_Z} - \tilde{\epsilon}_{T_Z})/2\hbar)}{(\tilde{\epsilon}_{P_Z} - \tilde{\epsilon}_{T_Z})^2/4}, \quad (7)$$



# Calculation of decay of dinuclear system

$$\theta_{DNS} = \theta_{cap} + \Omega_{DNS} \cdot \tau(T_Z(\ell, E_Z^*(\ell))). \quad \tau(T_Z) = \frac{\hbar}{\Gamma_{qf}(T_Z)},$$

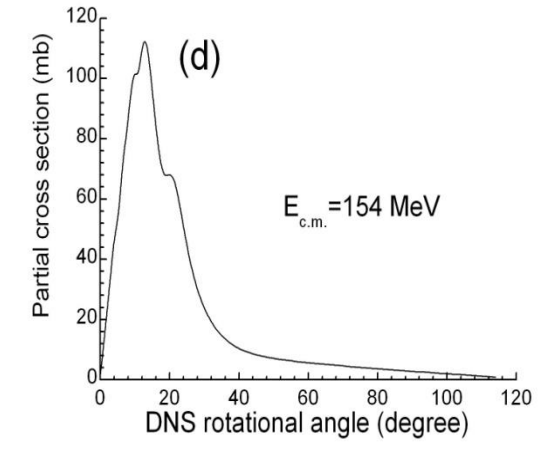
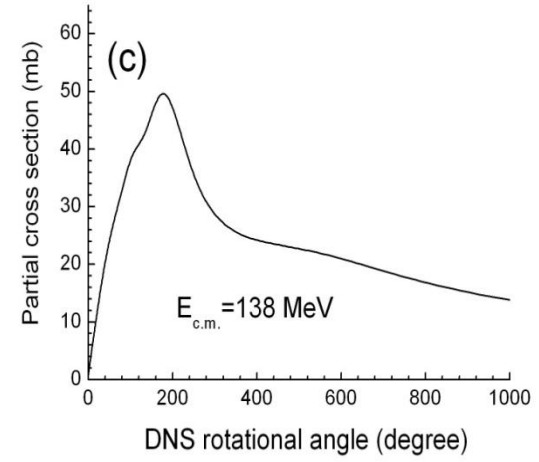
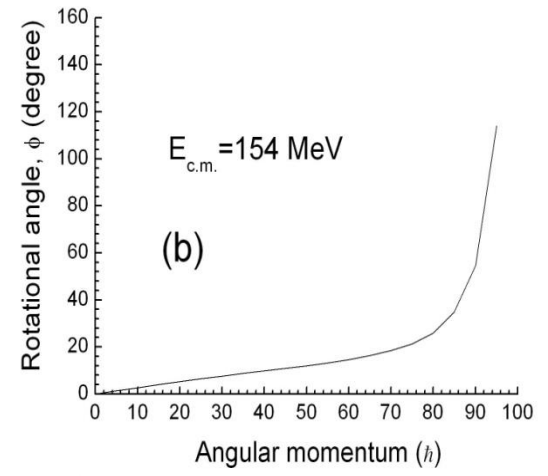
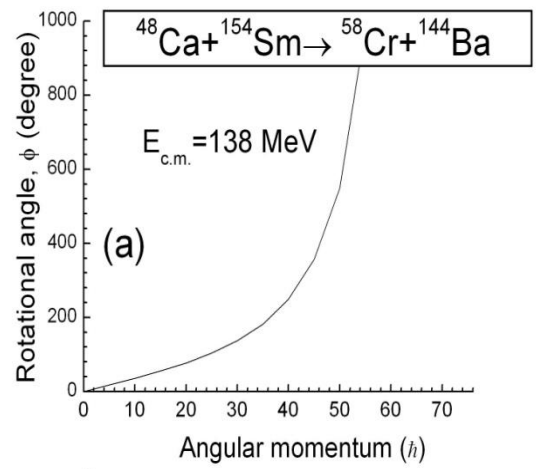
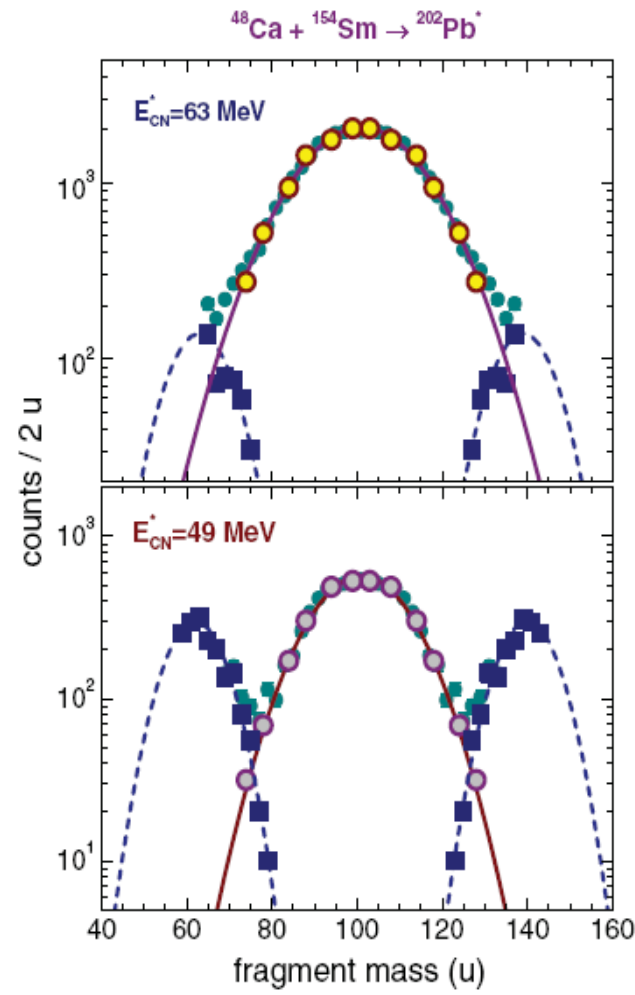
$$\Gamma_{qf}(\Theta) = K_{rot} \omega_m \left( \sqrt{\gamma^2 / (2\mu_{qf})^2 + \omega_{qf}^2} - \gamma / (2\mu_{qf}) \right) \times \exp(-B_{qf}/T_Z) / (2\pi\omega_{qf}). \quad (21)$$

$$\omega_m^2 = \mu_{qf}^{-1} \left| \frac{\partial^2 V(R)}{\partial R^2} \right|_{R=R_m},$$

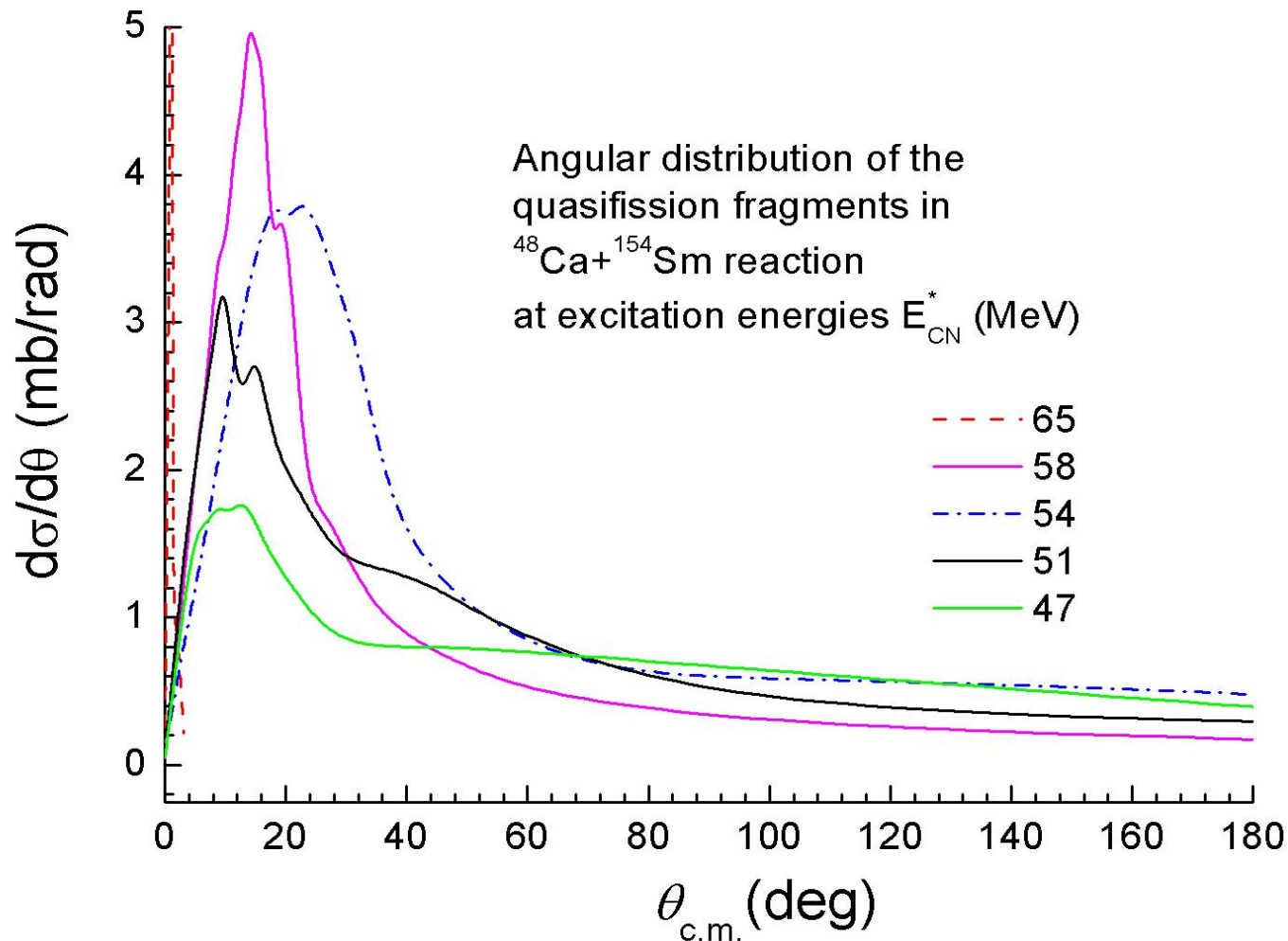
$$\omega_{qf}^2 = \mu_{qf}^{-1} \left| \frac{\partial^2 V(R)}{\partial R^2} \right|_{R=R_{qf}}.$$

The strong decrease of the yield of quasifission products by increase of beam energy in the  $^{48}\text{Ca} + ^{154}\text{Sm}$  reaction we explained by strong changing of the angular distribution of quasifission products: increase of beam energy leads to yield of quasifission products at angles close to the beam direction. Another reason is that maximum of mass distribution shifts to mass symmetric region.

Therefore, it is interesting to study mass-angle distribution of the reaction products.



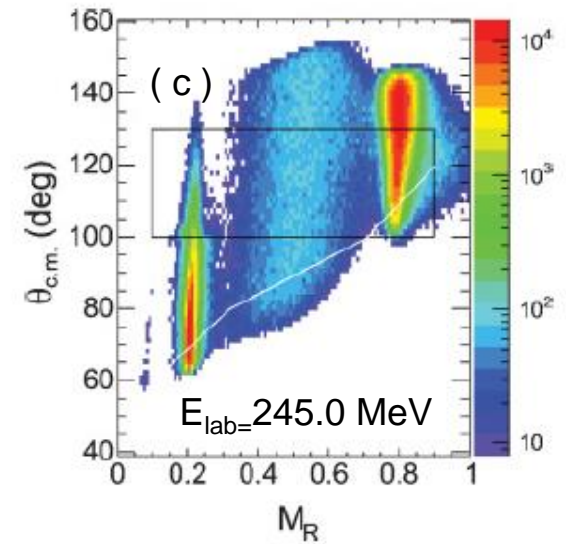
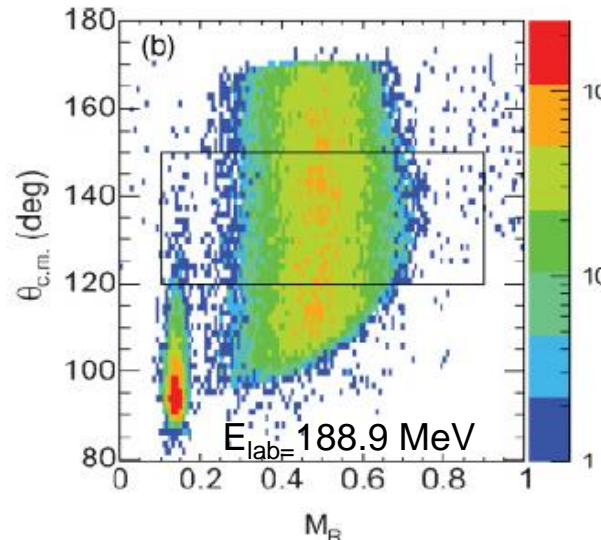
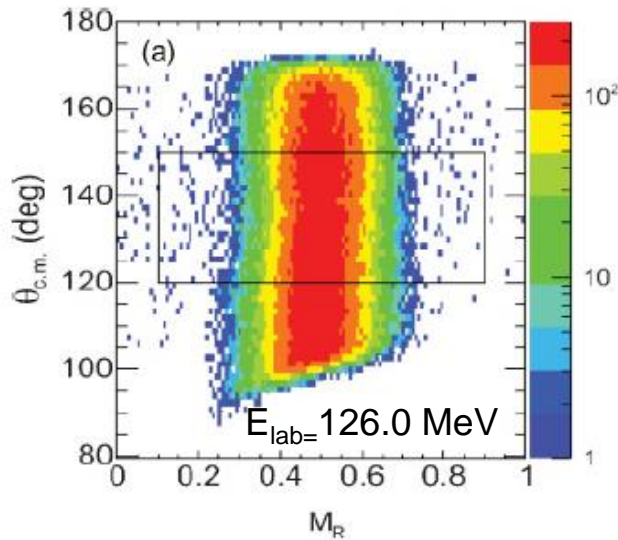
# Where we should look for quasifission fragments?



# Mass-angle distribution of the binary products in full momentum transfer (capture) reactions: $^{16}\text{O}+^{204}\text{Pb}$ (a), $^{34}\text{S}+^{186}\text{W}$ (b) and $^{48}\text{Ti}+^{170}\text{Er}$ (c,d).

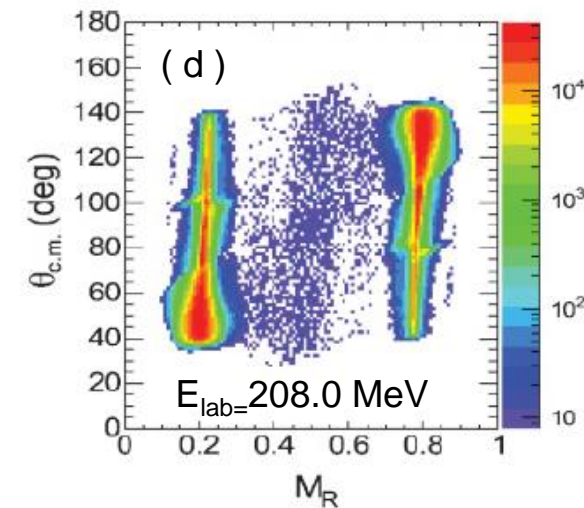
ENTRANCE CHANNEL DEPENDENCE OF QUASIFISSION ...

PHYSICAL REVIEW C 77, 034610 (2008)

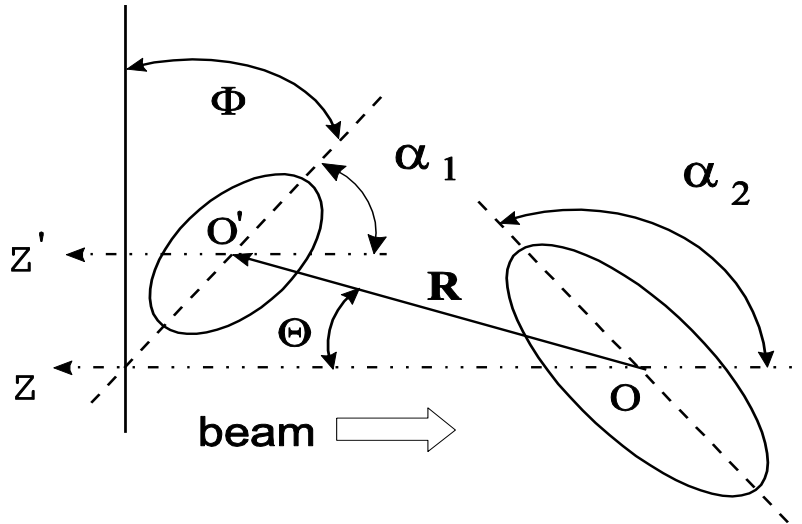


$$M_R = M_2 / (M_1 + M_2)$$

Dependence of the mass –angle distribution on the initial beam energy for the  $^{48}\text{Ti}+^{170}\text{Er}$  reaction (c,d): at small energy angular distribution of quasifission fragments becomes more isotropic. That is reason why quasifission seemed to be disappear for  $^{48}\text{Ca}+^{154}\text{Sm}$  reaction in the experiments discussed in [Knyazheva et al. Phys. Rev.C 75, 064602 \(2007\)](#). Our interpretation was presented in [A.K.N. et al. Phys.Rev. C 79 024606 \(2009\)](#).

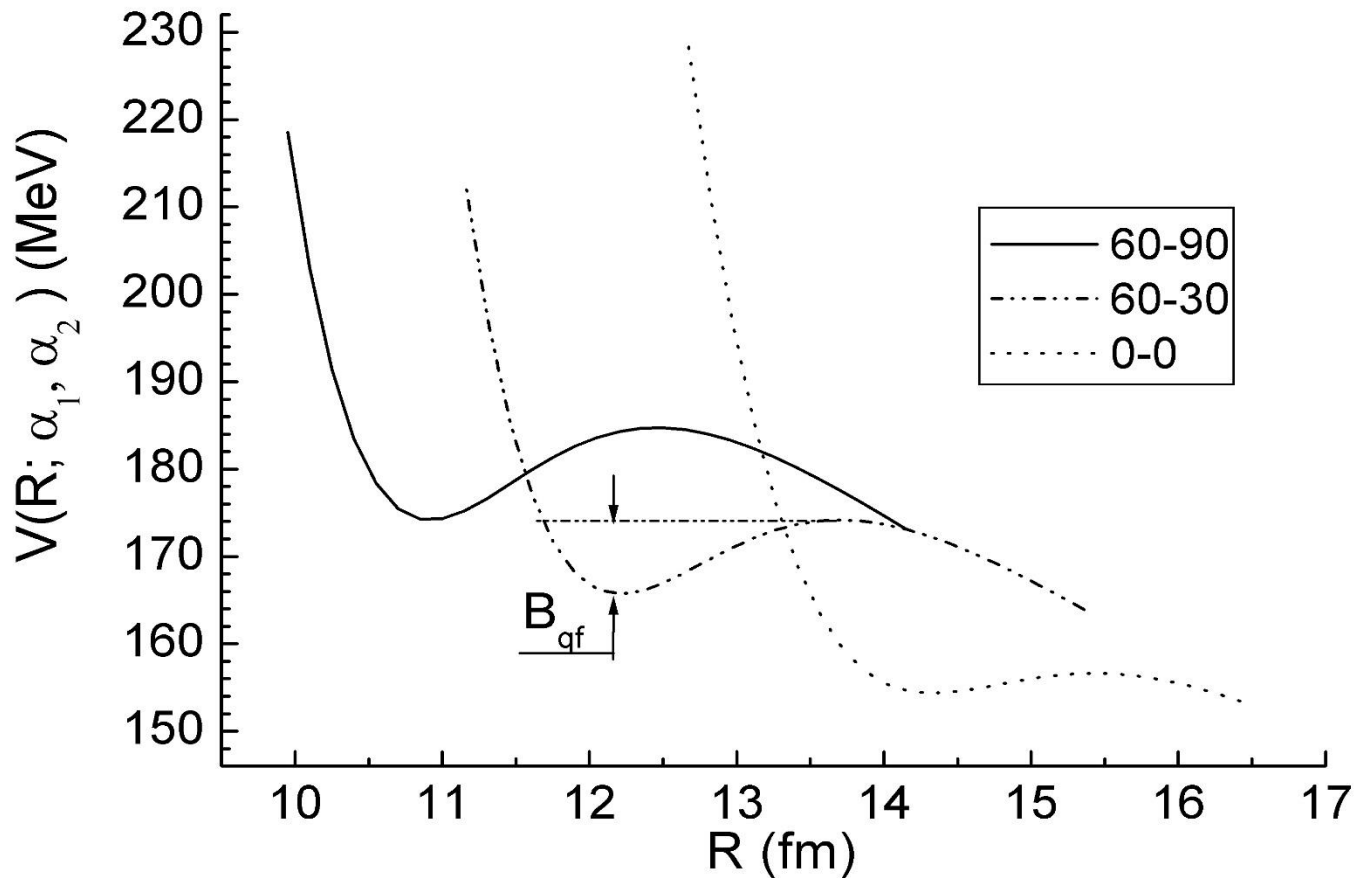


# Dependence of the capture and fusion cross sections on the orientation angle of the axial symmetry axis of reactants

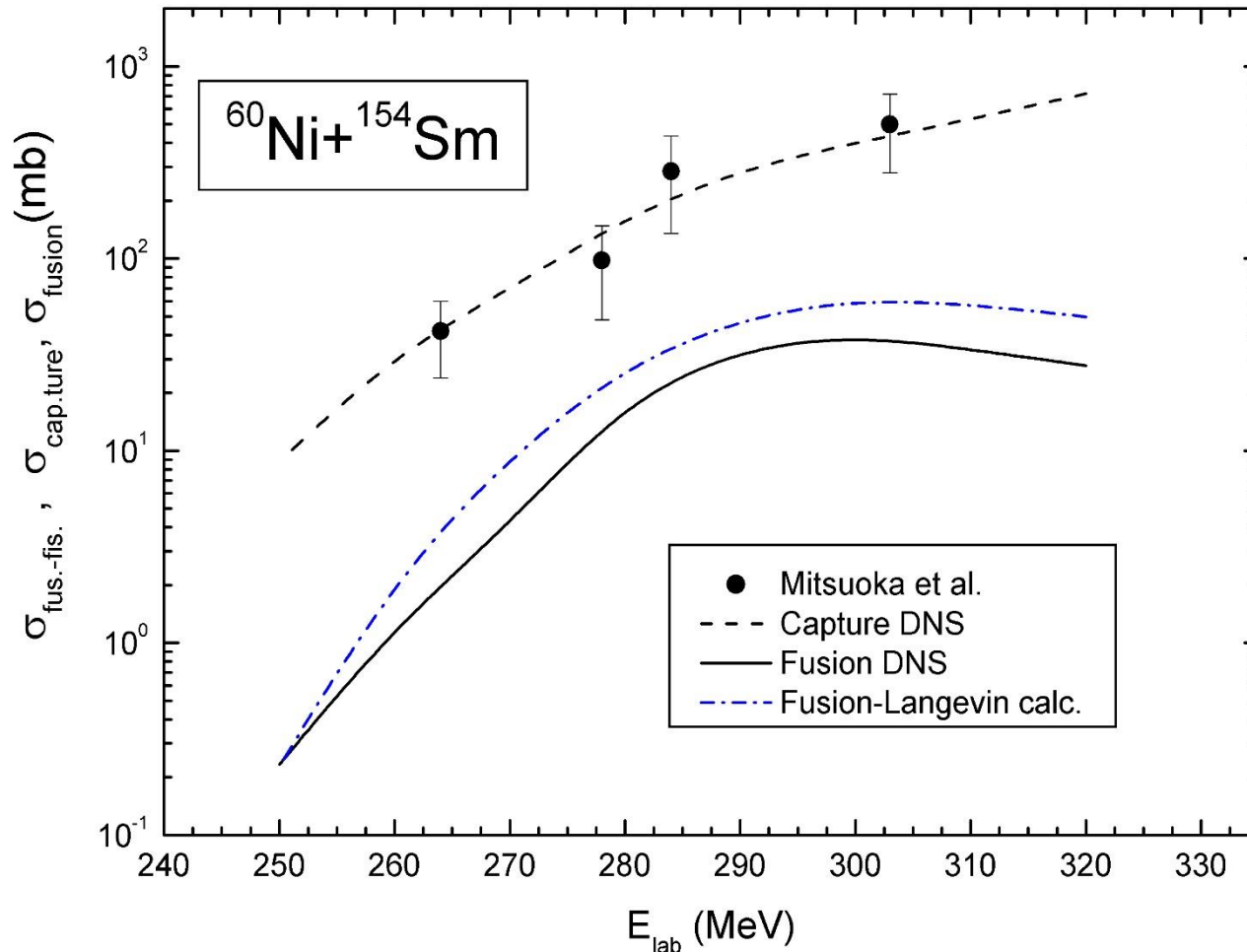


$$V_{nuc-nuc}(R, L; \{Z_i, A_i, \beta_i, \alpha_i\}) = V_{Coul}(R, L; \{Z_i, A_i, \beta_i, \alpha_i\}) + V_{nucl}(R, L, \{Z_i, A_i, \beta_i, \alpha_i\}) \\ + V_{rot}(R, L, \{Z_i, A_i, \beta_i, \alpha_i\})$$

# Nucleus-nucleus potential as a function of the distance between nuclei and orientation their axial symmetry axis



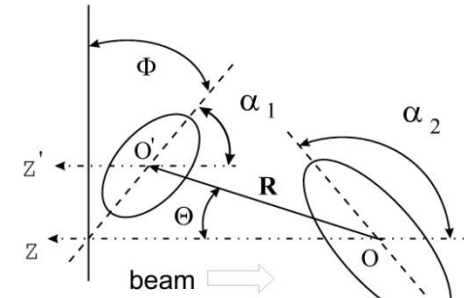
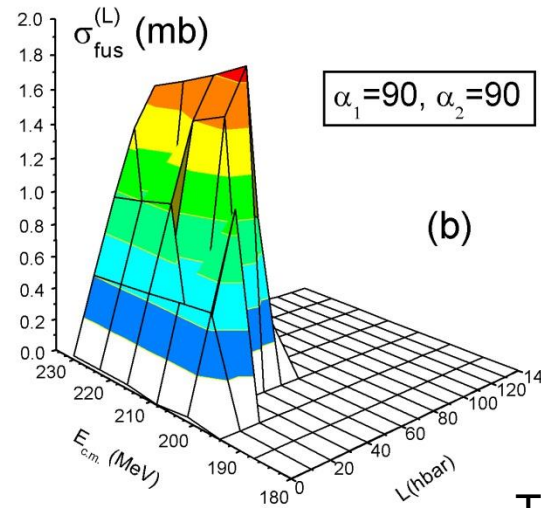
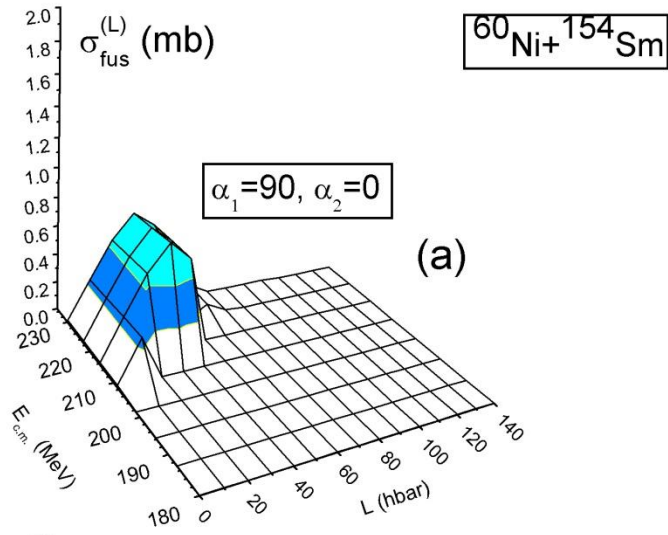
# Comparison of the capture and fusion excitation functions with the experimental data and Langevin calculations



S. Mitsuoka, et al.  
PRC 62 (2000) 054603.

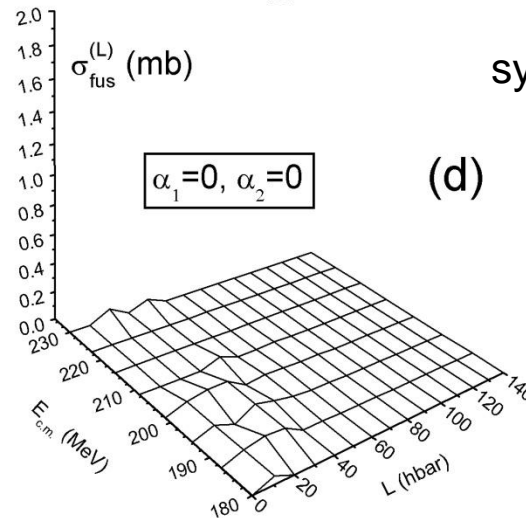
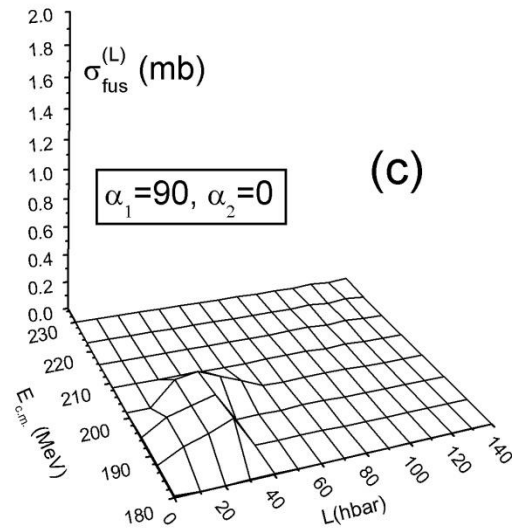
Y. Aritomo, M. Ohta,  
Nucl.Phys. A744  
(2004) 3

# Partial fusion cross section as a function of the orientation of axial symmetry axis reactants



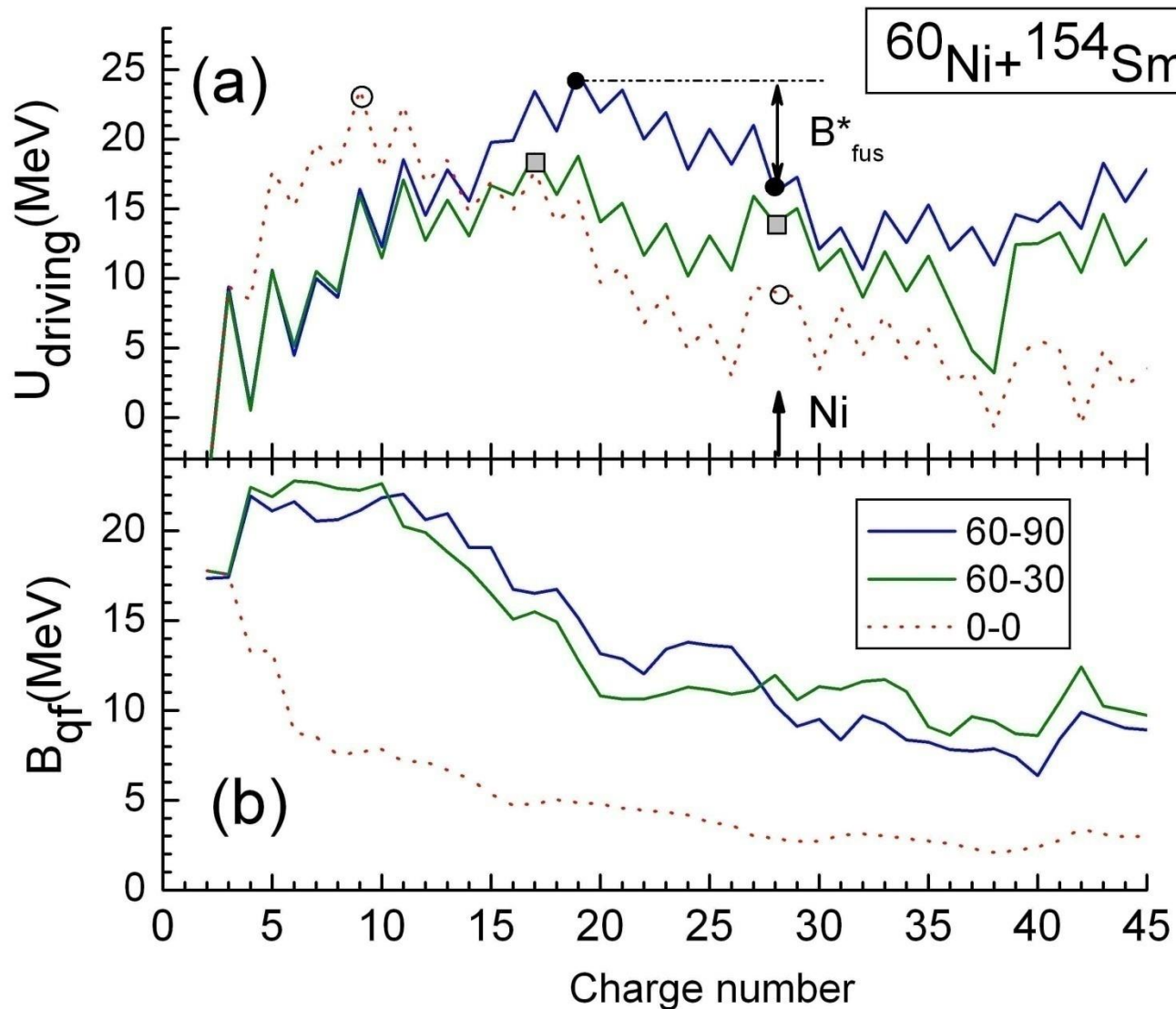
Nasirov A.K. et al.

The role of orientation of nuclei symmetry axis in fusion dynamics,  
[Nucl. Phys. A 759 \(2005\) 342](#)





Dependence of the driving potential (a) and quasifission barrier (b) on the mutual orientations of the axial symmetry axes of nuclei



# Conclusions from comparisons

- The study of dynamics of the heavy ion collision reactions at low energy and with different mass asymmetries and total masses are important to build whole presentation about capture, quasifission, fusion-fission and evaporation residue formation processes.
- The shell structure of interacting nuclei can lead to unexpected phenomena which should be studied by the use of dynamical calculation.
- The mutual dependence of the shell structure and deformation parameters of nuclei causes difficulties to make dynamics of collision at different orbital angular momentum.
- Dinuclear system model allows us to investigate different aspects of reaction although we use simplifications but keeping information about shell structure of nuclei.

# The formation of dinuclear systems

- Dinuclear system is formed due to shell effects as the quantum states of the neutron and proton systems of nuclei.
- Shell effects is observed as cluster states in the large amplitude collective motions of nuclei.
- The observed cluster emission, mass-charge distribution of the quasifission fragments and spontaneous asymmetric fission of Th, U and Cf isotopes proved the strong role of shell structure.
- Reactions of heavy ion collisions and fission (spontaneous and induced) processes can be studied well using dinuclear system concept.

# Manifestation of shell structure in fission

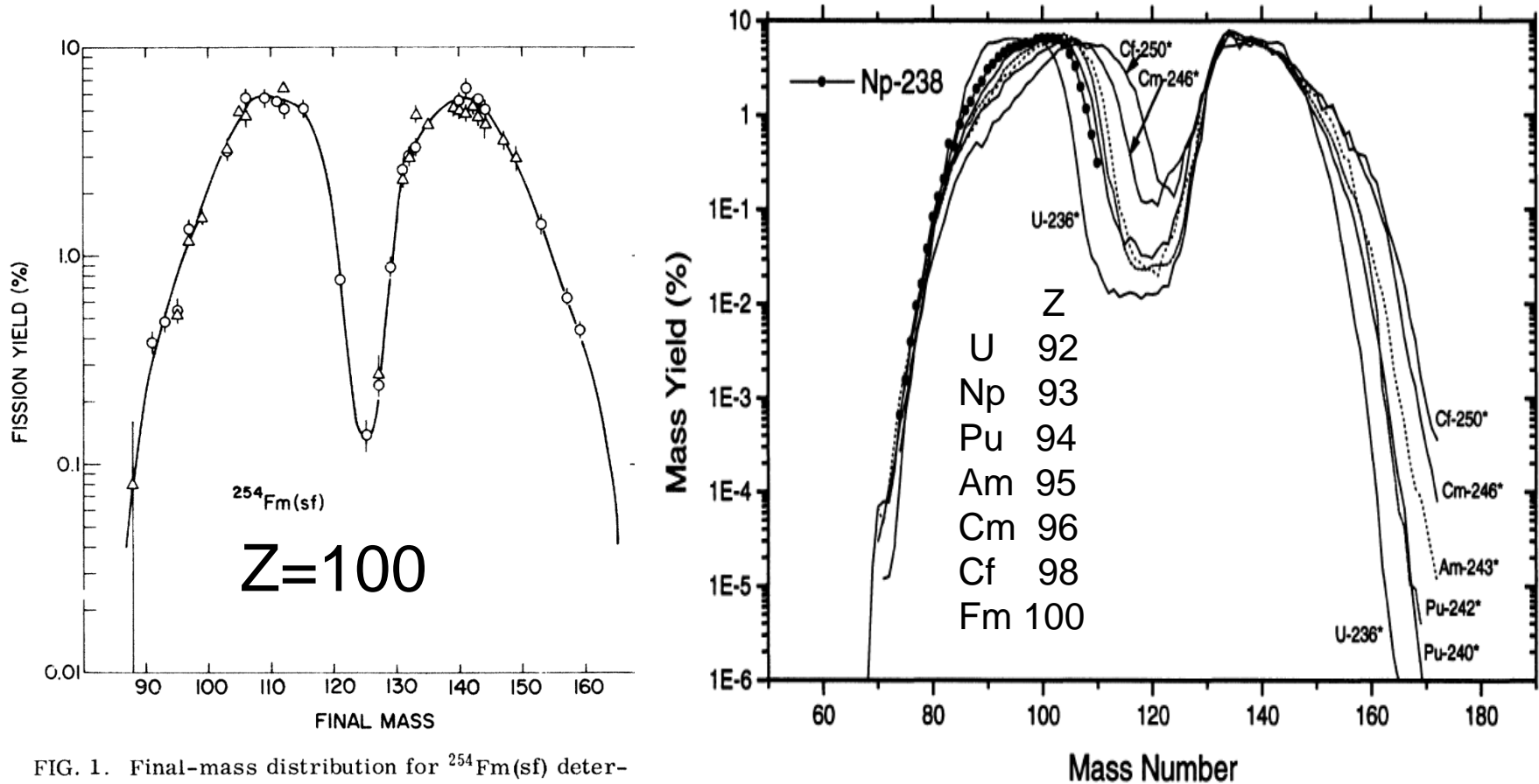
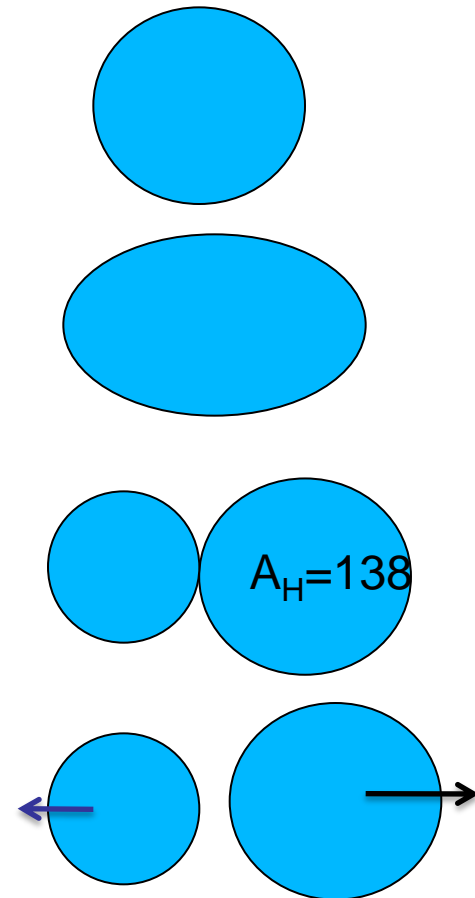
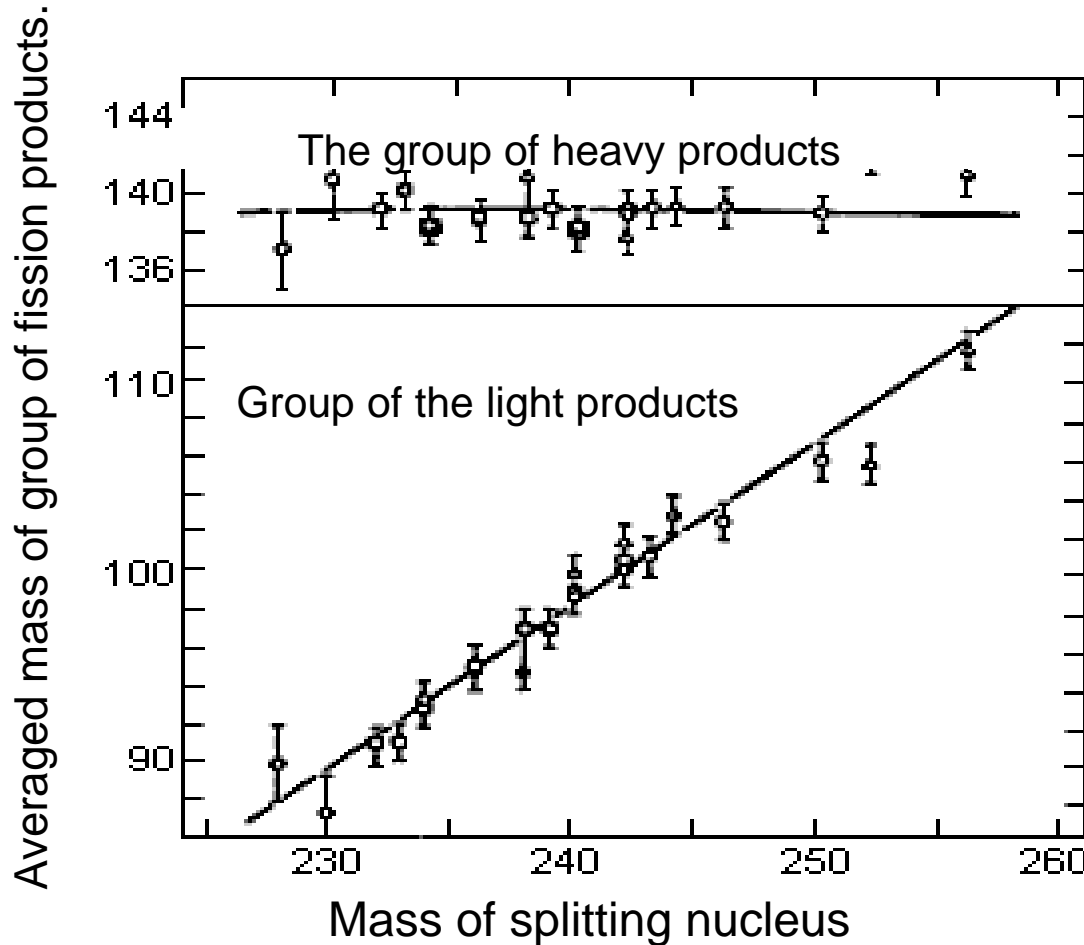


FIG. 1. Final-mass distribution for  $^{254}\text{Fm}(\text{sf})$  determined from radiochemical and  $\gamma$ -ray spectrometry measurements. Circles represent present data. Triangles represent data from Ref. 6. The solid curve represents a total yield of 200%.

I. Tsekhanovich, F. Gönnerwein et al.  
 Nuclear Physics A 688 (2001) 633–658

J.E. Gindler, Phys.Rev.C 16(1977) 1483

Appearance of shell effects as a heavy cluster at fission of massive nuclei. The cluster and conjugate fragment form dinuclear system.



$$A_L = F(Z_{\text{fiss}})$$

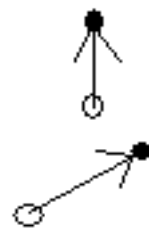
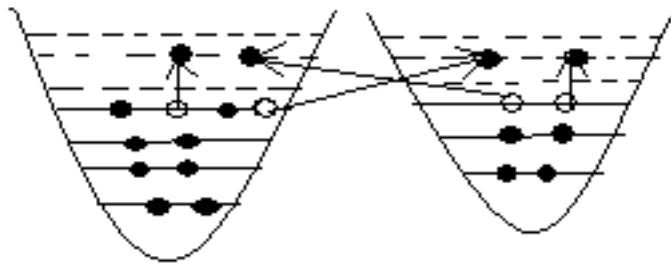
# Conditions allowing long lifetime of dinuclear systems at capture and fission processes

- Dinuclear system is formed due to shell effects as the quantum states of the neutron and proton subsystems of nuclei.
- Shell effects is observed as cluster states in the large amplitude collective motions of nuclei.
- The observed cluster emission, mass-charge distribution of the quasifission fragments and spontaneous asymmetric fission of Th, U and Cf isotopes proved the strong role of shell structure.
- Reactions of heavy ion collisions and fission (spontaneous and induced) processes can be studied well using dinuclear system concept.
- Presence of the potential well with enough depth ( $B_{fq}$ ) in nucleus-nucleus potential.

# Non-equilibrium processes in heavy ion collisions

At  $A_1 + A_2 \rightarrow A_1' + A_2'$  usually  $E_1^* : E_2^* \neq A_1' : A_2'$  (even at fission!).

At thermodynamic equilibrium must be  $T_1 = T_2 \rightarrow E_1^* : E_2^* = A_1' : A_2'$

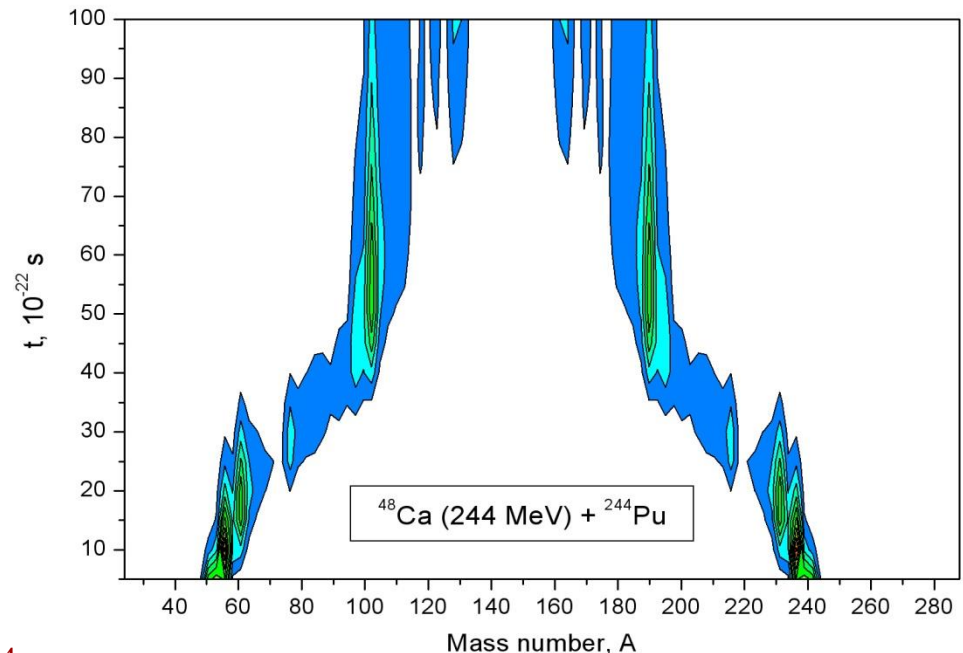
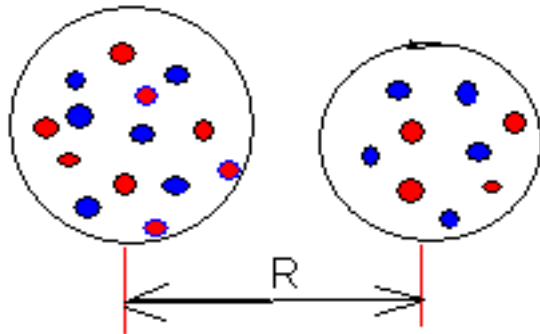


$V_{pp}^*$

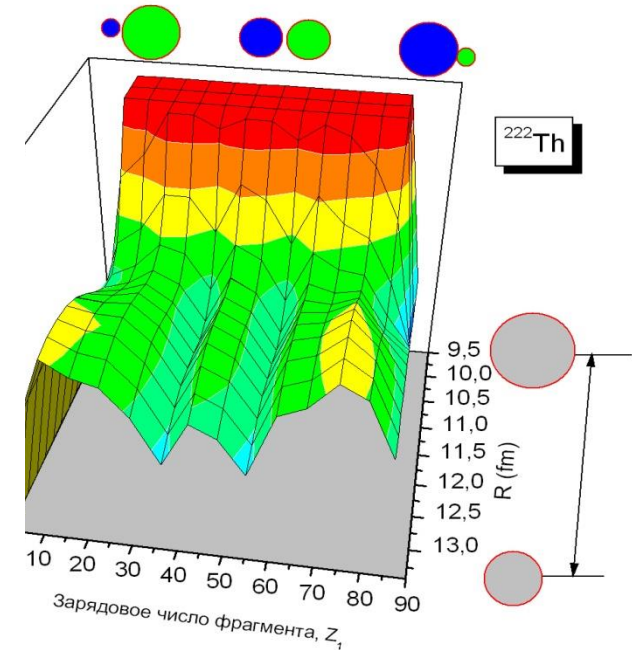
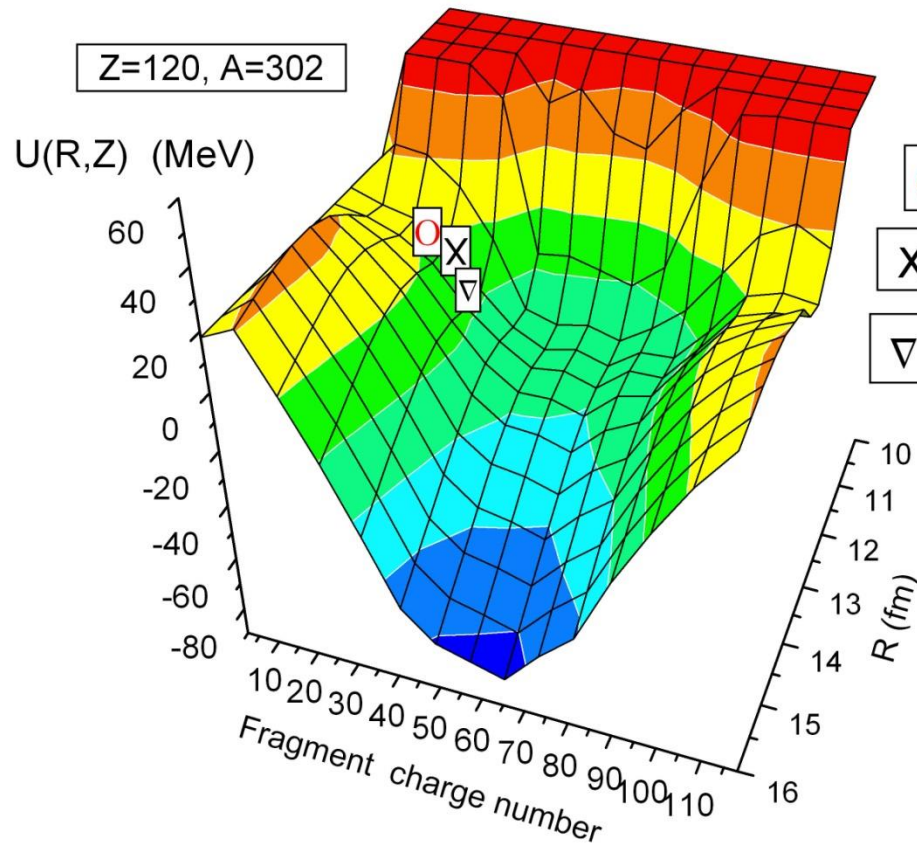
$g_{PT}$

$$T_i = 3.46 \sqrt{E_i / A_i}$$

$i = P, T$



# Potential energy surface of nuclear system



$$U_{dr}(A, Z, \beta_1, \beta_2) = B_1 + B_2 + V(A, Z, \beta_1; \beta_2; R) - B_{CN} - V_{CN}(L)$$



# Conclusions

The complete fusion mechanism in the heavy ion collisions strongly depends on the entrance channel peculiarities: mass (charge) asymmetry, shell structure of interacting nuclei, beam energy and angular momentum (impact parameter of collision).

The hindrance to formation of the compound nucleus is mainly caused by quasifission and fast-fission processes which are in competition with complete fusion.

The fission fragments of heavy nuclei (actinides) are mass symmetric or slightly mass asymmetric in dependence on the shell structure of fissioning nuclei and its excitation energy.

Therefore, the complete fusion of the main fission fragments has strong hindrance due to large intrinsic fusion barrier  $B_{fus}^*$  and small quasifission barrier  $B_{qf/}$ . As a result we have small fusion probability which was obtained in our calculations. Increasing the orbital angular momentum lead to increase the capture cross section but not fusion probability.